이학박사 학위논문

I. Efficient organic reactions and mechanistic studies based upon magnetically recyclable Pd–Fe_3O_4 heterodimer nanocrystals

II. Synthesis of core-shell type of Pd–Pt–Fe_3O_4 nanoparticles and their catalytic performance as magnetically reusable catalyst for organic reaction

I. 재사용 가능한 이종 팔라듐-산화철 나노결정을 이용한 효과적인 유기 반응 개발 및 메커니즘 규명

II. 재사용 가능한 코어-쉘 구조의 팔라듐-백금-산화철 나노입자의 합성 및 유기반응의 촉매 활성 연구

2017년 2월

서울대학교 대학원
화학부 유기화학 전공

변 상 문

Abstract

I. Efficient organic reactions and mechanistic studies based upon magnetically recyclable Pd–Fe_3O_4 heterodimer nanocrystals

In chapter I, we report the results of our investigation on the Wacker oxidation through the use of Pd–Fe_3O_4 heterodimer nanocrystals. Wacker oxidation is a useful process converting a terminal olefin to a methyl-ketone. We describe herein an environment-friendly and highly selective Wacker oxidation process employing superparamagnetic Pd–Fe_3O_4 heterodimer nano-particles as a reusable catalyst. Various reaction parameters were investigated for the determination of optimal reaction conditions. Consistently high yields and excellent reaction selectivities of the desired Wacker product were observed in almost all the reactions employing the Pd–Fe_3O_4 nano-catalysts in EtOH-H_2O under 1 atm O_2. This operationally simple oxidation protocol allows recycling of the Pd–Fe_3O_4 catalyst after the reaction through the use of an external magnet.

In chapter II, we also report an efficient, iterative, catalytic, Wacker-type oxidation of alkynes to 1,2-diketones using Pd–Fe_3O_4 heterodimeric nano-crystals. This process has a wide substrate scope affording 1,2-diketo derivatives in excellent yields under atmospheric pressure of O_2. The operational procedure using the Pd-Fe_3O_4 nano-praticles is extremely straightforward, and the catalyst can be reused through the

employment of simple magnetic separation, enabling the recycling of the catalyst for 5 times without loss of catalytic activity.

In chapter III, we report our mechanistic investigation on several useful catalytic reactions using Pd–Fe_3O_4 heterodimeric nanoparticles as magnetically recyclable catalysts. Successful applications of the nanocrystals toward various organic reactions such as Heck, Suzuki, and Sonogashira coupling reactions, direct C–H activation reaction, and Wacker oxidation have been reported. However, detailed mechanistic studies of these reactions have not been delineated. It has been unclear whether this processes proceeds through a heterogeneous or homogeneous mechanism. Herein, we report our detailed mechanistic investigations of the applications on Suzuki coupling reaction and Wacker oxidation as two representative heterogeneous reactions employing the Pd-Fe_3O_4 catalysts. Hot filtration tests, general kinetic studies and three-phase experiments were conducted for the two reactions. The results of our investigation led us to believe that these two reactions most likely proceed through the use of a solution-phase Pd species.

Key words: Heterodimeric nanocrystals, Palladium nanoparticle, Pd-Fe_3O_4, Wacker oxidation, Wacker-type oxidation, mechanism study, hot filtration test, kinetic study, three-phase test

II. Synthesis of core-shell type of Pd–Pt–Fe_3O_4 nanoparticles and their catalytic performance as magnetically reusable catalyst for organic reaction

Recently, we have documented several useful catalytic reactions using Pd–Fe_3O_4 heterodimeric nano-catalysts as novel magnetically recyclable catalysts. Successful applications of the Pd–Fe_3O_4 toward various organic reactions such as Heck-, Suzuki-, Sonogashira- cross coupling reactions, direct C–H arylation, Wacker and Wacker type oxidation have been reported.

In this study, we report the synthesis of bimetallic nanoflake-shaped Pd–Pt–Fe_3O_4 nanoparticles (NP's) and their application to the reduction of nitro- derivatives. Using hydrothermal method, we decorated nano sized crystals of palladium and platinum on the Fe_3O_4 NPs' surface. The Pd-Pt–Fe_3O_4 NPs were very efficient in effecting the one-pot cascade catalysis of dehydrogenation of ammonia borane (AB) and reduction of nitro- compounds to anilines in methanol within 5 minutes at room temperature. Development of efficient procedure for the reduction of nitro derivatives becomes one of the important synthetic methods in relation with the advent of various display materials and medicinal candidates. The reactions using the Pd–Pt–Fe_3O_4 catalyst proceeded faster than those using either Pd–Fe_3O_4, Pt–Fe_3O_4 or the combination of both Pt-Fe_3O_4 and Pd–Fe_3O_4 catalysts, confirming a unique "synergistic effect" of the bimetallic nano-catalyst system. The catalyst could be reused through the use of an external magnet in a very straightforward

manner and was recyclable for over 250 times without loss of its catalytic performance. Thus, this new catalyst could offer a very sustainable, useful and environment-friendly tool for potential industrial/medicinal applications in the reduction of nitro-compounds.

Key words: bimetallic nanocatalysts, synergistic effect, cascade reaction, chemo-selectivity, magnetically recyclable catalysts, heterogeneous catalysts, iron oxide, hydrogenation

CONTENTS

List of Figures

List of Schemes

List of Tables

Part I.

Chapter 1. Wacker oxidation of terminal alkenes using magnetically recyclable Pd–Fe_3O_4 heterodimeric nanocatalys*

*Part of this thesis was published in *RSC Advances* **2013**, 3(37), 16296-16299.

1. Introduction

Wacker oxidation was first invented by Smidt and co-workers[1] and is exemplified by the conversion of ethylene to acetaldehyde in the presence of a catalytic amount of Pd(II) and Cu(II) source in a mixture of water and an organic solvent (**Scheme I-1.1**). Since its discovery, this process has seen broad industrial applications. Recently, the conversion of terminal olefins to methyl ketones through the Wacker oxidation has been frequently used in many synthetic approaches to natural and non-natural products.[2] A variety of reaction conditions and solvent combinations has been investigated for the efficient oxidation of more complex substrates.[2a] Wacker oxidation generally involves Pd(II) catalyst and excess O_2 or hydrogen peroxide as an oxidant. The original conditions required the reaction to be performed in water containing hydrogen chloride and, showed some limitations, such as a low reaction selectivity and rate with the formation of unwanted side product(s). Therefore some efforts have been constantly focused on the refinement of the process through the use of a mixture of water and organic solvents (i.e. DMF, NMP, DMA and sulfolane) in the presence of a stoichiometric amount of $CuCl_2$. Other problems also appeared such as the formation of chlorinated derivatives[3] due to rearrangement followed by nucleophilic addition of the chloride anion. To overcome these limitations, chemists have continued to search for better catalysts, ligands, co-

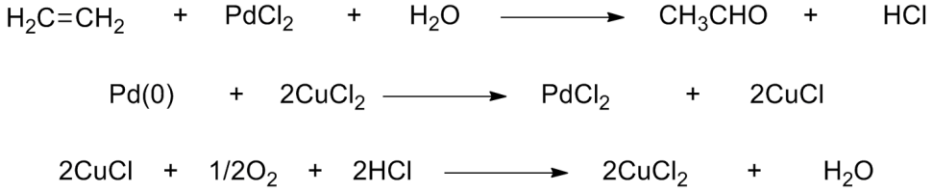

Scheme I-1.1 A general Wacker oxidation reaction

catalyst conditions,[4] new solvents including ionic liquids,[5] and new oxidant

systems using molecular oxygen.[6]

To recycle the expensive palladium catalyst in the Wacker process, the use of immobilized co-catalysts onto polymeric supports has been reported.[7] There has been an increasing interest in the use of magnetically separable nano-catalysts and nano-materials[8] in order to develop sustainable, heterogeneous catalysts as part of "green" processes. In our previous work, we reported on the simple synthesis of Pd–Fe_3O_4 and Rh–Fe_3O_4 bimetallic nanocrystal systems and their applications to Suzuki coupling and nitro-arene reduction, respectively.[9] Herein, we report on the Pd–Fe_3O_4 nanocrystals as a recyclable catalyst system for the Wacker oxidation of aryl and alkyl olefins in an environment friendly solvent combination under mild, aerobic conditions.

2. Results and Discussion

Wacker oxidations of styrene using excess hydrogen peroxide and molecular oxygen as the re-oxidant are known to be often accompanied by unwanted side products such as phenylacetaldehdye (3), benzaldehyde (4) and benzoic acid (5).[10]

In our optimized conditions, no hint of benzaldehyde or benzoic acid was detected. The GC analysis of the reaction products revealed that acetophenone (2) was the major product, and was accompanied by only a minute amount of phenylacetaldehyde (3) (**Scheme I-1.2**).

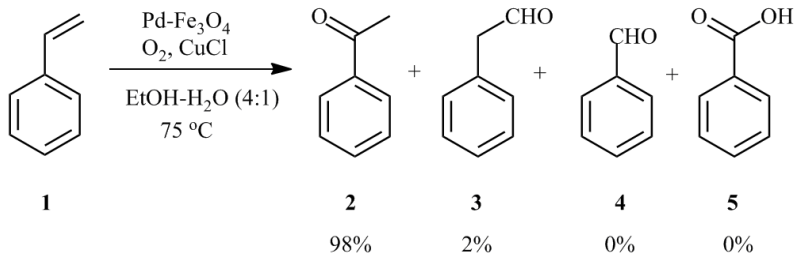

1 **2** **3** **4** **5**

98% 2% 0% 0%

Scheme I-1.2 Reaction selectivity of Wacker oxidation using the Pd–Fe_3O_4 catalyst

To optimize the reaction conditions, we first examined various solvents and solvent combinations. All reactions were carried out using 1 mol% Pd–Fe_3O_4 heterodimer nanocrystals in the presence of 10 mol% of CuCl under 1 atm O_2 unless otherwise noted. The results are collected in **Table I-1.1**. Reactions in solvents such as toluene, DMA and DMF gave no conversion at all (**Table I-1.1**, entries 1–3). When the reaction was carried out in water, however, some conversion to the desired product was observed (**Table I-1.1**, entry 4). Fortunately, when the solvent was changed to ethanol, both the conversion and reaction yield were remarkably enhanced, furnishing 75% of the desired methyl ketone (**Table I-1.1**, entry 5). With the same solvent we also explored the use of $CuCl_2$ instead of CuCl and the selectivity of the reaction was dramatically decreased giving only 20% of acetophenone (**Table I-1.1**, entry 6). Without any copper species, Wacker oxidation did not proceed at all (**Table I-1.1**, entry 7). Then we tried combinations of ethanol and water as solvent mixtures, and the results depended upon the volume ratio of the solvents (**Table I-1.1**, entries 8–10). We examined 2:1, 4:1, and 10:1 mixtures of EtOH-H_2O and the use of the 4:1 system furnished the best results giving >99% conversion and 85% yield of acetophenone (**Table I-1.1**, entry 9). Finally, upon testing a few temperature conditions, we found out that running the reaction at 75 °C in EtOH–H_2O (4:1) gave the best results, i.e. >99% conversion and 96% yield of the desired methyl

ketone product (**Table I-1.1**, entry 11).

Table I-1.1 Optimization of Wacker oxidation by using Pd–Fe_3O_4[a]

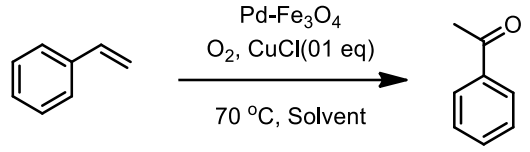

1

Entry	Solvent	Time (h)	Conversion(%)[b]	Yield(%)[b]
1	DMF	24	0	-
2	Toluene	24	0	-
3	DMA	24	0	-
4	Water	36	62	60
5	EtOH	24	>99	75
6	EtOH	18	>99	20
7	EtOH	24	0	-
8	EtOH+H2O (2:1)	36	76	73
9	EtOH+H2O (4:1)	36	>99	85
10	EtOH+H2O (10:1)	24	>99	75
11	EtOH+H2O (4:1)	36	>99	96

[a] Reaction condition: Compound 1 (1 mmol), Pd-Fe_3O_4(1 mol%), CuCl (0.1 mmol), Solvent (3 mL), mesitylene (1 mmol, internal standard), 70 °C, O_2 balloon. [b] All product composition and yields were characterized through GC analysis. [c] $CuCl_2$ (0.1 eq) instead of CuCl was used as a co-catalyst. [d] Reaction was run without CuCl. [e] EtOH (3 mL). [f] Reaction temperature was raised to 75 °C.

Table I-1.2 Wacker oxidation of different substrate by using Pd–Fe_3O_4[a]

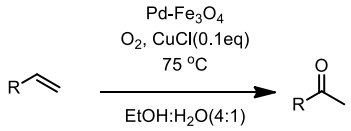

Entry	Substrate	Product	Conversion(%)[b]	Yield(%)[c]
1	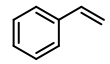	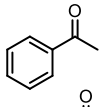	>99	96 (94)[d]
2	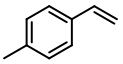	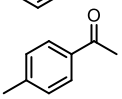	>99	91
3	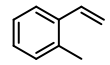	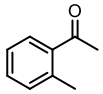	>99	97
4	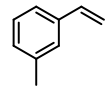	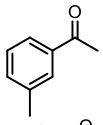	>99	93
5	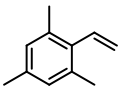	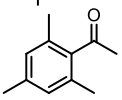	>99	98
6	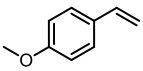	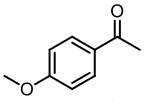	>99	90
7	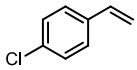	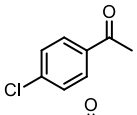	95	90
8	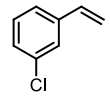	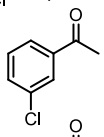	90	80
9	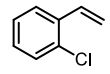	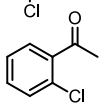	>99	56
10	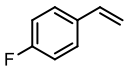	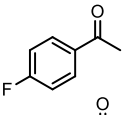	>99	96
11	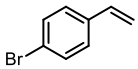	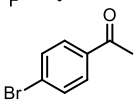	92	88
12	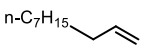	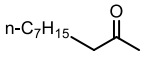	>99	78
13	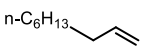	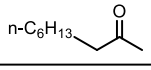	>99	60

[a] Reaction conditions: The substrates (1.0 mmol), Pd–Fe_3O_4 (1.0 mol%), CuCl (0.10 mmol), EtOH (3.0 mL), H_2O (0.75 mL) mesitylene (1.0 mmol, internal standard), 75 ^oC, O_2 balloon. [b] Numbers were determined through GC analysis. [c] Yields were determined through GC analysis based on comparison with an internal standard. [d] Yield of isolated product

With the optimized reaction conditions in hand, we set out to examine the scope of the reaction using various aryl- and alkyl-substituted terminal olefins. The results are collected in **Table I-1.2.** Reactions of electron-rich styrene derivatives gave the corresponding oxidation products in excellent conversions and high yields (**Table I-1.2.**, entries 2–6). Reaction of a sterically hindered styrene derivative also provided the desired ketone product in high yield (**Table I-1.2.**, entry 5). In addition, reactions of styrene derivatives with *para*- and *meta*-chloro-substitution exhibited good conversions and yields (**Table I-1.2.**, entries 7 and 8, respectively). However, in the case of *ortho*-chlorostyrene, though a good conversion was observed, only 56% yield of the desired methyl ketone was obtained (**Table I-1.2.**, entry 9) along with a substantial amount of side products. Also, reactions on *para*-fluoro- and *para*-bromo-substituted styrene proceeded with excellent conversions and yields (**Table I-1.2.**, entries 10 and 11, respectively). Furthermore, terminal alkenes substituted with alkyl groups were also smoothly converted to methyl ketones in moderate to good yields (**Table I-1.2.**, entries 12 and 13).

We have carried out recycling experiments using the Pd–Fe_3O_4 nanocrystals recovered from the previous run and the results are presented in **Table I-1.3**. The recovery of the catalyst was conveniently accomplished through the use of an external neodymium magnet for the collection of the nanocatalysts from the reaction mixture. The reactivity of the catalyst remained unchanged up to

Table I-1.3 Recyclability of the Pd–Fe_3O_4 nanocrystals for the Wacker-oxidation [a]

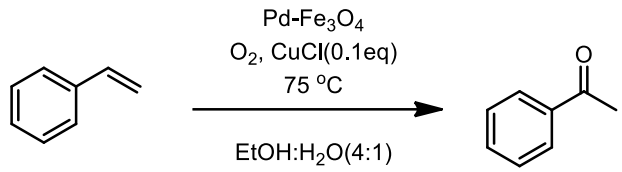

Entry	Conversion(%)[b]	Yield(%)[b]
1	99	95
2	99	93
3	99	92
4	99	89

[a] Reaction condition: Styrene (2 mmol), Pd-Fe_3O_4 (1 mol%), CuCl (0.2 mmol), EtOH (6 mL), H_2O (1.5 mL), mesitylene (2 mmol, internal standard). [b,c] All products were characterization by GC

the fourth recycling experiment. In the fifth run, however, the reaction rate decreased noticeably. The transmission electron microscope (TEM) images of the Pd–Fe_3O_4 heterodimer nanocrystals after the fifth recycling experiment did not show any significant morphological change compared to the images of the original sample, as shown in **Figure I-1.1**. Measurement of the palladium content in the Pd–Fe_3O_4 nanocrystals before the reaction and after five recycling runs using inductively coupled plasma atomic emission spectroscopy (ICP–AES) indicated 2.24 and 1.03 wt% of palladium, respectively. After first reaction, 4.9 ppm of palladium was detected in the solution. The reason for the reduction in the palladium content after five recycling runs is unclear and is currently being investigated. The nanocrystals after the fifth run were well separated through the use of an external magnet.

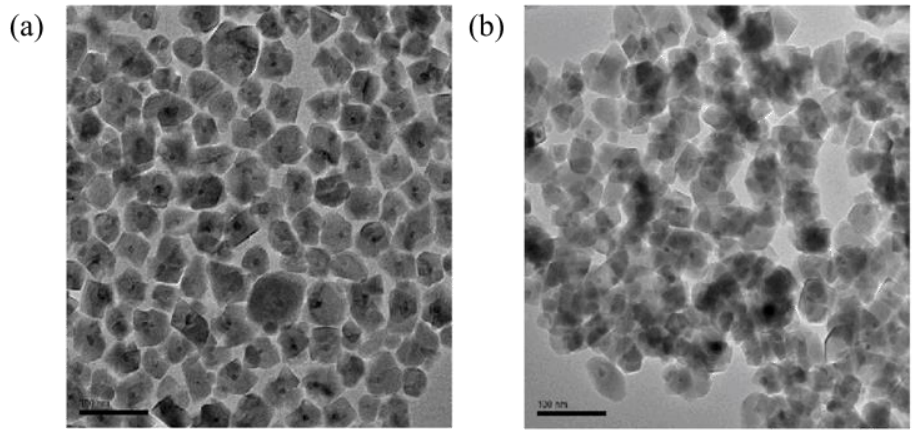

Figure I-1.1 (a) Pd–Fe_3O_4 TEM image, (b) After the fifth recylced Pd–Fe_3O_4 TEM image

Figure I-1.2 Magnetic separation of Pd–Fe_3O_4 after Wacker oxidation.

3. Conclusion

In summary, we describe herein a highly efficient catalytic process for the oxidation of various terminal olefins into methyl ketones using superparamagnetic Pd–Fe_3O_4 nanocrystals under 1 atm O_2 in EtOH-H_2O (4:1)

at 75 °C.. Reactions using Pd–Fe_3O_4 heterodimer nanocrystals (1 mol% in Pd) proceeded with exceedingly high selectivity to give the desired products in good to excellent yields. To the best of our knowledge, this work is the first use of heterodimeric Pd nanocrystals in the Wacker oxidation process. Also because of the superparamagnetic Fe_3O_4 nanocrystals, the catalyst can be easily recovered and recycled through the use of an external permanent magnet. The catalyst was reusable up to four times without losing its catalytic activity. It is particularly noteworthy that the reactions proceeded under mild oxidative conditions without the use of strong oxidants such as H_2O_2 or TBHP. We believe that the atom efficiency, cost effectiveness, and recyclability of the Pd–Fe_3O_4 nanocrystals indicate the potential for this catalyst system to be further developed to realize large scale applications. Further study of various palladium-catalyzed reactions is currently under investigation in our laboratory.

4. Experimental

General

All commercially available chemicals were purchased from Aldrich Chemical Co. or Tokyo Chemical Industry Co. and used without further purification unless otherwise noted. All reaction products were identified through comparison with the authentic compounds and quantified through GC analysis using a Hewlett Packard 5890 Gas Chromatograph using mesitylene as an internal standard.

Preparation of the catalyst

In a general experiment, 200 mg of $Pd(acac)_2$ (0.660 mmol) and 14.0 g of $Fe(acac)_3$ (40.0 mmol) were added to a solution containing 120 mL of oleylamine (350 mmol) and 80 mL of oleic acid (250 mmol). The mixture was heated to 120 ^oC under reduced pressure and agitated with vigorous stirring for 2 h. The resulting mixture was heated to 220 ^oC under Ar atmosphere at a heating rate of 2 ^oC /min and kept at this temperature for 30 min. Then it was further heated to 300 ^oC at the same heating rate and aged for 30 min. Subsequently the mixture was cooled to room temperature and washed with 250 mL of ethanol and a black supernatant was decanted. The residue was dispersed in EtOH (250 mL) through sonication and products were collected by centrifugation (1700 rpm, 15 min). The Pd–Fe_3O_4 was again dispersed in 150 mL of hexane and collected through the use of an external magnet. This washing process was repeated until the decanted hexane showed no color. After repeated washing cycles, the catalyst was collected and dried under vacuum to furnish 2.45 g of solid.

General procedure for Wacker oxidation

A mixture of Pd–Fe_3O_4 nanocrystal catalyst (1.0 mmol) in ethanol (3.0 mL) was placed in a sealed vial and the mixture was heated to 75 ^oC. After 60 min, styrene (1 mmol), CuCl (0.1 mmol) and H_2O (0.75 mL) were added to the mixture and the vial was equipped with an O_2 balloon. The sealed vial was sonicated for 1 minute for dispersion of to disperse the Pd-Fe_3O_4 and the reaction mixture was stirred for 36 h at 75 ^oC. Once the reaction was complete, the reaction mixture was separated from the catalyst using an external magnet.

General procedure for recycling

After the reaction was complete, ethanol (5 mL) was added and the mixture was sonicated for 1 min. Then, The Pd–Fe_3O_4 catalysts were separated with the use of an external magnet. The catalyst was washed with EtOH (20 mL) and the washing cycles were repeated five times. The catalyst was the washed twice with H_2O. Finally, the catalyst was washed with ethanol twice and dried before use for in the next reaction.

Part I.

Chapter 2. Wacker-type oxidation of alkyne to 1,2-diketones Using the Pd-Fe_3O_4 Heterodimeric nanocatalysts*

*Part of this thesis was published in *RSC Advances*, **2014**, *4(64)*, 34084-34088.

1. Introduction

1,2-Dicarbonyl derivatives are valuable structural motifs often embedded in many natural products[11] and biologically active compounds. [12] Among these derivatives, benzil derivatives are employed for a number of interesting applications, such as corrosion inhibitors of mild steel, [13] photosensitive agents in photocurable coatings, [14] and carboxylesterase (CE) inhibitors. [15] Moreover, 1,2-dicarbonyl derivatives can be used as precursors to many biologically active compounds or as building blocks for the synthesis of quinoxalines, triazines, and imidazoles. [16]

In light of their usefulness, the development of convenient synthetic pathways for 1,2-diketones has attracted much attention, and several synthetic methods have been reported, including substitutions of keto acid chloride or oxalyl chloride[17] and oxidations of hydroxyketone derivatives. [18] Among several other methods, [19] oxidation of 1,2-diarylalkynes[20] can be a very straightforward approach to the synthesis of diketones. The 1,2-diarylalkynes are easily prepared by standard Sonogashira coupling reactions of aryl alkynes and aryl halides.[21] A variety of reagents have been employed to oxidize 1,2-diarylalkynes for the synthesis of benzil compounds, such as manganese[22] and chromium reagents, [23] sulfur trioxide-dioxane complexes, [24] ozone, [25] dioxiranes, [26] iodo- or bromo-succinimide, [27] and orthoperiodic acid. [28] However, these reagents are highly toxic, and the procedures associated with their use are expensive, low yielding, limited in terms of functional group tolerance, poorly chemoselective, and produce environmentally hazardous wastes.

Recently, in an effort to provide a remedy to these drawbacks, new alkyne oxidation reactions have been developed that utilize homogenous catalysts such as iron(III) bromide,[29] palladium(II) sources with copper co-catalyst,[30] and

gold-catalyzed transformations.[31] The use of a heterogeneous palladium source such as palladium on carbon (Pd/C) has been reported for the synthesis of benzil derivatives with DMSO and molecular oxygen as dual oxidants.[32] There has been increased interest in the use of magnetically recyclable palladium nanoparticles and nanomaterials[33] for the development of sustainable, efficient, heterogeneous catalysts for practical organic synthesis. Iron oxide-based catalysts have many advantages including their facile recovery by an external neodymium magnet, thus obviating complicated separation/ filtration processes. Thus, magnetically recoverable iron oxide catalysts offer great potential for industrial applications.

Herein, we report the efficient synthesis of benzil derivatives from 1,2-diarylalkynes under oxygen atmosphere using Pd–Fe_3O_4 heterodimer nanocrystals as a reusable and durable catalyst system.

2. Results and Discussion

Our first attempt at the Pd–Fe_3O_4-catalyzed oxidation of an acetylene derivative was carried out using diphenylacetylene (1a) and 1 mol% catalyst in DMSO under 1 atm oxygen in the presence of 10 mol% $CuBr_2$. This reaction afforded the corresponding benzil (2a) in 62% yield after 28 h at 95 ^oC (**Table I-2.1**, entry 1). We then carried out an extensive screening of solvents, such as DMSO, DMF, H_2O, toluene and 1,4-dioxane with 10 mol% $CuBr_2$ under otherwise identical reaction conditions (**Table I-2.1**, entries 1-5). Among the solvents examined, 1,4-dioxane was identified as most effective for the Wacker-type oxidation. The addition of a Cu(II) salt was absolutely necessary since no product formation was observed in its absence (**Table I-2.1**, entry 7). Replacing

$CuBr_2$ by $CuCl_2$, $Cu(OAc)_2$, or CuI resulted in decreased reactivity in each case (**Table I-2.1**, entries 8-10). In fact, no reaction was observed with CuI. Finally, optimal conditions were identified by employing 1 mol% of Pd–Fe_3O_4 and 10 mol% of $CuBr_2$ in dioxane/H_2O under 1 atm of O_2 in a balloon, which yielded 98% of the desired product (**Table I-2.1**, entry 5). When the reaction temperature decrease to 75 °C, the yield was decreased slightly under otherwise the same conditions (**Table I-2.1**, entry 6).

Table I-2.1 Optimization of Wacker-type oxidation by using Pd–Fe_3O_4[a]

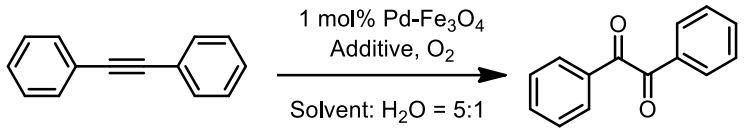

1

Entry	Solvent	Additive	Temp.(°C)	Time (h)	Yield(%)[b]
1	DMSO	$CuBr_2$	95	28	62
2	DMF	$CuBr_2$	95	28	3
3	H_2O	$CuBr_2$	95	28	6
4	Toluene	$CuBr_2$	95	28	-
5	1,4-Dioxane	$CuBr_2$	95	28	98
6	1,4-Dioxane	$CuBr_2$	75	28	85
7	1,4-Dioxane	-	95	28	-
8	1,4-Dioxane	$CuCl_2$	95	28	87
9	1,4-Dioxane	$Cu(OAc)_2$	95	28	5
10	1,4-Dioxane	CuI	95	28	-

[a] Reaction conditions: Compound 1 (0.5 mmol), Pd–Fe_3O_4 (1.0 mol%), additive (0.05 mmol), solvent (5.0 mL), H_2O (1.0 mL), O_2 balloon. [b] Yield of isolated product.

Table I-2.2 Study on the effect of H_2O content in solvent

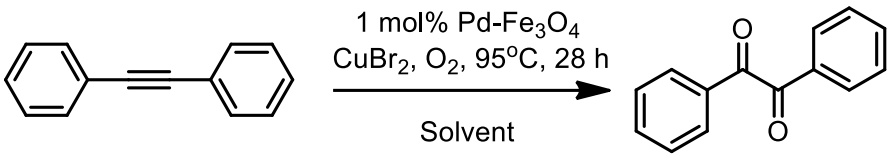

1

Entry	Solvnet	Yield (%)[a]
1	1,4-Dioxane	14
2	1,4-Dioxane : H_2O = 5 : 1	98
3	1,4-Dioxane : H_2O = 3 : 2	82
4	1,4-Dioxane : H_2O = 2 : 3	52
5	1,4-Dioxane : H_2O = 1 : 5	26
6	H_2O	6

[a] isolated yield.

Also, wecarried out reactions with varying amounts of water in the solvent mixture, and the yield of desired product was the highest in 1:5 water-dioxane solvent. (**Table I-2.2)**

Table I-2.3 Wacker-type oxidation of different substrate by using Pd–Fe_3O_4[a]

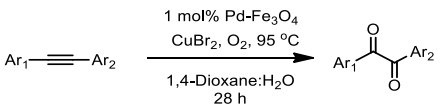

Entry	Substrate	Yield (%)[b]	Entry	Substrate	Yield (%)[b]
1	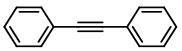	98	8	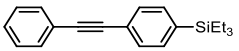	85
2	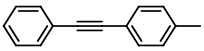	92	9	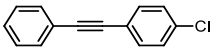	82
3	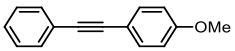	90	10	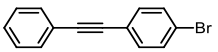	94
4	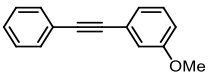	88	11	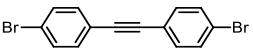	86
5	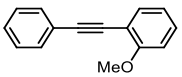	86	12	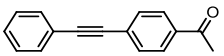	91
6	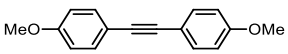	86	13	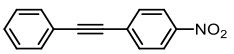	83
7	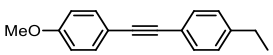	92	14	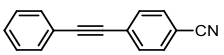	77

[a] Reaction conditions: Substrate (0.5 mmol), Pd–Fe_3O_4 (1.0 mol%), $CuBr_2$ (0.05 mmol), 1,4-dioxane (5.0 mL), H_2O (1.0 mL), O_2 balloon. 95 °C [b] Yield of isolated product.

With the optimized reaction conditions, the substrate scope was then examined. As shown in **Table I-2.3**, good to excellent product yields were obtained for a variety of diaryl-substituted alkyne derivatives. Reactions of substrates equipped with electron-donating substituents, such as *p*-methyl, *o*-, *m*-and *p*-methoxy groups, provided excellent yields of the desired products (**Table I-2.3**, entries 2-5). Sterically hindered, *o*-substituted substrate also gave

good yield of the desired product (**Table I-2.3**, entry 5). Reactions of diphenylacetylenes with two *p*-substitutions, such as 1,2-bis(4-methoxyphenyl)ethyne and 1-ethyl-4-((4-methoxyphenyl)ethynyl)benzene gave good yield to the corresponding diketo products (**Table I-2.3**, entries 6-7). A trimethylsilyl-substitution was also well tolerated under the reaction conditions (**Table I-2.3**, entry 8). In addition, reactions of substrates having one or two halide substitutions at the para position(s) also gave rise to good to excellent yields (**Table I-2.3**, entries 9-11). Reactions of substrates having other electron-withdrawing groups, such as *p*-acetyl and *p*-nitro groups proceeded with good yields (**Table I-2.3**, entries 12-13). The only reaction that provided a moderate yield (77%) was that employing *p*-cyano-substituted diphenylacetylene (**Table I-2.3**, entry 14).

Table I-2.4 Oxidation of alkyl-substituted acetylene derivatives

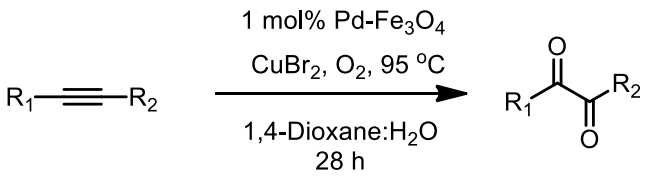

Entry	Substrate	Yield (%)[a]
1	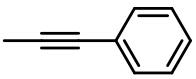	20
2	$CH_3(CH_2)_3$—≡—$(CH_2)_3CH_3$	-

[a] isolated yield.

Also, we carried out further experiments using alkyl, aryl and dialkyl substituted acetylenes. As seen from the table below, when 1-phenylpropyne was employed as substrate, only 20% yield of the desired product was isolated along with several other side products (**Table I-2.4**, entry 1). When 5-nonyne, a dialkyl-substituted acetylene, was used, the reaction was very sluggish, leaving almost unreacted starting material. The results are added in **Table I-2.4**.

The recyclability of the Pd–Fe_3O_4 nanocatalyst was confirmed by its ability to repeatedly catalyze the oxidation of diphenylacetylene (**Table I-2.3**). After the reaction, the catalyst from the reaction mixture was simply collected using an external neodymium magnet. Then, without filtration, the catalyst was washed five times with EtOAc, twice with water, and was dried in vaccum condition for 2 h. The recovered catalyst could then be reused immediately in the next reaction. In this experiment, more than 99% of the nanocrystals could be recovered through the use of an external magnet and through catalyst purification by dispersion and collection cycles. The results are presented in **Table I-2.5**. The reactivity of the catalyst consistently remained unchanged up to the fourth recycling experiment. After the fifth run, however, the yield of the product was slightly diminished to 83%, indicating a slight decrease in the activity of the Pd-Fe_3O_4 catalyst.

Table I-2.5 Recyclability of the Pd–Fe_3O_4 nanocrystals for the Wacker type -oxidation [a]

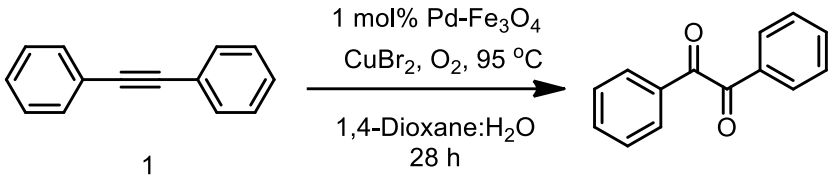

Entry	Yield(%)[b]
1	98
2	96
3	96
4	92
5	83

[a] Reaction conditions: **1** (0.5 mmol), Pd–Fe_3O_4 (1.0 mol%), $CuBr_2$ (0.05 mmol), 1,4-dioxane (5.0 mL), H_2O (1.0 mL), O_2 balloon. 95 °C [b] Yield of isolated product.

As shown in **Figure I-2.1**, the Pd–Fe_3O_4 nanocrystals exhibited very good dispersion during and after the oxidation reaction. After the reaction was complete, the nanocrystals could be gathered easily using an external magnet. The transmission electron microscope (TEM) image of the Pd–Fe_3O_4 nanocrystals after five oxidation cycles showed that the size and morphology of the nanocrystals had not changed (**Figure. I-2.2** and **I-2.3**). Moreover, the powder X-ray diffraction (XRD) pattern of the catalyst did not show any noticeable change from those of the catalyst before use (**Figure I-2.4** and **I-2.5**). In addition, when the catalyst system was analyzed after the first and fifth reaction by inductively coupled plasma atomic emission spectroscopy (ICP-AES), the nanoparticles showed 1.9 and 1.2 wt% of Pd, respectively. About 37%

of palladium was lost after 5 cycles. This observation indicates that a small amount of Pd might have leached out from the original catalyst system upon each recycling experiment. However, there was no detectable change in Fe content.

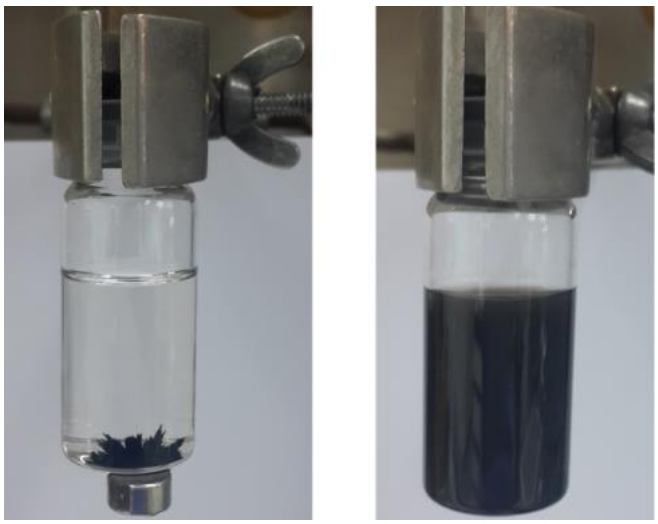

Figure 1-2.1 Magnetic separation of Pd–Fe_3O_4 after Wacker-type oxidation..

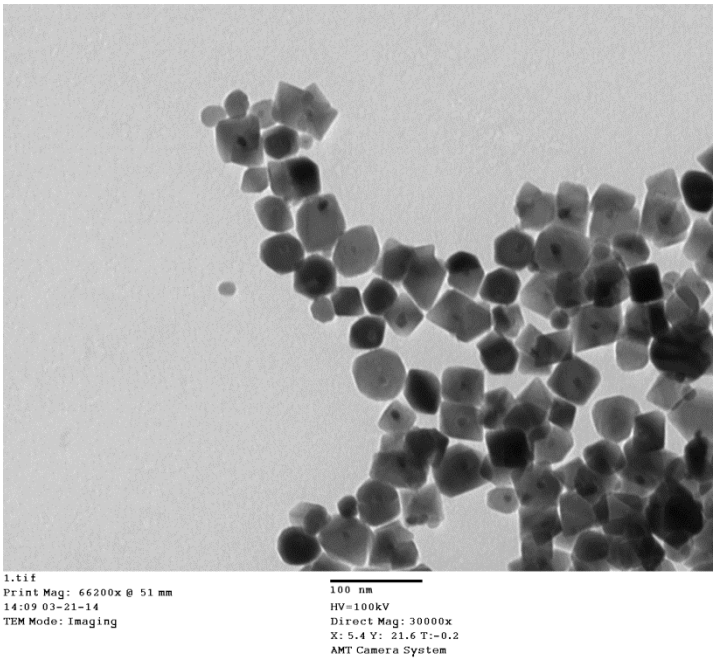

Figure I-2.2 TEM image of the fresh Pd–Fe_3O_4

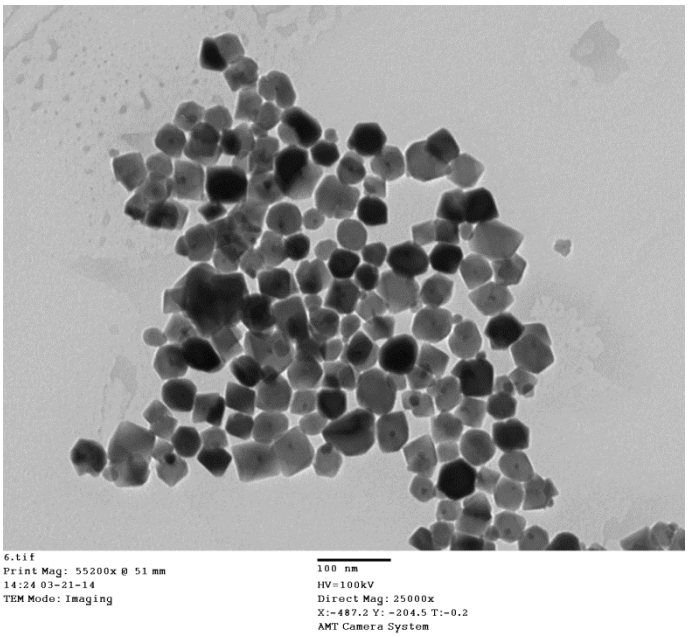

Figure I-2.3 TEM image of Pd–Fe_3O_4 after fifth reusing experiment

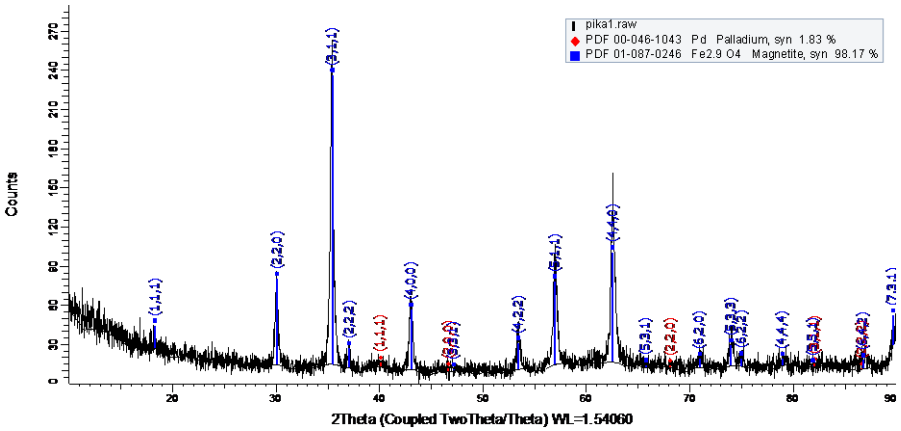

Figure I-2.4 XRD pattern of the fresh Pd–Fe_3O_4

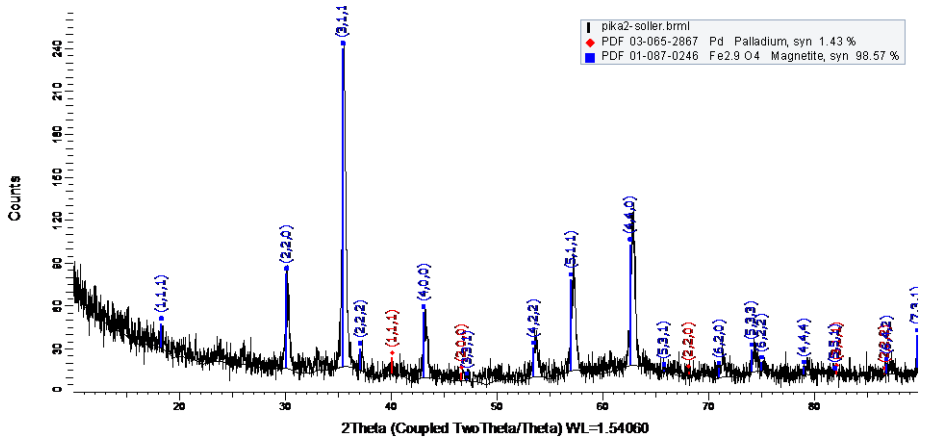

Figure I-2.5 XRD pattern of the Pd–Fe_3O_4 after the fifth reusing experiment

3. Conclusion

In summary, a convenient, heterogeneous, Wacker-type oxidation of alkynes to benzils under aerobic conditions using 1 mol% of Pd–Fe_3O_4 nanocatalyst was developed. This transformation showed high efficiency with a variety of substrates and excellent functional group tolerance. Moreover, owing to its magnetic property, the catalyst could be conveniently recovered using an external permanent magnet, obviating the need for filtration before reuse. The nanocatalyst was recycled five times without loss of its catalytic activity. Further studies to understand the detailed reaction mechanism and exact reacting species of the Pd–Fe_3O_4 catalyst system are in progress. Under the optimized reaction conditions, high yields, good functional group tolerance, and efficient recyclability of the Pd–Fe_3O_4 nanocrystals indicate that this system exhibits great applicability for large scale applications. Further research into various Pd–Fe_3O_4-catalyzed reactions is currently under progress in our laboratory.

4. Experimental

General

All commercially available chemicals were purchased from Aldrich Chemical Co. or Tokyo Chemical Industry Co. and used without further purification unless otherwise noted. All reaction products were identified through comparison with the authentic compounds and quantified through GC analysis using a Hewlett Packard 5890 Gas Chromatograph with mesitylene as an internal standard. All Transmission Electron Microscopy (TEM) images were obtained on a JEOL EM-2010 microscope at an accelerating voltage of 200 kV. The powder X-ray diffraction (XRD) was performed using a Bruker AXS D8 FOCUS (2 theta : 5-100, scanspeed : 2degree/min, Cu Kαradiation: λ=1.54056nm, Generator : 40kV, 40m)

Synthesis of substrates (General Procedure for the Sonogashira Reaction)

An oven-dried Schlenk flask equipped with a magnetic stirring bar was charged with Bu4NOAc (1.5 mmol) and $Pd(OAc)_2$ (1-3 mol%) or $Pd_2(dba)_3$ (2 mol % for aryl bromides) inside a nitrogen-filled flask. The flask was capped with a rubber septum, and then it was removed from the glove box. An aryl iodide or bromide (1.0 mmol) and DMF (3.0 mL) were then successively added, and after 5 min of stirring, the alkyne (1.0 mmol) was added. Stirring was continued at room temperature under argon for the corresponding reaction times indicated in the tables, after which time the reaction mixture was diluted

with water (10 mL) and extracted with diethyl ether (4x10 mL). The combined ether layers were dried over Na_2SO_4, filtered, concentrated, and purified through alumina gel flash chromatography using hexanes or hexanes/ether to elute the desired coupling product.

General procedure for Wacker-type oxidation

Pd–Fe_3O_4 nanocrystal catalyst (1.0 mmol) in 1,4-dioxane (5.0 mL) was put to a vial. Phenylacetylene (1 mmol), $CuBr_2$ (0.1 mmol) and H_2O (1 mL) were added to the mixture and an O_2 balloon was attached to the sealed vial. The vial was sonicated for 3 minute for dispersion of the catalyst and the reaction mixture was stirred for 28 h at 95 ºC. After the reaction mixture was cooled to room temperature, the catalyst was separated from the mixture through the use of an external magnet. The solution containing the product was diluted with EtOAc (15 mL) and H_2O (15 mL) and extracted with EtOAc (3x15 mL).And dried over anhydrous $MgSO_4$, filtered, and concentrated in vacuo. The residue was purified by silica-gel column chromatography using n-hexane/EtOAc as an eluent.

General procedure for recycling

After the reaction was complete, 1,4-dioxane (5 mL) was added and the mixture was sonicated 3 min for dispersion. Then the Pd–Fe3O4 catalyst was separated with the use of an external magnet. The recovered catalyst was washed five times with EtOAc (20 mL), twice with water H_2O (20 mL) and dried in vacuo.

Synthesis of Pd–Fe_3O_4 heterodimer nanocrystals.

The Pd–Fe_3O_4 synthesis was performed by two-step thermal decomposition of a mixture solution composed of iron acetate, palladium acetate, oleic acid and oleylamine. In a general synthesis, 10 mg of $Pd(acac)_2$ (0.033 mmol) and 0.7 g of $Fe(acac)_3$ (2.00 mmol) was added into a solution 4.0 mL of containing oleic acid (12.5 mmol) and 6.0 mL of oleylamine (17.5 mmol) and the mixture was heated to 120 ^oC in a vacuum with vigorous stirring for 3 h. Under Ar atmosphere, the dark mixture was heated to 220 ^oC at a heating rate of 2 ^oC /min and kept at this temperature for 30 min, and then it was further heated to 300 ^oC at the same heating rate and aged at 300 ^oC for 30 min. After cooling 3h, the mixture solution was precipitated by adding EtOH and 140 mg of the powdery Pd–Fe_3O_4 were obtained after the washing and vacuum drying processes. The nanocrystals were dispersible in many organic solvents such as chloroform and hexane.

Part I.

Chapter 3. Mechanistic studies on the organic reactions catalyzed by Pd–Fe_3O_4 heterodimeric nanocrystals[*]

[*]Part of this thesis was published in *Chem. Asian J*. **2015**, *80(9)*, 982-988.

1. Introduction

In organic synthesis, Pd is one of the most useful metal catalysts for various C–C bond-forming reactions and functional group transformations. Notably, the chemists who contributed to the development of the C–C bond cross-coupling reactions using Pd catalysts, such as the Heck, Suzuki, and Negishi reactions, won the Nobel Prize in Chemistry in 2010.[34] Many other related cross-coupling reactions have been developed apart from these three representative name reactions. Moreover, the Pd-catalyzed mechanisms have been utilized for many other reactions such as oxidation and reduction.[35] Pd-catalyzed organic reactions have also been well documented in many reviews and books.[36]

Despite the importance and wide application of Pd-catalyzed reactions, the use of soluble Pd catalysts poses significant problems, including the toxicity caused by residual Pd, safety issues because of the instability of Pd in air, and high costs attributed to the scarcity of the metal, thus hindering their industrial applications.[37] Some researchers developed palladium free coupling reactions to conquer these problems in case of Sonogashira coupling.[38] So, to overcome these drawbacks, heterogeneous Pd catalysts have been investigated.[39] Heterogeneous catalytic processes usually employ biphasic systems or immobilization on supports. For biphasic systems, separable ionic liquids[40] or phase-transfer methods have been used.[41] In the case of immobilization, materials such as carbon nanotubes, graphene, high-surface-area solids (silicates, zeolites, alumina, etc.), polymers, and metal oxides have been reported as metal supports.[42] Heterogeneous catalysts have several advantages such as lower amount of metallic residues in products, recyclable/reusable catalytic system, and easy handling and recovery with enhanced safety.

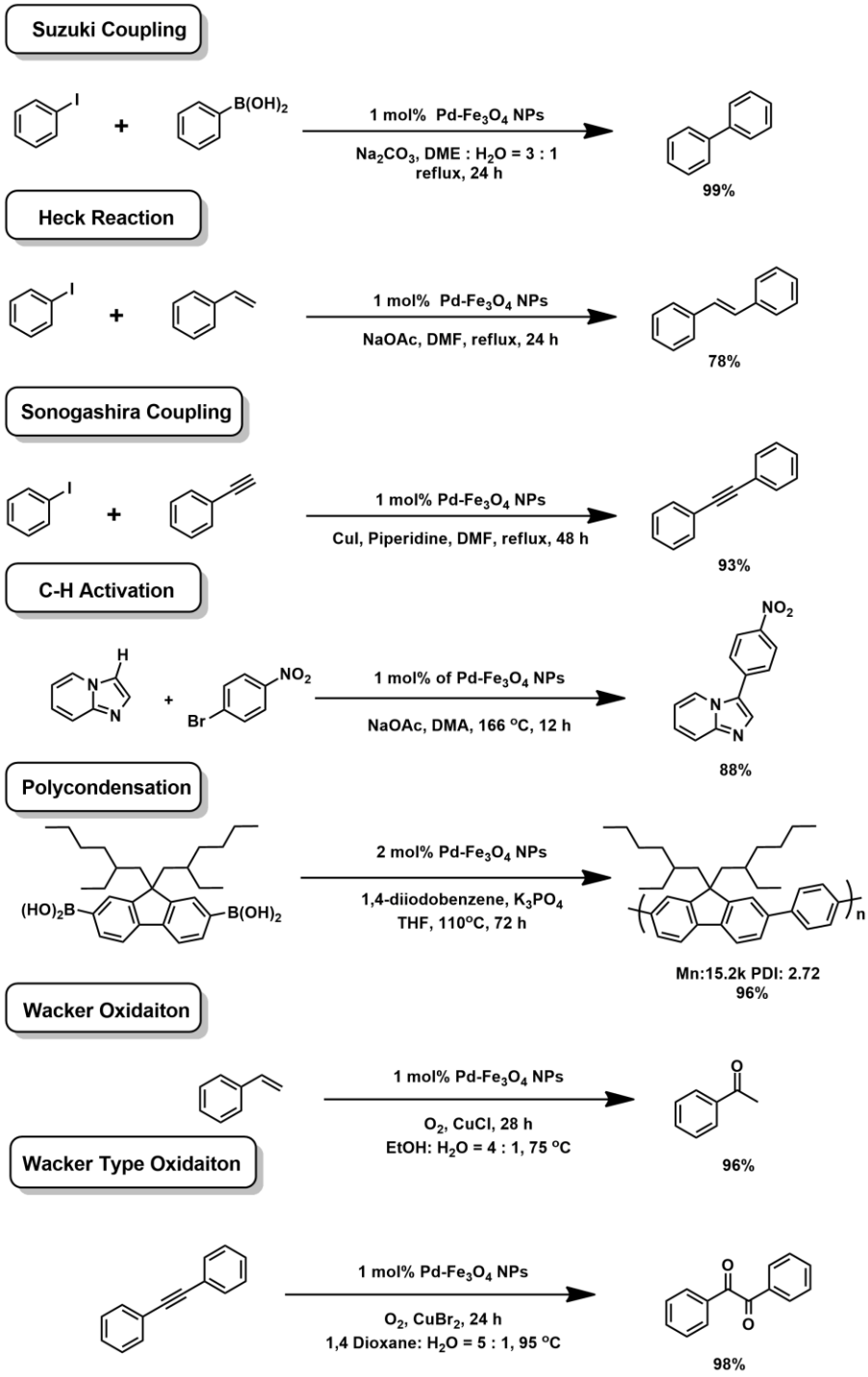

Scheme I-3.1. Different applications of heterodimeric Pd–Fe_3O_4 nanocratalyst

These advantages make heterogeneous catalysts suitable for bulk synthesis in industrial applications. Particularly, the existence of metal residues in products poses a serious problem in the pharmaceutical industry.

However, reactions that use heterogeneous catalysts often have lower selectivity and catalytic activity than those using homogeneous catalysts. Consequently, reactions employing heterogeneous catalyst systems often require harsher conditions or are limited to a narrow substrate scope. Therefore, new types of catalysts should be developed to maximize the benefits of both homogeneous and heterogeneous reactions and to minimize their disadvantages. To achieve this goal, increased attention has been focused to nanocrystals as catalysts.[43] Nanocrystals have a high surface area per volume and good dispersity, leading to high catalytic activity similar to that of homogeneous catalysts. Furthermore, the handling of nanocrystals is similar to that of heterogeneous catalysts. Because of these characteristics, nanocrystal catalysts are considered semi-heterogeneous catalysts with desirable attributes of both the systems, i.e., the efficiency of homogeneous reactions and the recyclability of heterogeneous materials. Therefore, nanocrystal catalysts have attracted much interest, and a large number of studies have been reported in the last decade.[44],[45]

Recently, hybrid nanocrystals containing two or more metals have attracted much attention; the synthesis and applications of such hybrid metal nanoparticles have been reported.[46] The properties of individual metal nanocrystals can be exploited in hybrid nanocrystals, possibly leading to synergistic and enhanced properties. Among them, heterodimeric nanocrystals have been synthesized from transition metals and metal oxides and used for multifunctional applications including biomedical sensing and catalytic

reactions.[47]

We reported a simple synthesis of Pd–Fe_3O_4 heterodimer nanocrystals by controlled one-pot thermal decomposition of metal acetylacetonate mixtures (**Figure I-3.1**).[9] The nascent nanocrystals were easily recovered using an external magnet without filtration or centrifugation. Using the magnetic heterodimeric nanoparticles, we reported several catalytic applications of Pd–Fe_3O_4 heterodimeric nanocrystals, e.g., Suzuki cross-coupling reaction[9(a)] Heck reaction, Sonogashira reaction,[48] direct catalytic C–H arylation,[49] polycondensation,[50] Wacker oxidation, and Wacker-type triple bond oxidation[51] (**Scheme I-3.1**). In almost all these reactions, the Pd–Fe_3O_4 heterodimeric nanocrystals exhibited consistently effective catalytic activities, even in the absence of ligands. This efficient and reusable nanocrystal catalyst system paves a way to green chemistry, with great potential for industrial applications.

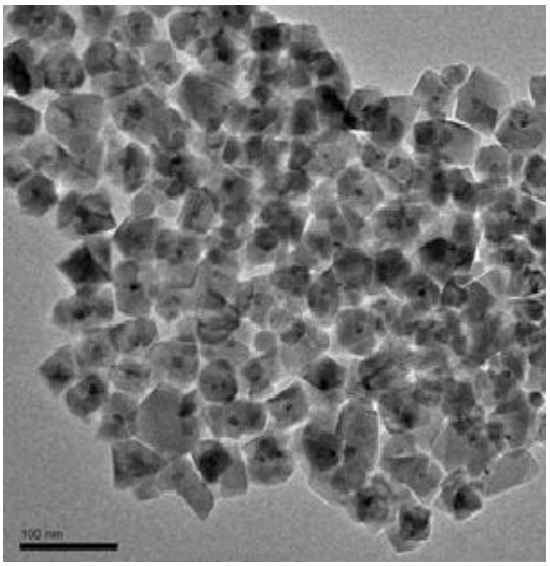

Figure 1-3.1 TEM image of heterodimeric Pd–Fe_3O_4 nanoparticles

While studying various reactions using magnetic Pd–Fe_3O_4 nanoparticles, we were intrigued by the true catalytic species involved in the so-called "heterogeneous" reactions. Are these reactions truly heterogeneous? Or is there a small amount of soluble Pd species released in each recycling experiment that is responsible for the iterative reactions? To answer these questions, detailed mechanistic investigations were carried out using previously reported experimental methods for elucidating the mechanism of heterogeneous catalytic reactions. [52] Use of Pd/C as a heterogeneous catalyst system that leaches out soluble Pd species has been well documented, however, it has been difficult to reuse the Pd/C system as a recyclable catalyst.[53] In this part III, we report our findings on the mechanism of the Pd–Fe_3O_4 nanoparticle-catalyzed Suzuki coupling reactions, based on experiments such as kinetics studies, hot filtration tests, and three-phase tests.

2. Results and Discussion

For mechanistic studies on the reactions using the magnetically recoverable Pd–Fe_3O_4 nanoparticle catalysts, two representative reactions were selected: Suzuki coupling and Wacker oxidation. Previously, we reported a series of representative cross-coupling reactions based on the catalytic activity of the Pd–Fe_3O_4 heterodimer nanocrystals. It was found that the Pd–Fe_3O_4 heterodimer nanocrystals have excellent catalytic activity for the Suzuki coupling reactions of arylboronic acids with various aryl iodides, even though the catalyst showed slightly lower activity towards less activated aryl bromides. After the completion of the Suzuki reaction of phenylboronic acid with iodobenzene, the Pd–Fe_3O_4 heterodimer nanocrystals could be easily separated from the reaction mixture using an external magnet, and the recovered nanocrystal catalyst could be recycled for >10 times without any

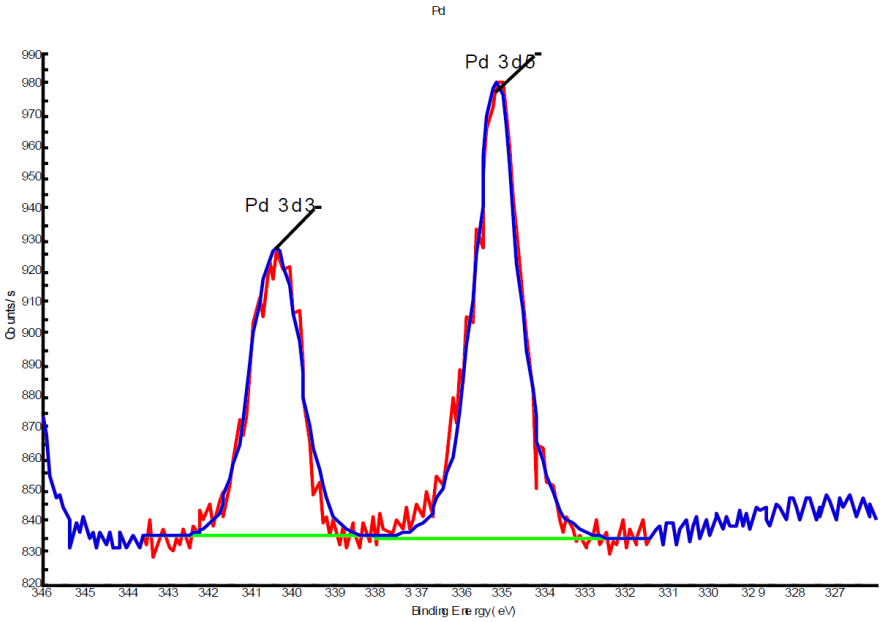

Figure I-3.2 XPS spectroscopy of fresh Pd–Fe_3O_4

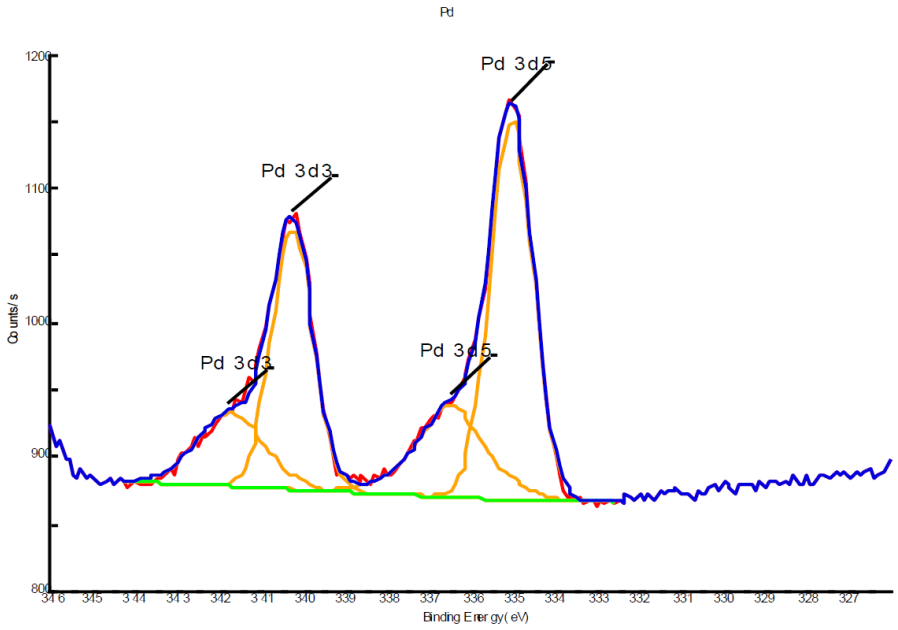

Figure I-3.3 XPS spectroscopy of spent Pd–Fe_3O_4

significant loss of the catalytic activity. Successful Wacker oxidation was also carried out through the iterative use of the Pd–Fe_3O_4 nanocrystal catalyst.[19] The Pd–Fe_3O_4 nanocrystal catalyst recovered using an external magnet retained catalytic activity for four times. At the end of the recycling runs, the transmission electron microscope (TEM) images, powder X-ray diffraction (XRD) patterns, and inductively coupled plasma atomic emission spectra (ICP-AES) of the Pd–Fe_3O_4 heterodimer nanocrystals were compared to those before the recycling. No significant morphological change was observed compared to those of the original catalyst. However, these morphological results cannot be considered as significantly contributing to the understanding of the mechanism of Pd–Fe_3O_4 nanocrystal catalysis. Also, the X-ray photoelectron spectroscopy (XPS) of the fresh and spent Pd–Fe_3O_4 were taken to see the change in the oxidation states of the Pd metal. The oxidation state of fresh catalyst was confirmed to be Pd(0) (**Figure I-3.2**). After the Suzuki reaction was complete, however, the XPS data indicated the presence of some Pd(II), as well as Pd(0) species (**Figure I-3.3**).

Kinetic Experiments

To gain insight into the mechanism of the reaction, kinetics of the Suzuki reaction and Wacker oxidation were studied using Pd–Fe_3O_4. Kinetic studies are very valuable for checking the presence of a precatalyst, which is characterized by a typical induction period in the catalytic reaction. The reaction rates of the Pd–Fe_3O_4 nanocrystal-catalyzed Suzuki coupling and Wacker oxidation reactions showed sigmoidal kinetic patterns in both the reactions. The substrate and product distributions were measured every hour by gas chromatography (GC). As shown in **Figure I-3.4**, a clear induction period

(1 and 2 h for Suzuki and Wacker oxidation reactions, respectively) was confirmed when the Pd–Fe_3O_4 nanocrystals were used. This observation strongly suggests that the Pd–Fe_3O_4 catalysis needs some time to generate an "active" catalytic species in the reaction mixture as a presumably homogeneous Pd species.[54] The soluble Pd species may dissolve out from the nanocrystals at high reaction temperatures.

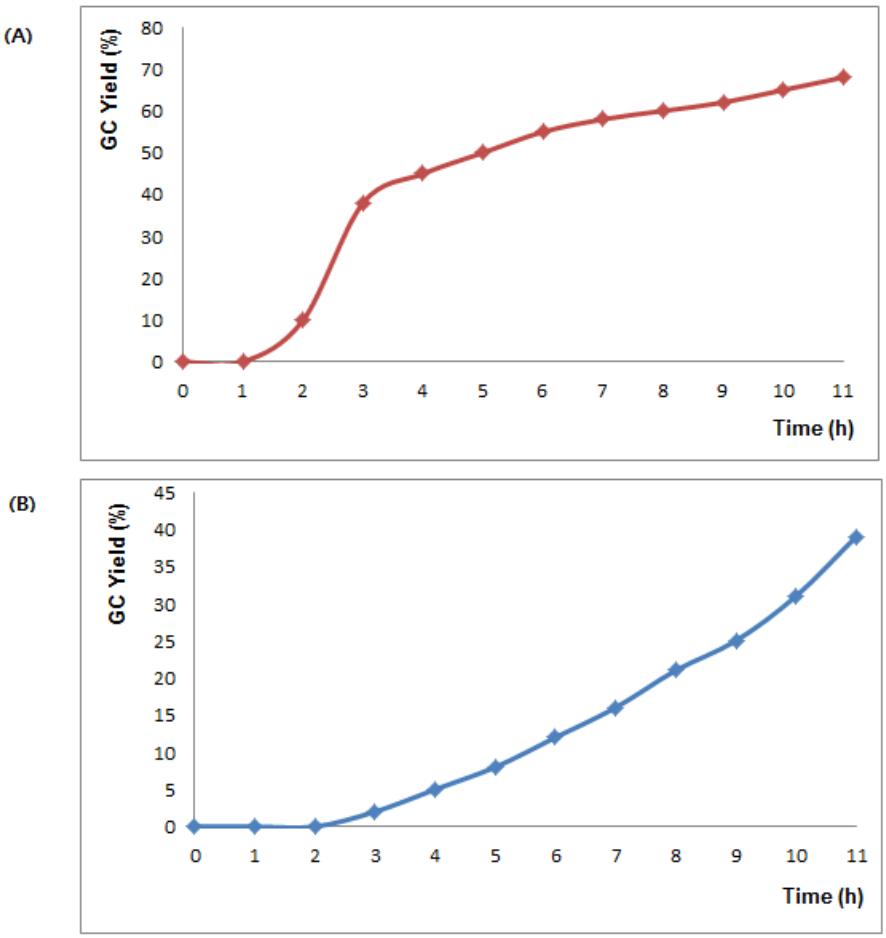

Figure I-3.4 Kinetics of Pd–Fe_3O_4 nanocrystal-catalyzed reactions. (A) Suzuki coupling reaction. (B) Wacker oxidation reaction

Hot Filtration Tests

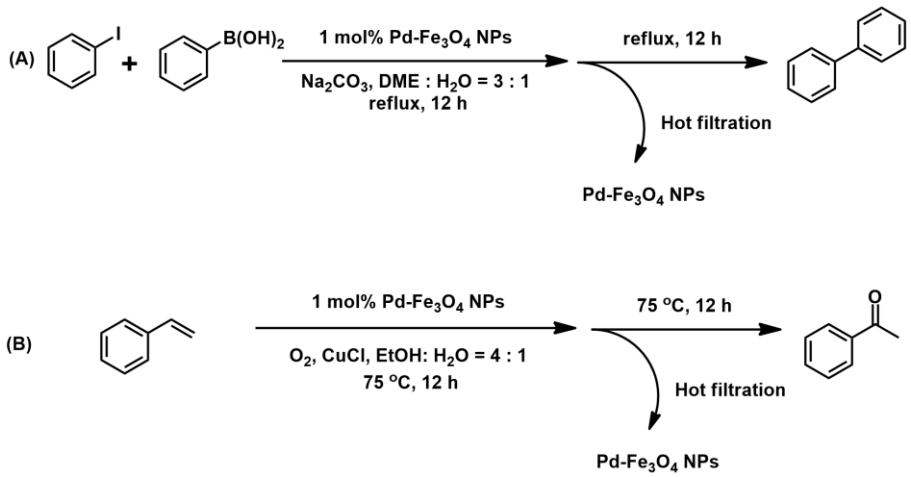

Scheme I-3.2 Hot filtration tests (A) Suzuki coupling reaction using Pd–Fe_3O_4 (B) Wacker oxidation reaction using Pd–Fe_3O_4.

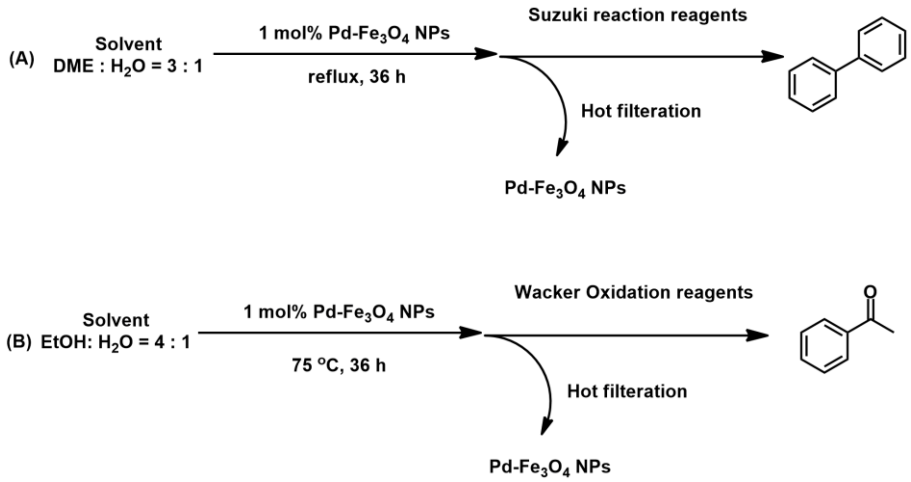

Scheme I-3.3 Blank tests (A) Suzuki coupling reaction using Pd–Fe_3O_4 (B) Wacker oxidation reaction using Pd–Fe_3O_4.

To further understand the leaching-out phenomenon, "hot filtration" tests[55] for both Suzuki and Wacker oxidation reactions were carried out (**Scheme I-3.2**). The Pd–Fe_3O_4 nanocrystals were collected at the bottom of the flask using

a neodymium magnet, and the supernatant solution was separated while the solution was hot. During the process, the high temperature was maintained. The catalytic activity of the obtained solution was then tested; if the remaining substrates converted to products, the yield was measured by GC. If the reaction occurred only at the surface of the nanocrystals, the supernatant solution would not show any catalytic activity. Conversely, if any soluble catalytic Pd species released from the nanocrystals remained in the solution phase, then the reaction would proceed in the obtained solution.

In the Wacker oxidation reaction, 20% additional conversion was observed. In the Suzuki coupling reaction, 7% additional conversion was observed. To observe the soluble Pd species in the solution in more detail, a blank hot filtration test was performed by heating a mixture of the Pd–Fe_3O_4 nanocrystal catalyst in a solvent for 36 h. While the flask was hot, the Pd–Fe_3O_4 catalyst and magnetic stir bar were removed using an external magnet. Then, the reagents for Suzuki or Wacker oxidation reaction were introduced along with a new stir bar (**Scheme I-3.3**). After 36 h, the Wacker product was obtained in 40% GC yield while the Suzuki product was obtained in 10% GC yield. The results indicate that the presence of a homogeneous Pd species in the solution phase was at least partially responsible for the observed reactivities. The difference between the two reactions can be attributed to the difference in the amounts of leached Pd under different reaction conditions; i.e., in the Wacker oxidation reaction conditions, more Pd was released from the nanocrystals, resulting in more conversion. When the palladium contents in the solution from the spent Pd–Fe_3O_4 nanocatalyst from the Suzuki and Wacker oxidation were measured using ICP–AES, 0.3 and 4.9 ppm of palladium, respectively, were detected. The result of the hot filtration test strongly alludes to the fact that the catalysis was carried out by dissolved Pd that leached into the solution from the

nanocrystals.

Three-Phase Tests

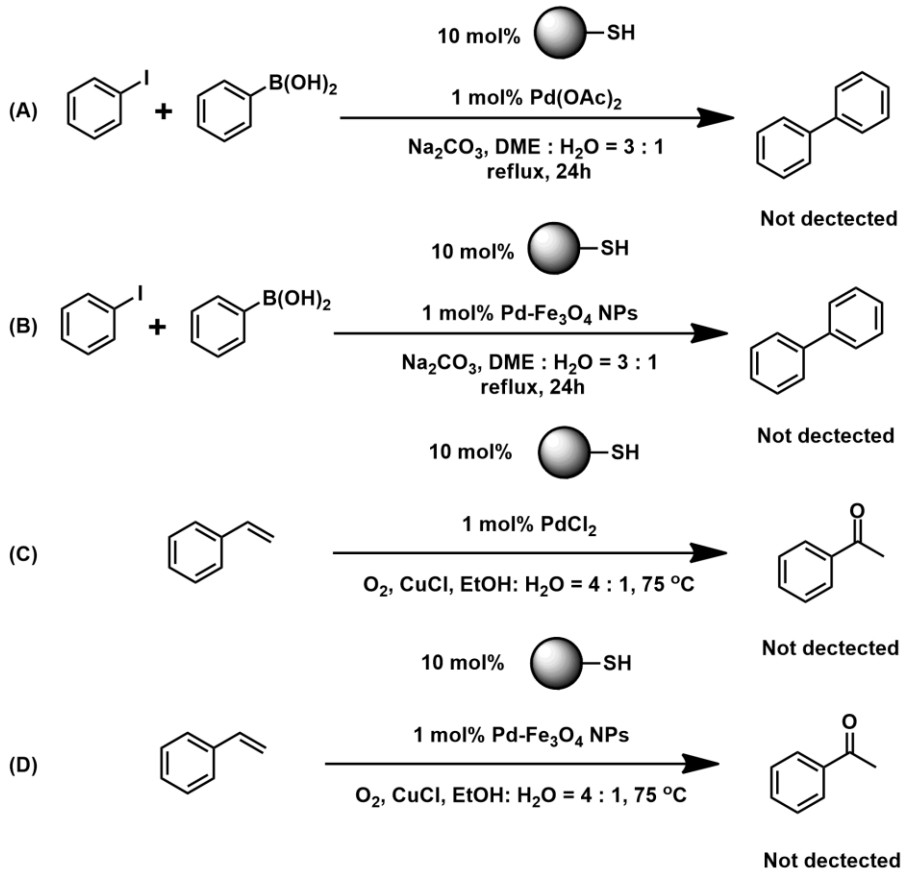

Scheme I-3.4 Three-phase tests. (A) Suzuki coupling reaction using homogeneous Pd sources. (B) Suzuki coupling reaction using Pd–Fe_3O_4. (C) Wacker oxidation using homogeneous Pd sources. (D) Wacker oxidation using Pd–Fe_3O_4.

To further determine the true catalyst species for the Pd–Fe_3O_4-catalyzed reactions, a three-phase test was designed to capture the homogeneous soluble Pd species using polymer-supported thiol as the immobilized scavenger.[56] Thus,

Suzuki and Wacker oxidation reactions were carried out in the presence of a thiol resin, polymer-bound 2-mercaptoethylamine (Aldrich No. 641022), as a transition-metal scavenger. For the three-phase test, both homogeneous and heterogeneous reactions using $PdCl_2$ and Pd–Fe_3O_4 nanocrystals, respectively, were carried out (**Scheme I-3.4**). Neither Suzuki nor Wacker oxidation product was detected by GC analysis. The results indicate that the Pd–Fe_3O_4 nanocrystals lost their reactivity in the presence of a scavenger similar to the reactions using $PdCl_2$. The soluble, active Pd source was trapped by the polymer-supported thiol resin, yielding neither Suzuki nor Wacker reaction products. The results also strongly indicate that the Pd–Fe_3O_4 nanocrystal-catalyzed reactions proceed because of the dissolved Pd species from the nanocrystals.

Proposed Mechanism of Pd–Fe_3O_4 Nanocrystal Catalysis

Careful studies have been carried out to delineate putative mechanism of palladium nanoparticle-catalyzed reactions. Results of our mechanistic studies such as kinetic experiments, hot filtration tests, and three-phase tests also corroborate the previously suggested leaching mechanism of Pd nanoparticles. After examining all the experimental data obtained so far, we suggest a reaction mechanism that incorporates a soluble Pd species as the true catalyst as shown in **Figure I-3.5**. The details of soluble Pd species in the solvent are still not clear. However, clearly a small amount of homogeneous Pd species leached into the solution phase on heating the reaction mixture. Once a soluble Pd species enters the solution phase, the standard catalytic cycle of the Suzuki cross-coupling reaction would be operative. The fact that the reaction does not proceed upon the addition of a polymer-supported thiol scavenger strongly

suggests that the true catalyst of the reaction is a soluble Pd species rather than a heterogeneous Pd catalyst. Thus, it can be concluded that the reactions are catalyzed by the soluble Pd species in the homogeneous phase originating from the Pd–Fe_3O_4 nanocrystals.

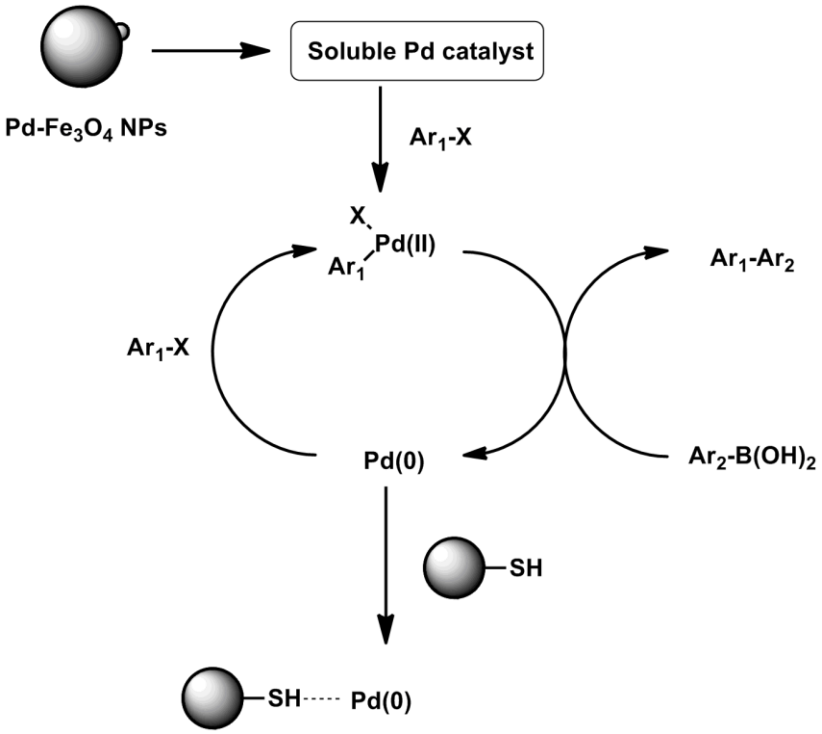

Figure I-3.5 Probable Suzuki reaction mechanism showing the generation of a homogeneous active catalyst.

3. Conclusion

In summary, the Pd–Fe_3O_4 heterodimeric nanocrystal catalytic system has several advantages over the conventional homogeneous and heterogeneous systems including good catalytic activity, reusability, and safe handling of the catalyst. Previously, we have demonstrated several catalytic applications of the Pd–Fe_3O_4 heterodimeric nanocrystals as magnetically separable catalysts. We successfully applied the nanocrystals as catalysts, often in the absence of ligands, to various organic reactions such as Suzuki, Heck, and Sonogashira coupling reactions, direct C–H arylation, and Wacker oxidation. However, it was not clear whether these processes involved a homogeneous or heterogeneous mechanism. Therefore, a systematic investigation was carried out using various approaches for identifying the true catalyst of the Pd–Fe_3O_4 nanocrystal-catalyzed reactions. General kinetic studies, hot filtration tests, and three-phase tests were carried out for Suzuki coupling and Wacker oxidation reactions. It was evident from the experimental results that a small amount of leached soluble Pd species was the true catalyst. The fact that the nanocrystal catalyst system provides an efficient and eco-friendly synthetic method for Pd-catalyzed reactions indicates that the Pd–Fe_3O_4 heterodimeric nanocrystals act as a good reservoir for supplying a small amount of soluble Pd species upon heating the reaction mixture. This heterogeneous catalyst system has great potential to further the development of greener synthetic methods for diverse applications that are not only restricted to laboratory, but can also be applied to large-scale synthesis.

4. Experimental

General

All commercially available chemicals were purchased from Aldrich Chemical Co. and used as received without further purification unless otherwise noted. All the reaction products were identified by comparing the data with those of the authentic compounds and quantified by GC using a Hewlett Packard 5890 Gas Chromatograph with mesitylene as the internal standard.

General procedure for Suzuki coupling

Degassed solvent (1,2-dimethoxyethane DME:H_2O = 3 mL:1 mL), iodobenzene (1.0 mmol), phenylboronic acid (1.2 mmol), Na_2CO_3 (1.3 mmol), mesitylene (1.0 mmol) as the internal standard, and the Pd–Fe_3O_4 nanocrystal catalyst (1.0 mol%) were added to a round-bottom flask and backfilled with argon. The reaction mixture was refluxed for 24 h under vigorous stirring. The yield was determined by GC analysis.

General procedure for Wacker oxidation

The Pd–Fe_3O_4 nanocrystal catalyst (1.0 mol%), styrene (1 mmol), CuCl (0.1 mmol), mesitylene (1.0 mmol) as the internal standard, and solvent (EtOH:H_2O = 3 mL:0.75 mL) were added to a vial, and an O_2 balloon was attached to the vial. The vial was sonicated for 3 min for the dispersion of the Pd–Fe_3O_4 nanocrystal catalyst, and the reaction mixture was stirred at 75 °C for 36 h. The

yield was determined by GC analysis.

Typical procedure for hot filtration test for Suzuki coupling

Degassed solvent (DME:H_2O = 3 mL:1 mL), iodobenzene (1.0 mmol), phenylboronic acid (1.2 mmol), Na2CO3 (1.3 mmol), mesitylene (1.0 mmol) as the internal standard, and the Pd–Fe_3O_4 nanocrystal catalyst (1.0 mol%) were added to a round-bottom flask and backfilled with argon. The reaction mixture was refluxed for 12 h under vigorous stirring. Then, while the flask was hot, the Pd–Fe_3O_4 nanocrystal catalyst and magnetic stir bar were removed using an external magnet. A new stir bar was added, and the reaction was allowed to proceed for 12 h more.

Typical procedure for hot filtration test for Wacker oxidation

The Pd–Fe_3O_4 nanocrystal catalyst (1.0 mol%), styrene (1 mmol), CuCl (0.1 mmol), mesitylene (1.0 mmol) as the internal standard, and solvent (EtOH : H_2O = 3 mL:0.75 mL) were added to a vial, and an O_2 balloon was attached to the vial. The vial was sonicated for 3 min for the dispersion of the Pd–Fe_3O_4 nanocrystal catalyst, and the reaction mixture was stirred at 75 °C for 12 h. Then, while the vial was hot, the Pd–Fe_3O_4 nanocrystal catalyst and magnetic stir bar were removed using an external magnet. Another stir bar was added, and the reaction was allowed to proceed for 12 h more.

Typical procedure for blank and hot filtration tests for Suzuki coupling

Degassed solvent (DME:H_2O = 3 mL:1 mL) and the Pd–Fe_3O_4 nanocrystal catalyst (1.0 mol%) were added to a round-bottom flask and backfilled with argon. The reaction mixture was refluxed for 36 h under vigorous stirring. Then, while the flask was hot, the Pd–Fe_3O_4 nanocrystal catalyst and magnetic stir bar were removed using an external magnet. A new stir bar, iodobenzene (1.0 mmol), phenylboronic acid (1.2 mmol), Na_2CO_3 (1.3 mmol), and mesitylene (1.0 mmol) as the internal standard were added, and the reaction was allowed to proceed for 36 h more.

Typical procedure for blank and hot filtration tests for Wacker oxidation

The Pd–Fe_3O_4 nanocrystal catalyst (1.0 mol%) and solvent (EtOH:H_2O = 3 mL:0.75 mL) were added to a vial, and an O_2 balloon was attached to the vial. The vial was sonicated for 3 min for the dispersion of the Pd–Fe_3O_4 nanocrystal catalyst, and the reaction mixture was stirred at 75 °C for 36 h. Then, while the vial was hot, the Pd–Fe_3O_4 nanocrystal catalyst and magnetic stir bar were removed using an external magnet. A new stir bar, styrene (1 mmol), CuCl (0.1 mmol), and mesitylene (1.0 mmol) as the internal standard were added, and the reaction was allowed to proceed for 36 h more.

Typical procedure for three-phase tests for Suzuki coupling

Degassed solvent (DME:H_2O = 3 mL:1 mL), iodobenzene (1.0 mmol), phenylboronic acid (1.2 mmol), Na_2CO_3 (1.3 mmol), mesitylene (1.0 mmol) as the internal standard, a polymer-bound resin (2-mercaptoethylamine, Aldrich No. 641022) (0.1 mmol), and the Pd–Fe_3O_4 nanocrystal catalyst (1.0 mol%)

were added to a round-bottom flask and backfilled with argon. The reaction mixture was refluxed for 24 h under vigorous stirring. The yield was determined by GC analysis.

Typical procedure for three-phase tests for Wacker oxidation

The Pd–Fe_3O_4 nanocrystal catalyst (1.0 mol%), styrene (1 mmol), CuCl (0.1 mmol) mesitylene (1.0 mmol) as the internal standard, a polymer-bound resin (2-mercaptoethylamine, Aldrich No. 641022) (0.1 mmol), and solvent (EtOH:H_2O = 3 mL:0.75 mL) were added to a vial, and an O_2 balloon was attached to the vial. The vial was sonicated for 3 min for the dispersion of the Pd–Fe_3O_4 nanocrystal catalyst, and the reaction mixture was stirred at 75 °C for 36 h. The yield was determined by GC analysis.

Reference of part I

(1) (a) J. Smidt, W. Hafner, R. Jira, J. Sedlmeier, R. Sieber, R. Rüttinger and H. Kojer, *Angew. Chem.*, 1959, **71**, 176-182; (b) J. Smidt, W. Hafner, R. Jira, R. Sieber, J. Sedlmeier and A. Sabel, *Angew. Chem. Int. Ed.*, 1962, **1**, 80-88.

(2) (a) J. Takacs and X.-t. Jiang, *Curr. Org. Chem.*, 2003, **7**, 369-396; (b) C. N. Cornell and M. S. Sigman, *Inorg. Chem.*, 2007, **46**, 1903-1909. (c) J. Tsuji, *Synthesis*, 1984, 369. (d) J. Tsuji, *PalladiumReagents and Catalysts. Applications in Organic Synthesis*, Wiley, New York, 1995; P. M.Henry, in *Handbook of Organopalladium Chemistry for Organic Synthesis*, ed. E.-I. Negishi, Wiley Interscience, New York, 2002, vol. 2, pp. 2119-2140.

(3) (a) W. Hafner, R. Jira, J. Sedlmeier and J. Smidt, *Chem. Ber.*, 1962, **95**, 1575-1581.

(4) (a) J. E. Baeckvall, A. K. Awasthi and Z. D. Renko, *J. Am. Chem. Soc.*, 1987, **109**, 4750-4752; (b) J.-E. Baeckvall, R. B. Hopkins, H. Grennberg, M. Mader and A. K. Awasthi, *J. Am. Chem. Soc.*, 1990, **112**, 5160-5166; (c) Z.-Y. Wang, H.-F. Jiang, C.-R. Qi, Y.-G. Wang, Y.-S. Dong and H.-L. Liu, *Green Chemistry*, 2005, **7**, 582; (d) H. Ogawa, H. Fujinami, K. Taya and S. Teratani, *Bull. Chem. Soc. Jpn.*, 1984, **57**, 1908-1913; (e) S. N. Shelke, G. R. Mhaske, V. D. Bonifacio and M. B. Gawande, *Bioorg. Med. Chem. Lett.*, 2012, **22**, 5727-5730; (f) Y. Zhang and M. S. Sigman, *J. Am. Chem. Soc.*, 2007, **129**, 3076-3077.

(5) (a) H. Jiang, L. Jia and J. Li, *Green Chemistry*, 2000, **2**, 161-164; (b) V. V. Namboodiri, R. S. Varma, E. Sahle-Demessie and U. R. Pillai, *Green Chemistry*, 2002, **4**, 170-173; (c) A. Haimov and R. Neumann, *Chem. Commun.*, 2002, 876-877; (d) Z. Hou, B. Han, L. Gao, T. Jiang, Z. Liu, Y. Chang, X. Zhang and J. He, *New J. Chem.*, 2002, **26**, 1246-1248; (e) J.-Q. Wang, F. Cai, E. Wang and L.-N. He, *Green Chemistry*, 2007, **9**, 882; (f) I. A. Ansari, S. Joyasawal, M. K. Gupta, J. S. Yadav and R. Gree, *Tetrahedron Lett.*, 2005, **46**, 7507-7510; (g) C. Chiappe, A. Sanzone and P. J. Dyson, *Green Chemistry*, 2011, **13**, 1437-1441.

(6) (a) G.-J. T. Brink, I. W. C. E. Arends, G. Papadogianakis and R. A. Sheldon, *Chem. Commun.*, 1998, 2359-2360; (b) G.-J. T. Brink, I. W. C. E. Arends, G. Papadogianakis and R. A. Sheldon, *Applied Catalysis A: General*, 2000, **194-195**, 435-442; (c) K. Muniz, *Adv. Synth. Catal.*, 2004, **346**, 1425-1428; (d) T. Mitsudome, T. Umetani, N. Nosaka, K. Mori, T. Mizugaki, K. Ebitani and K. Kaneda, *Angew. Chem. Int. Ed.*, 2006, **45**, 481-485.

(7) (a) H.-G. Tang and D. C. Sherrington, *Polymer*, 1993, **34**, 2821-2829; (b) H. Tang, *J. Catal.*, 1993, **142**, 540-551; (c) J.-H. Ahn and D. C. Sherrington, *Macromolecules*, 1996, **29**, 4164-4165.

(8) (a) E. J. García-Suárez, A. M. Balu, M. Tristany, A. B. García, K. Philippot and R. Luque, *Green Chemistry*, 2012, **14**, 1434; (b) V. L. Budarin, J. H. Clark, R. Luque, D. J. Macquarrie and R. J. White, *Green Chemistry*, 2008, **10**, 382; (c) M. B. Gawande, R. K. Pandey and R. V. Jayaram, *Catalysis Science & Technology*, 2012, **2**, 1113; (d) C. Han, R. Luque and D.

D. Dionysiou, *Chem. Commun.*, 2012, **48**, 1860-1862; (e) S. N. Shelke, G. R. Mhaske, V. D. Bonifacio and M. B. Gawande, *Bioorg. Med. Chem. Lett.*, 2012, **22**, 5727-5730.; (f) M. B. Gawande, H. Guo, A. K. Rathi, P. S. Branco, Y. Chen, R. S. Varma and D.-L. Peng, *RSC Advances*, 2013, **3**, 1050; (g) M. B. Gawande, A. K. Rathi, P. S. Branco, I. D. Nogueira, A. Velhinho, J. J. Shrikhande, U. U. Indulkar, R. V. Jayaram, C. A. Ghumman, N. Bundaleski and O. M. Teodoro, *Chemistry*, 2012, **18**, 12628-12632; (h) M. B. Gawande, A. Velhinho, I. D. Nogueira, C. A. A. Ghumman, O. M. N. D. Teodoro and P. S. Branco, *RSC Advances*, 2012, **2**, 6144; (i) A. M. Balu, B. Baruwati, E. Serrano, J. Cot, J. Garcia-Martinez, R. S. Varma and R. Luque, *Green Chemistry*, 2011, **13**, 2750 (j) F. Rajabi, N. Karimi, M. R. Saidi, A. Primo, R. S. Varma and R. Luque, *Adv. Synth. Catal.*, 2012, **354**, 1707-1711.

(9) (a) Y. Jang, J. Chung, S. Kim, S. W. Jun, B. H. Kim, D. W. Lee, B. M. Kim and T. Hyeon, *Phys. Chem. Chem. Phys.*, 2011, **13**, 2512-2516; (b) Y. Jang, S. Kim, S. W. Jun, B. H. Kim, S. Hwang, I. K. Song, B. M. Kim and T. Hyeon, *Chem. Commun.*, 2011, **47**, 3601-3603.

(10) (a) J. Tsuji, H. Nagashima and K. Hori, *Chem. Lett.*, 1980, 257-260; (b) A. C. Bueno, Á. O. de Souza and E. V. Gusevskaya, *Adv. Synth. Catal.*, 2009, **351**, 2491-2495; (c) M. H. Xie, X. L. Yang and C. D. Wu, *Chem. Commun.*, 2011, **47**, 5521-5523; (d) D. G. Miller and D. D. M. Wayner, *J. Org. Chem*, 1990, **55**, 2924-2927.

(11) (a) L. Re, B. Maurer and G. Ohloff, *Helv. Chim. Acta*, 1973, **56**, 1882-1894; (b) M. D. Rozwadowska and M. Chrzanowska, *Tetrahedron*, 1985, **41**,

2885-2890; (c) W. Mahabusarakam, S. Deachathai, S. Phongpaichit, C. Jansakul and W. C. Taylor, *Phytochemistry*, 2004, **65**, 1185-1191.

(12) (a) M. D. Rozwadowska and M. Chrzanowska, *Tetrahedron*, 1985, **41**, 2885-2890; (b) M. R. Angelastro, S. Mehdi, J. P. Burkhart, N. P. Peet and P. Bey, *J. Med. Chem*, 1990, **33**, 11-13; (c) R. Maurya, R. Singh, M. Deepak, S. S. Handa, P. P. Yadav and P. K. Mishra, *Phytochemistry*, 2004, **65**, 915-920; (d) K. C. Nicolaou, D. L. Gray and J. Tae, *J. Am. Chem. Soc.*, 2004, **126**, 613-627; (e) R. M. Wadkins, J. L. Hyatt, X. Wei, K. J. Yoon, M. Wierdl, C. C. Edwards, C. L. Morton, J. C. Obenauer, K. Damodaran, P. Beroza, M. K. Danks and P. M. Potter, *J. Med. Chem*, 2005, **48**, 2906-2915.

(13) B. I. Ita and O. E. Offiong, *Mater. Chem. Phys, 2*001, **70**, 330-335.

(14) Matsushita Electric Industrial Co. Ltd. Jpn. Kokai Tokkyo Koho 1981, 203, 8198; *Chem. Abstr.*, 1981, **95**, 188163u.

(15) (a) T. Harada, Y. Nakagawa, R. M. Wadkins, P. M. Potter and C. E. Wheelock, *Bioorg. Med. Chem.*, 2009, **17**, 149-164; (b) C. D. Fleming, S. Bencharit, C. C. Edwards, J. L. Hyatt, L. Tsurkan, F. Bai, C. Fraga, C. L. Morton, E. L. Howard-Williams, P. M. Potter and M. R. Redinbo, *J. Mol. Biol.*, 2005, **352**, 165-177.

(16) (a) S. E. Wolkenberg, D. D. Wisnoski, W. H. Leister, Y. Wang, Z. Zhao and C. W. Lindsley, *Org. Lett.*, 2004, **6**, 1453-1456; (b) W. D. Shipe, F. Yang, Z. Zhao, S. E. Wolkenberg, M. B. Nolt and C. W. Lindsley, *Heterocycles*, 2006, **70**, 655; (c) X. Deng and N. S. Mani, *Org Lett*, 2006, **8**, 269-272; (d) H. Zipse, I. Held and S. Xu, *Synthesis*, 2007, **8** 1185-1196; (e) F. Rong, S.

Chow, S. Yan, G. Larson, Z. Hong and J. Wu, *Bioorg. Med. Chem. Lett.*, 2007, **17**, 1663-1666; (f) A. J. Herrera, M. Rondon and E. Suarez, *J. Org. Chem.*, 2008, **73**, 3384-3391; (g) G. R. Boyce and J. S. Johnson, *Angew. Chem. Int. Ed.* 2010, **49**, 8930-8933.

(17) (a) R. Sanz, M. P. Castroviejo, V. Guilarte, A. Perez and F. J. Fananas, *J. Org. Chem.*, 2007, **72**, 5113-5118; (b) J. J. Maresh, L. A. Giddings, A. Friedrich, E. A. Loris, S. Panjikar, B. L. Trout, J. Stockigt, B. Peters and S. E. O'Connor, *J. Am. Chem. Soc.*, 2008, **130**, 710-723; (c) T. Kashiwabara and M. Tanaka, *J. Org. Chem.*, 2009, **74**, 3958-3961.

(18) (a) M. Kirihara, Y. Ochiai, S. Takizawa, H. Takahata and H. Nemoto, *Chem. Commun.*, 1999, 1387-1388; (b) S. A. Tymonko, B. A. Nattier and R. S. Mohan, *Tetrahedron Lett.*, 1999, **40**, 7657-7659; (c) M. Okimoto, Y. Takahashi, Y. Nagata, G. Sasaki and K. Numata, *Synthesis*, 2005, **2005**, 705-707; (d) C. Joo, S. Kang, S. M. Kim, H. Han and J. W. Yang, *Tetrahedron Lett.*, 2010, **51**, 6006-6007.

(19) (a) J. Rodriguez, T. Constantieux and C. Allais, *Synthesis*, 2009, **2009**, 2523-2530; (b) N. Tada, M. Shomura, H. Nakayama, T. Miura and A. Itoh, *Synlett*, 2010, **2010**, 1979-1983; (c) M. Bouma, G. Masson and J. Zhu, *J. Org. Chem.*, 2010, **75**, 2748-2751; (d) R. Mossetti, T. Pirali, G. C. Tron and J. Zhu, *Org. Lett.*, 2010, **12**, 820-823.

(20) (a) A. R. Katritzky, D. Zhang and K. Kirichenko, *J. Org. Chem.*, 2005, **70**, 3271-3274; (b) S. Mori, M. Takubo, T. Yanase, T. Maegawa, Y. Monguchi and H. Sajiki, *Adv. Synth. Catal.*, 2010, **352**, 1630-1634; (c) Z.

Wan, C. D. Jones, D. Mitchell, J. Y. Pu and T. Y. Zhang, *J. Org. Chem.*, 2006, **71**, 826-828; (d) C. Mousset, O. Provot, A. Hamze, J. Bignon, J.-D. Brion and M. Alami, *Tetrahedron*, 2008, **64**, 4287-4294; (e) H. Fu, M. Niu, Y. Jiang and Y. Zhao, *Synthesis*, 2008, **2008**, 2879-2882; (f) K. J. Tan and U. Wille, *Chem. Commun.*, 2008, 6239-624; (g) M.-J. Wu, J.-H. Chu and Y.-J. Chen, *Synthesis*, 2009, **2009**, 2155-2162; (h) W. Ren, Y. Xia, S. J. Ji, Y. Zhang, X. Wan and J. Zhao, *Org Lett*, 2009, **11**, 1841-1844; (i) W. Ren, J. Liu, L. Chen and X. Wan, *Adv. Synth. Catal.*, 2010, **352**, 1424-1428.

(21) (a) H. Doucet and J. C. Hierso, *Angew. Chem. Int. Ed.*, 2007, **46**, 834-871; (b) R. Chinchilla and C. Najera, *Chem Rev.*, 2007, **107**, 874-922.

(22) (a) D. G. Lee and V. S. Chang, *Synthesis*, 1978, **1978**, 462-463; (b) N. S. Srinivasan and G. Lee Donald, *J. Org. Chem.*, 1979, **44**, 1574-1574; (c) D. G. Lee and V. S. Chang, *J. Org. Chem.*, 1979, **44**, 2726-2730.

(23) (a) H. Firouzabadi, A. R. Sardarian, H. Moosavipour and G. M. Afshari, *Synthesis*, 1986, **1986**, 285-288; (b) B. Rihter and J. Masnovi, *J. Chem. Soc., Chem. Commun.*, 1988, 35.

(24) V. O. Rogatchov, V. D. Filimonov and M. S. Yusubov, *Synthesis*, 2001, **2001**, 1001-1003.

(25) L. Re, B. Maurer and G. Ohloff, *Helv. Chim. Acta*, 1973, **56**, 1882-1894.

(26) (a) R. Curci, M. Fiorentino, C. Fusco, R. Mello, F. P. Ballistreri, S. Failla and G. A. Tomaselli, *Tetrahedron Lett.*, 1992, **33**, 7929-7932; (b) Z. F. Al-Rashid, W. L. Johnson, R. P. Hsung, Y. Wei, P. Y. Yao, R. Liu and K. Zhao, *J. Org. Chem.*, 2008, **73**, 8780-8784.

(27) H. Fu, M. Niu, Y. Jiang and Y. Zhao, *Synthesis*, 2008, **2008**, 2879-2882.

(28) G. Gebeyehu and E. McNelis, *J. Org. Chem.*, 1980, **45**, 4280-4283.

(29) A. Giraud, O. Provot, J.-F. Peyrat, M. Alami and J.-D. Brion, *Tetrahedron*, 2006, **62**, 7667-7673.

(30) (a) W. Ren, Y. Xia, S. J. Ji, Y. Zhang, X. Wan and J. Zhao, *Org. Lett.*, 2009, **11**, 1841-1844; (b) M. S. Yusubov, G. A. Zholobova, S. F. Vasilevsky, E. V. Tretyakov and D. W. Knight, *Tetrahedron*, 2002, **58**, 1607-1610; (c) A. Gao, F. Yang, J. Li and Y. Wu, *Tetrahedron*, 2012, **68**, 4950-4954.

(31) C. F. Xu, M. Xu, Y. X. Jia and C. Y. Li, *Org. Lett.*, 2011, **13**, 1556-1559.

(32) S. Mori, M. Takubo, T. Yanase, T. Maegawa, Y. Monguchi and H. Sajiki, *Adv. Synth. Catal.*, 2010, **352**, 1630-1634.

(33) (a) V. Polshettiwar, R. Luque, A. Fihri, H. Zhu, M. Bouhrara and J. M. Basset, *Chem. Rev.*, 2011, **111**, 3036-3075; (b) C. W. Lim and I. S. Lee, *Nano Today*, 2010, **5**, 412-434; (c) R. L. Oliveira, P. K. Kiyohara and L. M. Rossi, *Green Chem.*, 2010, **12**, 144-149; (d) X. B. Zhang, J. M. Yan, S. Han, H. Shioyama and Q. Xu, *J. Am. Chem. Soc.*, 2009, **131**, 2778-2779; (e) T. Hara, T. Kaneta, K. Mori, T. Mitsudome, T. Mizugaki, K. Ebitani and K. Kaneda, *Green Chem.*, 2007, **9**, 1246-1251; (f) V. Polshettiwar, B. Baruwati and R. S. Varma, *Green Chem.*, 2009, **11**, 127-131; (g) M. B. Gawande, H. Z. Guo, A. K. Rathi, P. S. Branco, Y. Z. Chen, R. S. Varma and D. L. Peng, *RSC Adv.*, 2013, **3**, 1050-1054; (h) M. B. Gawande, A. K. Rathi, P. S. Branco, I. D. Nogueira, A. Velhinho, J. J. Shrikhande, U. U. Indulkar, R. V. Jayaram,

C. A. Ghumman, N. Bundaleski and O. M. Teodoro, *Chem. Eur. J.*, 2012, **18**, 12628-12632; (i) V. Polshettiwar and R. S. Varma, *Org. Biomol. Chem.*, 2009, **7**, 37-40; (j) A. M. Balu, B. Baruwati, E. Serrano, J. Cot, J. Garcia-Martinez, R. S. Varma and R. Luque, *Green Chem.*, 2011, **13**, 2750-2758; (k) H. Yoon, S. Ko and J. Jang, *Chem. Commun.*, 2007, **43**, 1468-1470; (l) M. S. Kwon, I. S. Park, J. S. Jang, J. S. Lee and J. Park, *Org. Lett.*, 2007, **9**, 3417-3419; (m) K. Mori, Y. Kondo and H. Yamashita, *Phys. Chem. Chem. Phys.*, 2009, **11**, 8949-8954; (n) M. L. Kantam, J. Yadav, S. Laha, P. Srinivas, B. Sreedhar and F. Figueras, *J. Org. Chem*, 2009, **74**, 4608-4611; (o) Q. Du, W. Zhang, H. Ma, J. Zheng, B. Zhou and Y. Li, *Tettrahedron*, 2012, **68**, 3577-3584; (p) J. Zhang, Y. Wang, H. Ji, Y. Wei, N. Wu, B. Zuo and Q. Wang, *J. Catal.*, 2005, **229**, 114-118; (q) Y. W. Jun, J. S. Choi and J. Cheon, *Chem. Commun.*, 2007, 12031-1214; (r) S. C. Tsang, V. Caps, I. Paraskevas, D. Chadwick and D. Thompsett, *Angew. Chem. Int. Ed.*, 2004, **43**, 5645-5649; (s) J. Kim, J. E. Lee, J. Lee, Y. Jang, S. W. Kim, K. An, J. H. Yu and T. Hyeon, *Angew. Chem. Int. Ed.*, 2006, **45**, 4789-4793; (t) D. K. Yi, S. S. Lee and J. Y. Ying, *Chem. Mater.*, 2006, **18**, 2459-2461; (u) C. H. Jun, Y. J. Park, Y. R. Yeon, J. R. Choi, W. R. Lee, S. J. Ko and J. Cheon, *Chem. Commun.*, 2006, 1619-1621; (v) P. D. Stevens, J. Fan, H. M. Gardimalla, M. Yen and Y. Gao, *Org. Lett.*, 2005, **7**, 2085-2088; (w) D. Guin, B. Baruwati and S. V. Manorama, *Org. Lett.*, 2007, **9**, 1419-1421;

(34) (a) R. F. Heck, J. P. Nolley, *J. Org. Chem.* **1972**, *37*, 2320–2322; (b) H. A. Dieck, F. R. Heck, *J. Organomet. Chem.* **1975**, *93*, 259–263; (c) K.

Sonogashira, Y. Tohda, N. Hagihara, *Tetrahedron Lett.* **1975**, *16*, 4467–4470; (d) S. Baba, E. Negishi, *J. Am. Chem. Soc.* **1976**, *98*, 6729–6731; (e) D. Milstein, J. K. Stille; (f)*J. Am. Chem. Soc.* **1978**, *100*, 3636–3638; f) N. Miyaura, K. Yamada, A. Suzuki, *Tetrahedron Lett.* **1979**, *20*, 3437–3440; (g) A. S. Guram, S. L. Buchwald, *J. Am. Chem. Soc.* **1994**, *116*, 7901–7902.

(35) (a) J. Smidt, W. Hafner, R. Jira, J. Sedlmeier, R. Sieber, R. Rüttinger, H. Kojer, *Angew. Chem.* **1959**, *71*, 176–182; (b) S. S. Stahl, J. L. Thorman, R. C. Nelson, M. A. Kozee, *J. Am. Chem. Soc.* **2001**, *123*, 7188–7189; (c) H.-U. Blaser, C. Malan, B. Pugin, F. Spindler, H. Steiner, M. Studer, *Adv. Synth. Catal.* **2003**, *345*, 103–151; (d) B. A. Steinhoff, I. A. Guzei, S. S. Stahl, *J. Am. Chem. Soc.* **2004**, *126*, 11268–11278; (e) S. S. Stahl, *Science* **2005**, *309*, 1824–1826; (f) K. M. Gligorich, M. S. Sigman, *Chem. Commun.* **2009**, 3854–3867; (g) R. Jira, *Angew. Chem. Int. Ed.* **2009**, *48*, 9034–9037; (h) A. N. Campbell, S. S. Stahl, *Acc. Chem. Res.* **2012**, *45*, 851–863.

(36) (a) A. F. Littke, G. C. Fu, *Angew. Chem. Int. Ed.* **2002**, *41*, 4176-4211; (b) S. Kotha, K. Lahiri, D. Kashinath, *Tetrahedron* **2002**, *58*, 9633-9695; (c) K. C. Nicolaou, P. G. Bulger, D. Sarlah, *Angew. Chem. Int. Ed.* **2005**, *44*, 4442-4489; (d) T. W. Lyons, M. S. Sanford, *Chem. Rev.* **2010**, *110*, 1147-1169; (e) R. Chinchilla, C. Najera, *Chem. Rev.* **2007**, *107*, 874-922.

(37) D. Astruc, *Inorg. Chem.* **2007**, *46*, 1884–1894.

(38) (a) M. B. Thathagar, J. Beckers, G. Rothenberg, *Green Chem.* **2004**, *6*, 215-218; (b) R. K. Gujadhur, C. G. Bates, D. Venkataraman, *Org. Lett.* **2001**, *3*, 4315-4317; (c) S.-K. Kang, S.-K. Yoon, Y.-M. Kim, *Org. Lett.* **2001**,

3, 2697-2699; (d) S. Cacchi, G. Fabrizi, L. M. Parisi, *Org. Lett.* **2003**, *5*, 3843-3846; (e) I. P. Beletskaya, G. V. Latyshev, A. V. Tsvetkov, N. V. Lukashev, *Tetrahedron Lett.* **2003**, *44*, 5011-5013.

(39) (a) D. Y. Murzin, P. Mäki-Arvela, E. Toukoniitty, T. Salmi, *Catal. Rev.* **2005**, *47*, 175–256; (b) M. Seki, *Synthesis* **2006**, *2006*, 2975–2992; (c) L. Yin, J. Liebscher, *Chem. Rev.* **2007**, *107*, 133–173; (d) I. Beletskaya, V. Tyurin, *Molecules* **2010**, *15*, 4792–4814; (e) M. Lamblin, L. Nassar-Hardy, J.-C. Hierso, E. Fouquet, F.-X. Felpin, *Adv. Synth. Catal.* **2010**, *352*, 33–79.

(40) (a) H.-T. Wong, C. J. Pink, F. C. Ferreira, A. G. Livingston, *Green Chem.* **2006**, *8*, 373; (b) H. Hagiwara, K. H. Ko, T. Hoshi, T. Suzuki, *Chem. Commun.* **2007**, 2838–2840; (c) F. Li, C. Xia, *Tetrahedron Lett.* **2007**, *48*, 4845–4848; (d) Y. Zhang, X.-Y. Quek, L. Wu, Y. Guan, E. J. Hensen, *J. Mol. Catal. A: Chem.* **2013**, *379*, 53–58.

(41) (a) R. Abu-Reziq, D. Avnir, I. Miloslavski, H. Schumann, J. Blum, *J. Mol. Catal. A: Chem.* **2002**, *185*, 179–185; (b) D. Lee, H. Lee, S. Kim, C.-E. Yeom, B. M. Kim, *Adv. Synth. Catal.* **2006**, *348*, 1021–1024.

(42) (a) I. Fenger, C. Le Drian, *Tetrahedron Lett.* **1998**, *39*, 4287–4290; (b) K. Köhler, R. G. Heidenreich, J. G. E. Krauter, J. Pietsch, *Chem. Eur. J.* **2002**, *8*, 622–631; (c) M. Lysén, K. Köhler, *Synlett* **2005**, 1671–1674.

(43) (a) D. Astruc, F. Lu, J. R. Aranzaes, *Angew. Chem. Int. Ed.* **2005**, *44*, 7852–7872; (b) A. Fihri, M. Bouhrara, B. Nekoueishahraki, J. M. Basset, V. Polshettiwar, *Chem. Soc. Rev.* **2011**, *40*, 5181–5203.

(44) (a) V. Polshettiwar, R. Luque, A. Fihri, H. Zhu, M. Bouhrara, J. M.

Basset, *Chem. Rev.* **2011**, *111*, 3036–3075; (b) D. Wang, D. Astruc, *Chem. Rev.* **2014**, *114*, 6949-6985; (c) M. B. Gawande, P. S. Branco, R. S. Varma, *Chem. Soc. Rev.* **2013**, *42*, 3371-3393; (d)

(45) (a) M. B. Thathagar, J. E. ten Elshof, G. Rothenberg, *Angew. Chem. Int. Ed.* **2006**, *45*, 2886–2890; (b) V. R. Calderone, N. R. Shiju, D. Curulla-Ferre, S. Chambrey, A. Khodakov, A. Rose, J. Thiessen, A. Jess, G. Rothenberg, *Angew. Chem. Int. Ed.* **2013**, *52*, 4397-4401; b) R. Hudson, Y. Feng, R. S. Varma, A. Moores, *Green Chem.* **2014**, *16*, 4493-4505; (c) M. R. Nabid, Y. Bide, M. Niknezhad, *ChemCatChem* **2014**, *6*, 538-546; (d) A. J. Amali, B. Sharma, R. K. Rana, *Chem. Eur. J.* **2014**, *20*, 12239-12244.

(46) (a) H. Gu, R. Zheng, X. Zhang, B. Xu, *J. Am. Chem. Soc.* **2004**, *126*, 5664–5665; (b) A. Figuerola, A. Fiore, R. Di Corato, A. Falqui, C. Giannini, E. Micotti, A. Lascialfari, M. Corti, R. Cingolani, T. Pellegrino, P. D. Cozzoli, L. Manna, *J. Am. Chem. Soc.* **2008**, *130*, 1477–1487; (c) G. J. Hutchings, *Chem. Commun.* **2008**, 1148–1164.

(47) (a) H. Gu, Z. Yang, J. Gao, C. K. Chang, B. Xu, *J. Am. Chem. Soc.* **2005**, *127*, 34–35; (b) Y. Li, Q. Zhang, A. V. Nurmikko, S. Sun, *Nano Lett.* **2005**, *5*, 1689–1692; (c) H. Yu, M. Chen, P. M. Rice, S. X. Wang, R. L. White, S. Sun, *Nano Lett.* **2005**, *5*, 379–382;)d) S. H. Choi, H. B. Na, Y. I. Park, K. An, S. G. Kwon, Y. Jang, M. H. Park, J. Moon, J. S. Son, I. C. Song, W. K. Moon, T. Hyeon, *J. Am. Chem. Soc.* **2008**, *130*, 15573–15580.

(48) J. Chung, J. Kim, Y. Jang, S. Byun, T. Hyeon, B. M. Kim, *Tetrahedron Lett.* **2013**, *54*, 5192–5196.

(49) J. Lee, J. Chung, S. M. Byun, B. M. Kim, C. Lee, *Tetrahedron* **2013**, *69*, 5660–5664.

(50) I. H. Bae, I.-H. Lee, S. Byun, J. Chung, B. M. Kim, T.-L. Choi, *J. Polym. Sci., Part A: Polym. Chem.* **2014**, *52*, 1525–1528.

(51) (a) S. Byun, J. Chung, Y. Jang, J. Kwon, T. Hyeon, B. M. Kim, *RSC Adv.* **2013**, *3*, 16296–16299; (b) S. Byun, J. Chung, T. Lim, J. Kwon, B. M. Kim, *RSC Adv*. **2014**, *4*, 34084–34088.

(52) (a) J. A. Widegren, M. A. Bennett, R. G. Finke, *J. Am. Chem. Soc.* **2003**, *125*, 10301–10310; (b) J. A. Widegren, R. G. Finke, *J. Mol. Catal. A: Chem.* **2003**, *198*, 317–341; (c) B. H. Lipshutz, S. Tasler, W. Chrisman, B. Spliethoff, B. Tesche, *J. Org. Chem.* **2003**, *68*, 1177–1189; (d) N. T. S. Phan, M. Van Der Sluys, C. W. Jones, *Adv. Synth. Catal.* **2006**, *348*, 609–679; (e) C. M. Crudden, M. Sateesh, R. Lewis, *J. Am. Chem. Soc.* **2005**, *127*, 10045–10050; (f) J. E. Mondloch, E. Bayram, R. G. Finke, *J. Mol. Catal. A: Chem.* **2012**, *355*, 1–38; (g) R. A. Sheldon, M. Wallau, I. W. C. E. Arends, U. Schuchardt, *Acc. Chem. Res.* **1998**, *31*, 485–493.

(53) a) R. G. Heidenreich, J. G. E. Krauter, J. Pietsch, K. Köhler, *J. Mol. Catal. A: Chem.* **2002**, *182-183*, 499-509; b) K. Köhler, R. G. Heidenreich, J. G. E. Krauter, J. Pietsch, *Chem. Eur. J.* **2002**, *8*, 622-631.

(54) (a) M. B. Thathagar, J. E. ten Elshof, G. Rothenberg, *Angew. Chem. Int. Ed.* **2006**, *45*, 2886–2890; (b) J. G. de Vries, *Dalton Trans.* **2006**, 421–429; (c) A. K. Diallo, C. Ornelas, L. Salmon, J. Ruiz Aranzaes, D. Astruc, *Angew. Chem. Int. Ed.* **2007**, *46*, 8644–8648; (d) Z. Niu, Q. Peng, Z. Zhuang, W. He,

Y. Li, *Chem. Eur. J.* **2012**, *18*, 9813–9817; (e) A. V. Gaikwad, A. Holuigue, M. B. Thathagar, J. E. ten Elshof, G. Rothenberg, *Chem. Eur. J.* **2007**, *13*, 6908–6913.

(55) R. A. Sheldon, M. Wallau, I. W. C. E. Arends, U. Schuchardt, *Acc. Chem. Res.* **1998**, *31*, 485–493.

(56) S. P. Andrews, A. F. Stepan, H. Tanaka, S. V. Ley, M. D. Smith, *Adv. Synth. Catal.* **2005**, *347*, 647–654.

Part II.

Synthesis of core-shell type of Pd–Pt–Fe_3O_4 nanoparticles and their catalytic performance as magnetically reusable catalyst for organic reaction*

*Part of this thesis was published in *ACS Appl. Mater. Interfaces* 2016, 8, 14637−14647.

1. Introduction

The development of new type of nano-particles (NPs) with controlled surface shapes, textures, and sizes has been relentlessly pursued for attaining desirable catalytic activities.[1-3] In the last decade, much effort has been concentrated in this field, and numerous novel NPs possessing unique physical (optical,[4] structural,[5] electronic,[6] and magnetic[7]) properties for various applications have been documented. Significant research has been dedicated to the development of controllable synthetic pathways for diverse noble monometallic nanoparticles, including nanoboxes,[8] rods,[9] cages,[10] and hollow spheres.[11] Recently, bimetallic nano-materials,[12,13] including bimetallic nanoparticles, have attracted significant attention from theoretical and practical perspectives. In fact, bimetallic nanoparticles have been investigated for many applications because they exhibit extraordinary chemical activities that are clearly different from those of the parent metals.[14-16] For example, bimetallic nanoparticle-loaded clusters reported to provide "synergistic effects"[17-18] for the catalysis of synthetic organic reactions because of the interaction between each metal species.[19]

Magnetically recoverable nanoparticles have attracted increasing interest because of their scientific, technological, and industrial importance as excellent durable catalysts.[20-25] Magnetic nanocatalysts can be very easily and efficiently isolated from reaction media through the use of an external magnet. This approach greatly enhances the efficiency of these catalysts, warranting practical industrial applications. Because of these merits, new catalyst types, reactions, trends, and systems based on magnetic separation are emerging at a rapid rate. Thus, further enhancement of their catalytic performance, utilization efficiency, and recyclability continues to be a significant issue.

Functionalized aromatic amines are ubiquitously found in pharmaceuticals,[26] natural products,[27] pigments,[28] and polymers.[29] Consequently, various metal catalysts based on Pd,[30,31] Pt,[32-34] Au, [35-37] Fe, [38,39] Co[40] and Ni[41] have been investigated for their preparation via the reduction of nitro compounds. Both the use of stoichiometric reductants[42] and catalytic reduction conditions[43] employing metal-catalyzed hydrogenation with advanced methodologies have been developed.[44] In general, between the two approaches, catalytic reduction is preferred because of its atom efficiency, compatibility with industrial applications, and eco-friendliness. Sustainable processes for the reduction of substituted nitro-compounds require highly active and selective catalysts. For more environmentally friendly conditions, alcohols such as isopropanol,[45] glycerol,[46] and ethanol[47] have been utilized as alternative hydrogen providers. However, reductions using alcohols as the hydrogen source typically exhibit low selectivity and slow reaction rates. Recently, ammonia-borane ($NH_3 \cdot BH_3$, AB) has become an attractive hydrogen carrier for hydrogenation because of its nontoxicity, high volume/mass hydrogen density, good solubility in water and alcoholic solvents and facile release of H_2 through hydrolysis and alcoholysis catalyzed by noble metals.[48,49] In particular, it has gained wide popularity for the reduction of double bonds, carbonyls, imines, nitriles, and nitro compounds under ambient conditions in aqueous solutions.[50]

Previously, we reported the synthesis and application of novel heterodimeric nano-particles such as Rh–Fe_3O_4 and Pd–Fe_3O_4. Selective reduction of nitro compounds and alkenes[51], Suzuki cross-coupling[52], Sonogashira and Heck reactions[53], direct catalytic C-H arylation[54], polycondensations[55], and Wacker[56] and Wacker-type triple-bond oxidations[57] were successfully demonstrated, and mechanistic studies of Pd–Fe_3O_4 heterodimeric nanocrystals were conducted.[58]

In the present study, we report a highly efficient of magnetically recyclable catalytic system using Pd–Pt–Fe_3O_4 nano-particles for reducing nitroarenes and nitroalkanes to amines derivatives. The noble nano-catalysts were simply prepared using a facile one-pot hydrothermal method on a multi-gram scale and exhibited unique surface morphologies and textures and exceedingly fast catalytic nitro reduction performance. Excellent yields of the desired products were obtained with long-term recyclability of the Pd–Pt–Fe_3O_4. In addition, the reactivity and chemo-selectivity of this novel, recoverable bimetallic nano-catalysts were compared with those of each component metal constituent (i.e., the monometallic systems).

2. Results and Discussion

The Pd–Pt–Fe_3O_4 NPs were prepared via the simultaneous reduction of palladium chloride (II) and potassium tetrachloroplatinate (II) in polyvinylpyrrolidone (PVP) and ethylene glycol (EG), followed by deposition of the two metal nanocrystals on commercially available Fe_3O_4 nanocrystals in a simple one-pot solution phase hydrothermal process. In particular, 1.92 mmol each of $PdCl_2$ and K_2PtCl_4 was reduced, resulting in a Pd:Pt molar ratio in the Pd–Pt–Fe_3O_4 NPs of nearly 1.0:1.0. PVP served as a dispersant[59] and sterically stabilized the nanoparticles[60], whereas EG functioned as both the solvent and a reductant. Inductively coupled plasma-atomic emission spectroscopic (ICP-AES) analysis confirmed that the Pd–Pt–Fe_3O_4 NPs contained 5.1 wt% palladium and 8.3 wt% platinum.

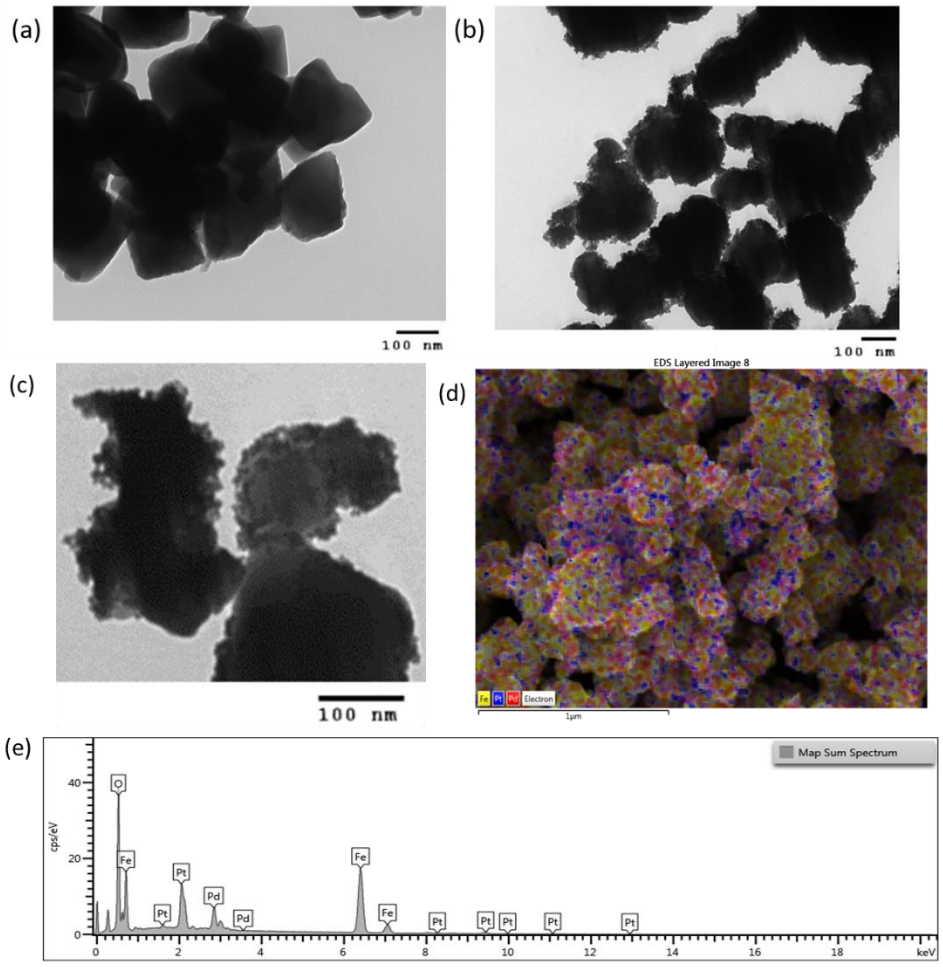

Figure II-1. (a) TEM image of Fe_3O_4 NPs (b) TEM image of Pd–Pt–Fe_3O_4 NPs (c) TEM image of Pd–Pt–Fe_3O_4 NPs (d) The mapping image of Pd–Pt–Fe_3O_4 NPs (e) EDS map sum spectrum pattern of Pd–Pt–Fe_3O_4 NPs

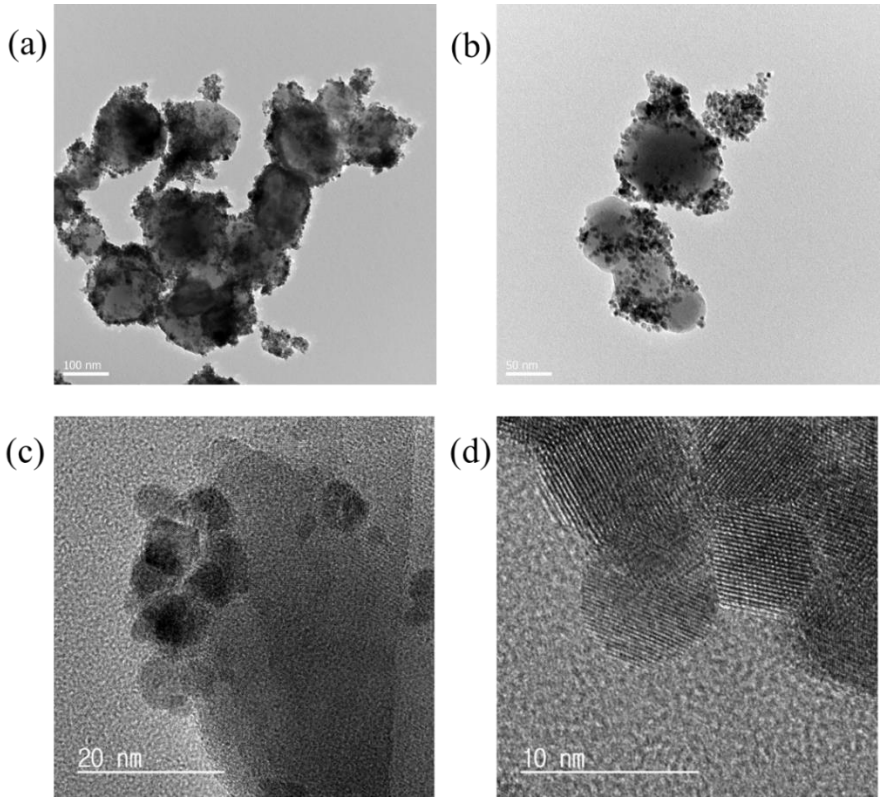

Figure II-2. (a) and (b) HR-TEM image of Pd–Pt–Fe_3O_4 NPs (c) and (d) Cs-TEM images of Pd–Pt–Fe_3O_4 NPs

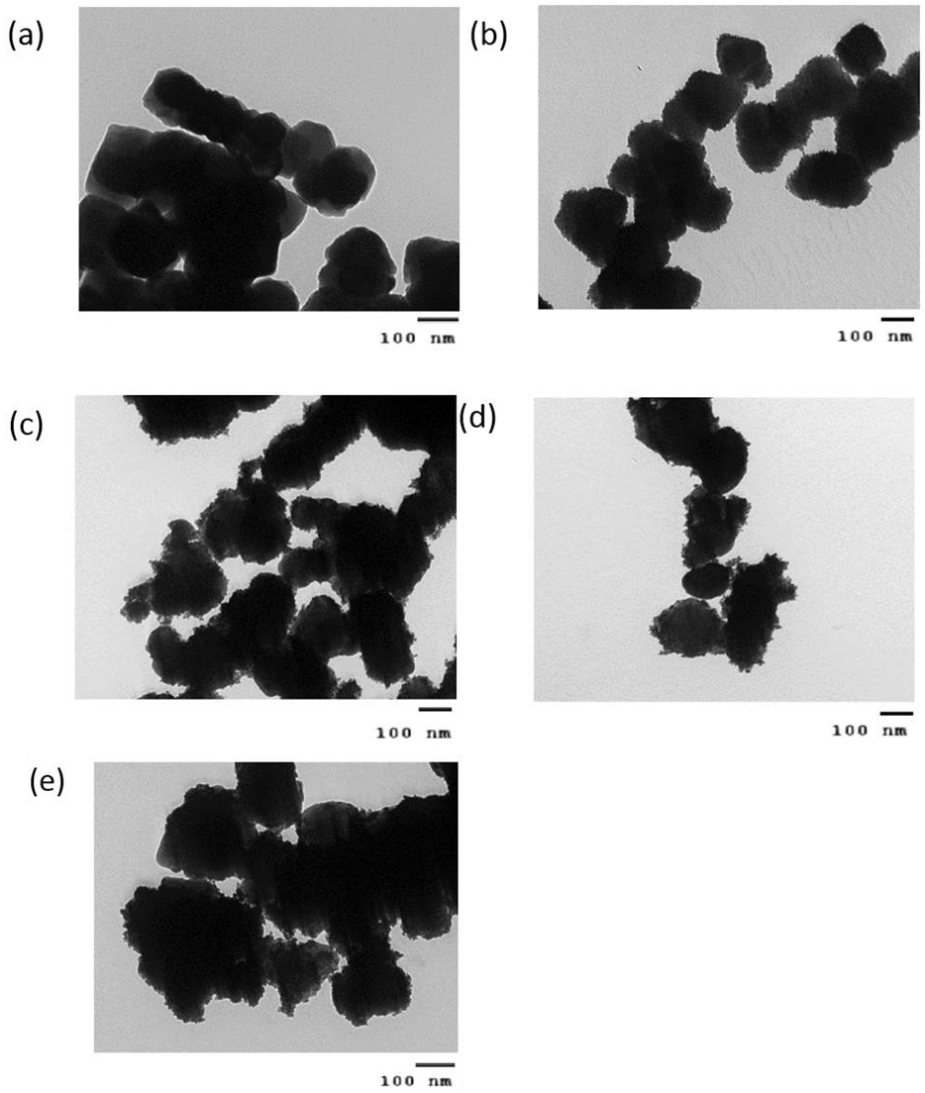

Figure II-3. TEM images of NPs: (a) Fe_3O_4 NPs; (b) Pd–Fe_3O_4 NPs; (c) fresh Pd–Pt–Fe_3O_4 NPs; (d) Pd–Pt–Fe_3O_4 NPs after 1 cycle of the catalytic reaction; (e) Pd–Pt–Fe_3O_4 NPs after 10 cycles of the catalytic reaction.

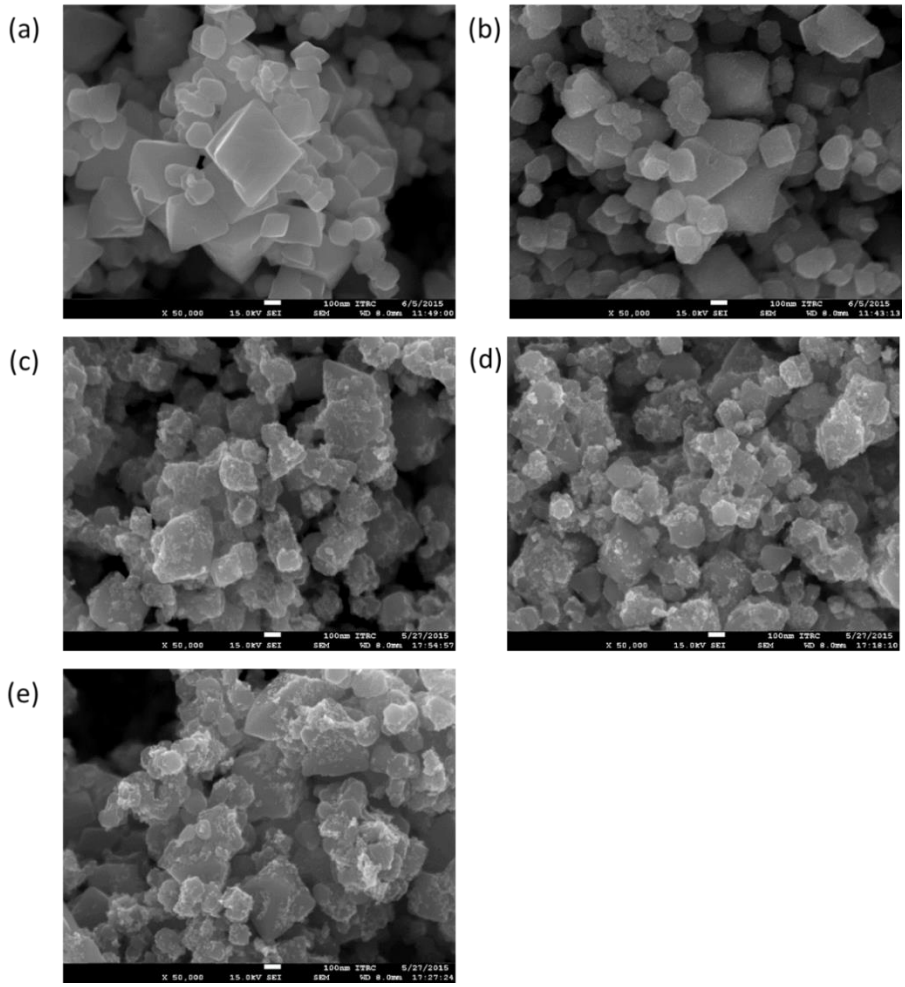

Figure II-4. SEM images of NPs: (a) Fe_3O_4 NPs; (b) Pd–Fe_3O_4 NPs; (c) fresh Pd–Pt–Fe_3O_4 NPs; (d) Pd–Pt–Fe_3O_4 NPs after 1 cycle of the catalytic reaction; (e) Pd–Pt–Fe_3O_4 NPs after 10 cycles of the catalytic reaction.

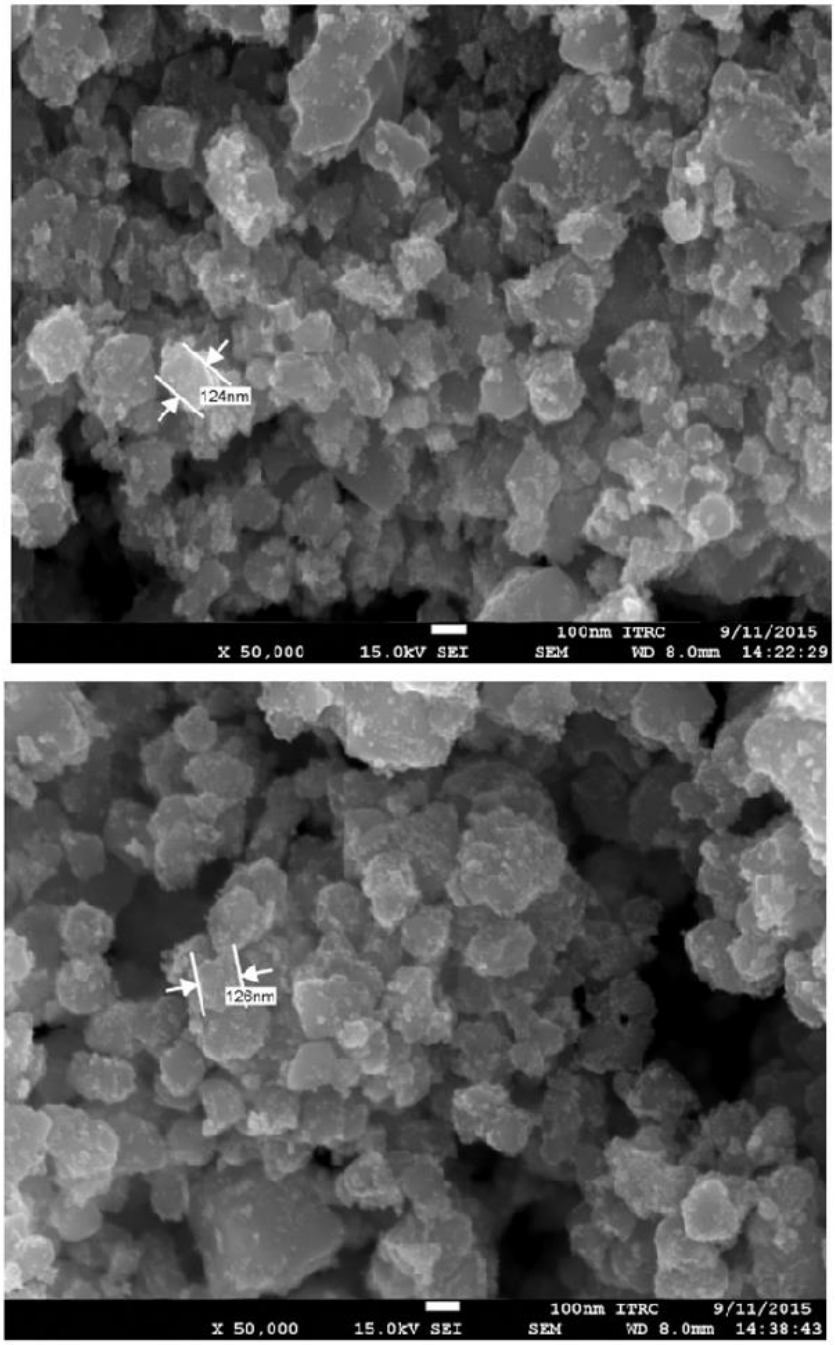

Figure II-5. SEM images of the Pd–Pt–Fe_3O_4 NPs

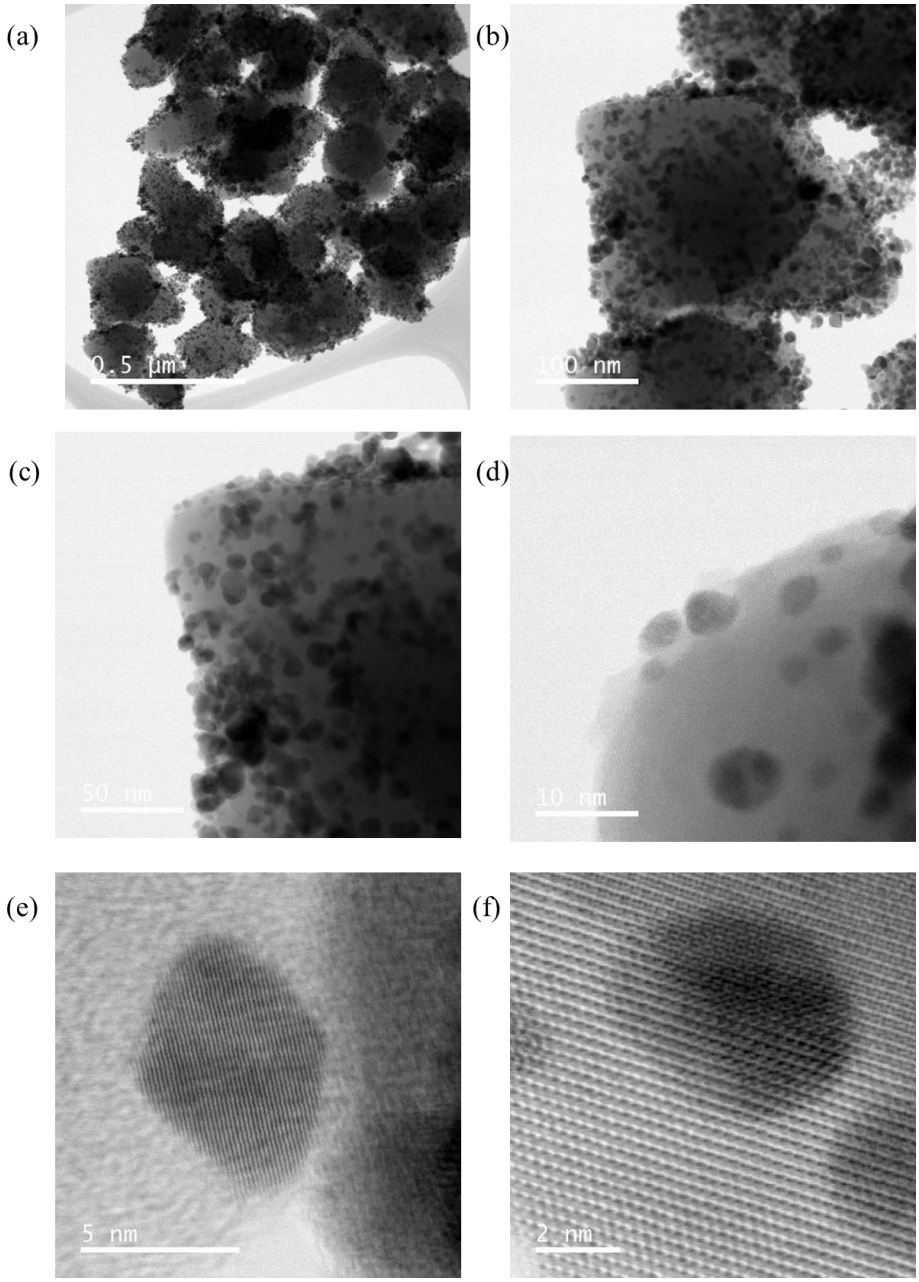

Figure II-6. Representative BF-STEM images of Pd–Pt–Fe_3O_4 NP_s

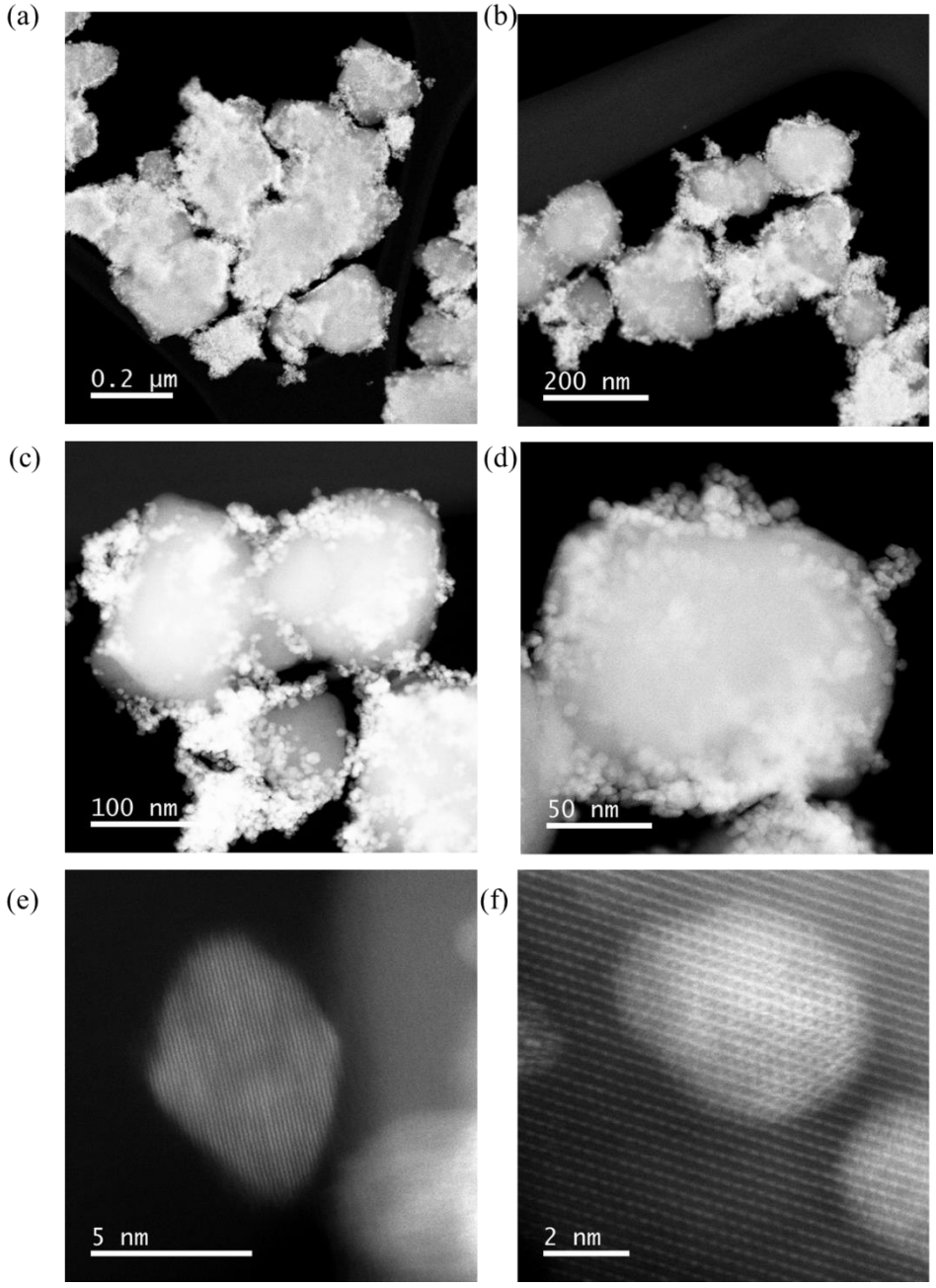

Figure II-7. Representative HAADF-STEM images of Pd–Pt–Fe_3O_4 NP_s

Figure II-1. (a) illustrates a transmission electron microscopy (TEM) image of the commercially available Pd–Pt–Fe_3O_4 NPs used as a magnetic and recyclable support. The Pd–Pt–Fe_3O_4 NPs were monodispersed and had diameters of approximately 90 to 180 nm. **Figures II-1, 2**, **3, 4, 5, 6** and **7** show representative TEM images, scanning electron microscopy (SEM) images, high resolution transmission electron microscopy images (HR-TEM), Cs-TEM images, bright-field scanning TEM (BF-STEM) images and high-angle annular dark-field scanning transmission electron microscopy (HAADF-STEM) images of the nanoflake Pd–Pt–Fe_3O_4 NPs. As can be seen in these images, the surfaces of the Pd–Pt–Fe_3O_4 NPs were well decorated with well-dispersed metal NPs having diameters ranging from 5 to 8 nm. These results demonstrate that Pt and Pd NPs were well immobilized on the surfaces of the Fe_3O_4 NPs. As can be seen in the mapping image of the catalyst in **Figure II-1** (d), the surface of the Fe_3O_4 support (yellow) was nearly evenly loaded with Pd (red) and Pt (blue). The close location of Pd and Pt in a bimetallic alloy form is believed to contribute to the observed synergistic effect for catalyzing the dehydrogenation of AB and nitro-reduction reaction. Moreover, the energy dispersive spectroscopy (EDS) pattern revealed the presence of Pd, Pt, and Fe elements in the Pd–Pt–Fe_3O_4 NPs (**Figure II-1** (e)).

To determine the oxidation states of the metals in the nanocatalyst, X-ray photoelectron spectroscopy (XPS) was performed, and the results are shown in **Figure II-8** (a) and (b). Several characteristic peaks for Pt 4f are present in **Figure II-8** (a). Two Pt $4f_{7/2}$ and Pt $4f_{5/2}$ peaks were identified at approximately 71.2 and 74.5 eV, respectively, and these two binding energies in particular indicate a Pt(0) species.[61] At the same time, peaks for different oxidation states of Pt (Pt(II) and Pt(IV)) were detected at 74.1 and 74.9 eV, respectively.[62] In **Figure II-8** (b), the characteristic peaks for metallic Pd can be clearly seen,

with the peaks at 335.0 and 340.5 eV assigned to Pd $3d_{5/2}$ and Pd $3d_{3/2}$, respectively, revealing that Pd(0) was present in the nanocatalyst. However, the XPS peaks for $3d_{5/2}$ at 337 eV and $3d_{3/2}$ at 342 eV indicated that the Pd–Pt–Fe_3O_4 nanocatalyst also contained a minor amount of Pd(II).[63] As can be seen in **Figure II-8** (c), the X-ray diffraction (XRD) pattern confirmed the presence of all three constituent elements in the Pd–Pt–Fe_3O_4 NPs. Importantly, however, no impurity peaks were detected by XRD. Clearly, the Pd–Pt–Fe_3O_4 NPs comprised Pd, Pt, and Fe_3O_4

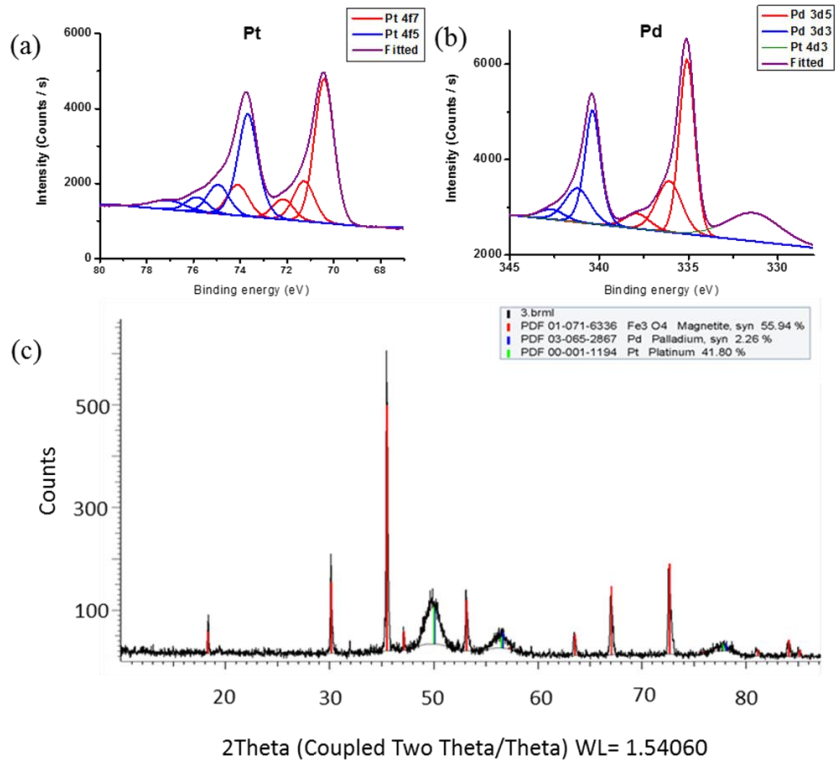

Figure II-8. XPS spectrum for the prepared Pd–Pt–Fe_3O_4 NPs (a) Pt 4f (b) Pd 4d (c) XRD spectrum data of Pd–Pt–Fe_3O_4 NPs

The formation of an alloy with two different metals could be confirmed by XRD of particles. When a random alloy is made, a change of lattice peak can be detected, which is different from the own metal. On the contrary, when two metal species do not form an alloy, XRD can usually distinguish two different phases.[64] Therefore, we compared the combined XRD of Pd–Fe_3O_4, Pt–Fe_3O_4 and Pd–Pt–Fe_3O_4 (**Figure II-9**). As can be seen in **Figure II-10**, there was a little different lattice peak in Pd–Pt–Fe_3O_4 compared to Pd-Fe_3O_4 and Pd–Pt–F_3O_4. This subtle difference led us to conclude that Pd and Pt Nps on Pd–Pt–Fe_3O_4 are Pd–Pt bimetallic alloy dispersed on Fe_3O_4 surface (**Figure II-10**).The detection of alloy was also confirmed by Cs-TEM. Cs-TEM and Cs- scanning transmission electron microscopy (STEM) images were analyzed by EDS to check the presence of the two different metals (Pd, Pt). Immobilized metals are forming together small round shapes, leading to the synthesis of nanoflake-shaped nanoparticles. **Figure II-11** and **12** shows in detail the dispersion of Pt and Pd on the surface by color detection. The picture shows a mixture of two different colors spread all over the supporting particles. Based on this analysis, we concluded that there is Pd–Pt bimetallic alloy on the surface of our catalyst (**Figure II-11** and **12**).

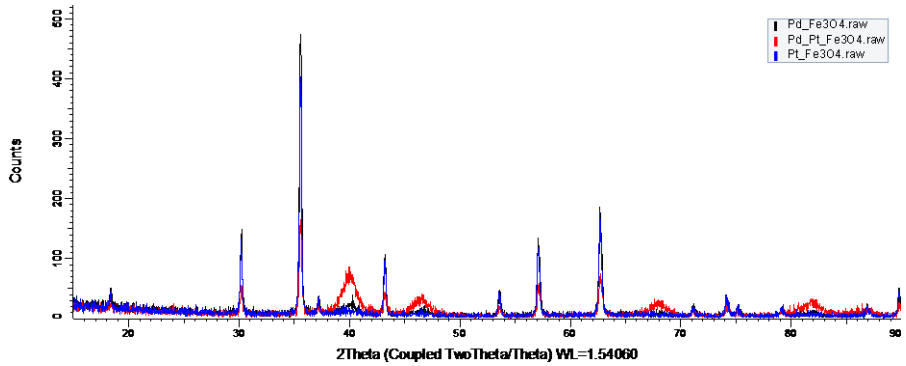

Figure II-9. XRD of Pd-Fe_3O_4, Pt-Fe_3O_4 and Pd-Pt-Fe_3O_4

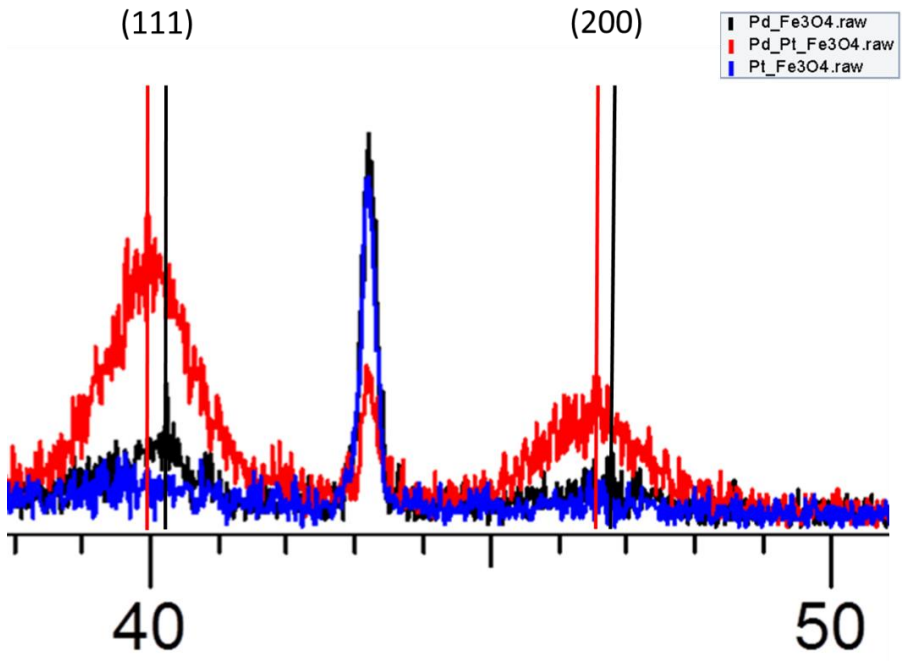

Figure II-10. XRD data of Pd-Fe_3O_4, Pt-Fe_3O_4 and Pd-Pt-Fe_3O_4

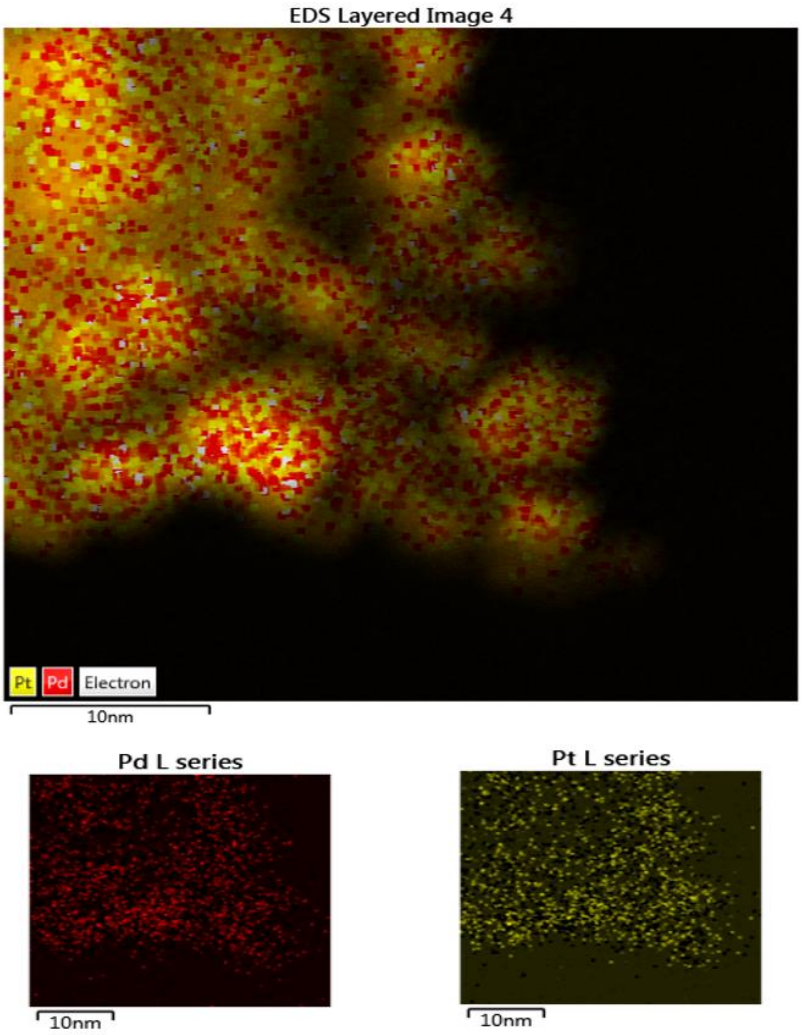

Figure II-11. The elemental analysis of Pd-Pt-Fe_3O_4 NPs mapping imag es by Cs-TEM-EDS

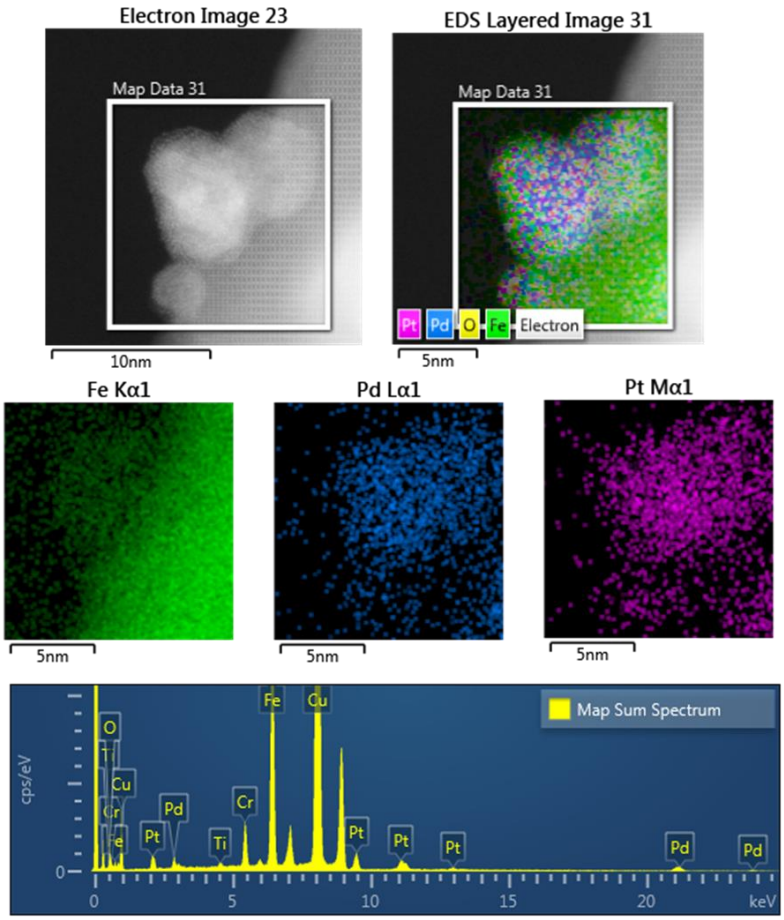

Figure II-12. The elemental analysis of Pd-Pt-Fe_3O_4 NPs mapping images by Cs-STEM-EDS

The magnetic properties of the Pd–Pt–Fe_3O_4 NPs were determined using a magnetic property measurement system (MPMS) in fields ranging from +30 to −30 kOe at room temperature (**Figure 4** (c)). The MPMS data clearly indicated that the Pd–Pt–Fe_3O_4 NPs, whose saturation magnetization value was 58.4 emu g−1 (Fe) at 300 K, were superparamagnetic. The Pd–Pt–Fe_3O_4 NPs, were also shown to be separable using an external magnet (**Figure 4** (a) and (b)), indicating that they should be useful as magnetically separable catalysts.

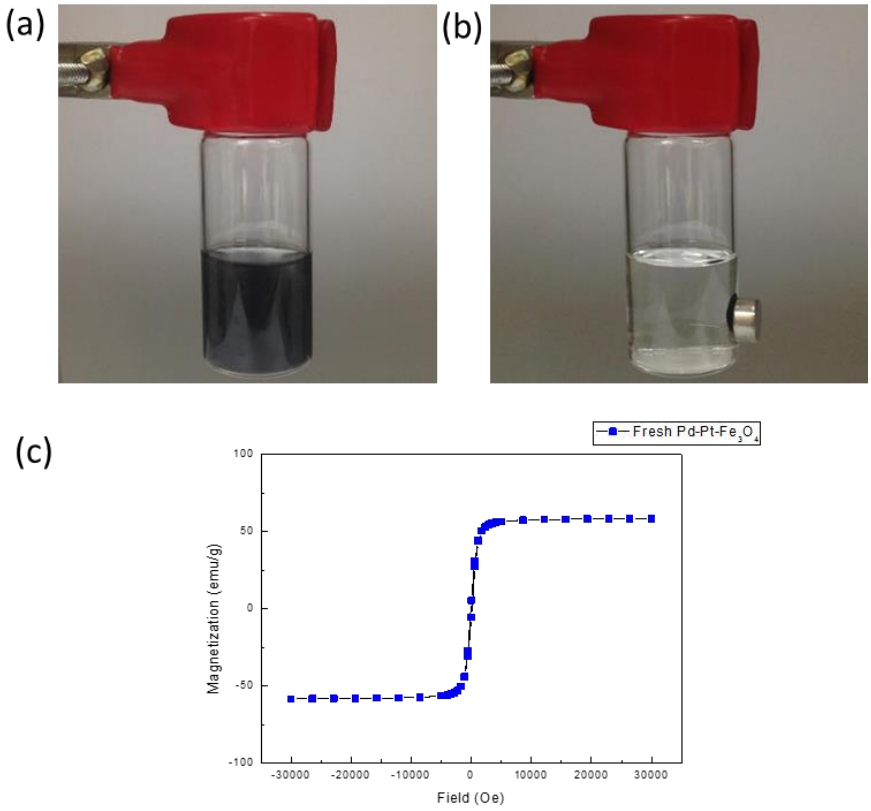

Figure II-13. Photographs of the magnetically separable Pd–Pt–Fe_3O_4 NPs (a) dispersion state of Pd–Pt–Fe_3O_4 NPs (b) magnetic separation of Pd–Pt–Fe_3O_4 NPs after reaction (c) MPMS data of Pd–Pt–Fe_3O_4 NPs

Table II-1. Optimization of the cascade dehydrogenation/reduction reaction catalyzed by Pd–Pt–Fe_3O_4 Nps [a]

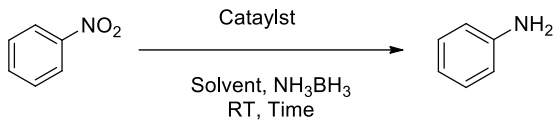

Entry	Catalyst	Solvent	Time	Yield (%)[b]	Conversion (%)[b]
1	None	MeOH	5 min	0	0
2	Fe_3O_4	MeOH	5 min	0	0
3	1 mol% Pd–Fe_3O_4	MeOH	5 min	40	68
4	1 mol% Pt–Fe_3O_4	MeOH	5 min	56	69
5[c]	1 mol% Pd–Fe_3O_4 & Pt–Fe_3O_4	MeOH	5 min	57	90
6	1 mol% Pd–Pt–Fe_3O_4	MeOH	5 min	>99	>99
7	1 mol% Pd–Pt–Fe_3O_4	H_2O	5 min	84	93
8	1 mol% Pd–Pt–Fe_3O_4	EtOH	5 min	64	75
9[d]	1 mol% Pd–Pt–Fe_3O_4	H_2O:EtOH	5 min	>99	>99
10[d]	1 mol% Pd–Pt–Fe_3O_4	H_2O:MeOH	5 min	>99	>99
11	0.1 mol% Pd–Pt–Fe_3O_4	MeOH	30 min	>99	>99
12	0.01 mol% Pd–Pt–Fe_3O_4	MeOH	3 h	>99	>99
13	0.001 mol% Pd–P–Fe_3O_4	MeOH	30 h	>99	>99
14[e]	1 mol% Pd–Pt–Fe_3O_4	MeOH	5 min	>99	>99

[a] Reaction conditions: 0.5 mmol nitrobenzene, 1.5 mmol NH_3BH_3, 5 mL solvent , room temperature. [b] Yields and conversions were determined via GC analysis using anisole as an internal standard. [c] 1mol% of each catalyst. [d] 5 mL of water/solvent (v/v=3:7). [e] 10 mmol nitro benzene.

With the Pd–Pt–Fe_3O_4 bimetallic NPs in hand, we initiated our search for the optimized reaction conditions for the dehydrogenation of ammonia-borane and reduction of $ArNO_2$. A series of catalysts and solvents were tested using nitrobenzene as a representative substrate (**Table II-1**). When the reactions was conducted without any catalyst or in the presence of Fe_3O_4 NPs at room temperature, no formation of the desired product was observed (**Table II-1**, entries 1–2). Next, an array of different catalysts, i.e., Pd–Fe_3O_4, Pt–Fe_3O_4, a combination of Pd–Fe_3O_4 and Pt–Fe_3O_4, and Pd–Pt–Fe_3O_4 were screened for the cascade reaction with the aim of finding the best catalyst system for nitrobenzene reduction (**Table II-1**, entries 3–6). Among the three Fe_3O_4-based NP catalysts, the Pd–Pt–Fe_3O_4 NPs exhibited the best catalytic activity in methanol, furnishing the highest conversion (>99%) and yield (>99%) (**Table II-1**, entry 6). Note that the catalyst comparison experiment revealed a significant synergistic effect[65] for the reaction with the bimetallic Pd–Pt–Fe_3O_4 NPs catalyst system compared with those with the other monometallic catalysts or a physical combination of the two. When the cascade reaction was performed in water or ethanol, the conversion and yield deteriorated (**Table II-1**, entries 7 and 8, respectively). In contrast, reactions in binary solvent systems (water–ethanol (v/v 3:7) or water–methanol (v/v 3:7) proceeded quite efficiently (**Table II-1**, entries 9 and 10, respectively). Noble metal-catalyzed hydrolysis of AB is faster than alcoholysis of AB.[66] Therefore, the addition of water to ethanol or methanol is beneficial for fast generation of H_2 (**Table II-1**, entries 8-10). However, alcoholic solvent is needed for better solubility of the substrates, hence the mixture of water and an alcohol as ideal solvent systems (**Table II-1**, entries 7, 9 and 10). Therefore, it can be said that binary solvent systems have a promising effect for reduction reactions of nitro compounds. Reaction conditions using 1.5 equiv ammonia-borane also can be successfully

applied to nitrobenzene (for example, see **Table II-2**), but not for all the substrates listed in our scope study. For this reason, we carried out the screening studies with uniform 3 equiv of ammonia-borane. When the Pd–Pt–Fe_3O_4 catalyst loading was reduced to 0.1, 0.01, and 0.001 mol%, completion of the reaction was observed at elongated reaction times (1, 3, and 30 h for **Table II-1,** entries 11, 12, and 13, respectively). The turnover numbers and turnover frequencies based on the concentration of Pd–Pt–Fe_3O_4 NPs are provided in the Supplementary Material (**Table II-3**). A larger scale (10 mmol) reaction proceeded with >99% yield and conversion (**Table II-1**, entry 14). These results indicate that even with a very small amount of the Pd–Pt–Fe_3O_4 NPs, the catalytic reaction proceeds quite efficiently, allowing potential industrial-scale applications. When hydrazine[67] or 1,1,3,3,-tetramethyldisiloxane[68] was used instead of ammonia-borane (AB) as a reductant, poor yield was detected over the same reaction time. Reduction using hydrazine hydrate was investigated in more detail and the results are shown in **Table II-4**, entry1. The conversion with hydrazine hydrate was very slow, taking 2 h to complete, however, only 5 min was required for the completion of the reduction with ammonia-borane and the initial comparison was made at 5 min from the start of the reaction. Bubbling hydrogen and $NaBH_4$ were equally effective as a hydrogen source leading to complete reaction in 5 min, however, reaction under atmospheric hydrogen was slow (1 h) as seen in the Supporting Information (**Table II-5)**.

Table II-2. Equivalent test of ammonia-borane for nitro-redcution[a]

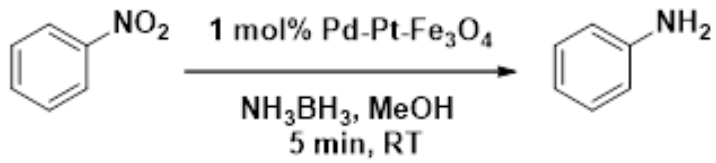

Entry	Eq. of AB	Yield(%)[b]	Conversion(%)[b]
1	1 eq	84	88
2	1.5 eq	>99	>99

[a]Reaction conditions: 0.5mmol substrate, 1 mol% Pd–Pt–Fe_3O_4 catalyst, 5mL of methanol and room temperature. [b]Yield and conversion were determined from GC analysis using anisole as an internal standard.

Table II-3. Turnover number and turnover frequency of nitro-redcution[a]

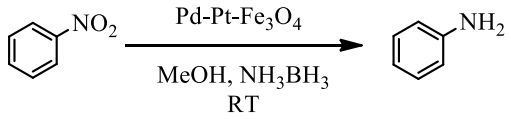

Entry	Catalyst	Reaction time	TON	TOF (h^{-1})
1	1mol%	5 min	100	1200
2	0.1mol%	30 min	1000	2000
3	0.01mol%	180 min	10000	3333
4[b]	0.001mol%	1800 min	100000	3333

[a] Reaction conditions: 0.5 mmol nitrobenzene, 1.5 mmol NH_3BH_3, 5mL of solvent and room temperature.[b] 5 mmol of nitrobenzene, 50ml of solvent

Table II-4. Test of hydrazine as an alternative hydrogen source[a]

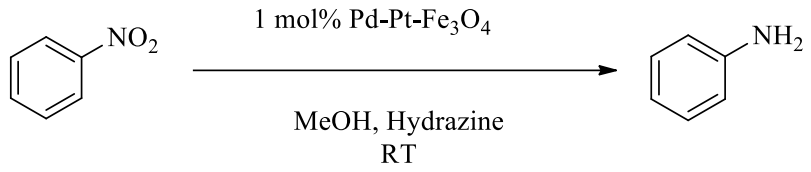

Entry	Time	Yield (%)[b]	Conversion (%)[b]
1	5min	16	24
2	30min	62	89
3	1h	78	89
4	2h	>99	>99

[a] Reaction conditions: 0.5 mmol substrate, 1.5 mmol reduciong agent, 1 mol% Pd–Pt–Fe_3O_4 catalyst, 5mL of solvent and room temperature.[b] Yields and conversion were determined by GC analysis using anisole as internal standard.

Table II-5. Variation of the reducing agent[a]

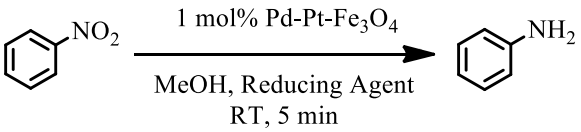

Entry	Reducing Agent	Yield (%)[b]	Conversion (%)[b]
1	Hydrazine	16	24
2	1,1,3,3- Tetramethyldisiloxane	0	0
3	NH_3BH_3	>99	100
4[c]	H_2 (1 atm)	>99	100
5	H_2 (bubbling)	>99	100
6	$NaBH_4$	>99	100

[a] Reaction conditions: 0.5 mmol substrate, 1.5 mmol reduciong agent, 1 mol% Pd–Pt–Fe_3O_4 catalyst, 5mL of solvent and room temperature.[b] Yields and conversion were determined by GC analysis using anisole as internal standard. [c] Reaction time 1h instead of 5 min.

To test the substrate scope of the Pd–Pt–Fe_3O_4 catalyzed nitro compounds reduction reaction, a diverse array of nitro compounds was subjected to the optimized conditions. The conversion of these compounds to their respective primary amines was achieved with high efficiency at room temperature in 5 min (**Table II-6.**). Perfect selectivity for nitro reduction was observed for substrates containing halogen atoms, without a hint of dehalogenation (**Table II-6**, entries 2−4). High yields and conversions were also obtained for nitroarenes containing both electron-donating groups (**Table II-6**, entries 5–9) and an electron-withdrawing substituent (**Table II-6**, entry 10). Notably, the reaction was also extended to the dinitro compound 2,6-dinitrotoluene, and both nitro groups were efficiently reduced to give the corresponding diamino product (**Table II-6**, entry 11). Furthermore, the catalytic reaction was easily extended to 1-nitronaphthalene, 4-nitrobiphenyl, and 2,7-dinitrofluorene, all of which afforded the desired products in excellent yields (**Table II-6**, entries 12, 13, and 14, respectively). These heteroaromatic amine derivatives are important intermediates for the production of drug molecules, insecticidal/antimicrobial agents, dyes, and recently compounds used in organic displays. Nitrile-containing compounds such as 4-nitrobenzonitrile and 2-chloro-5-nitrobenzonitrile were also smoothly reduced to the corresponding anilines without reduction of the nitrile or dehalogenation (**Table II-6**, entries 15 and 16, respectively). These results suggest that our catalyst is highly selective for nitro-reduction. A sterically hindered substrate was also reduced to the corresponding aniline product (**Table II-6**, entry 17). Finally, the reduction protocol was found to be equally effective for aliphatic nitro substrates such as nitrocyclohexane and 1-nitrohexane, which were quantitatively converted to the desired primary amines under the same reaction conditions (**Table II-6**, entries 18 and 19, respectively).

Table II-6. Pd–Pt–Fe_3O_4 catalyzed reduction of various substituted nitro compounds[a]

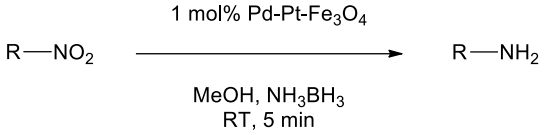

Entry	Substrate	Product	Yield (%)[b]	Conversion (%)[b]
1	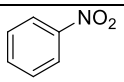	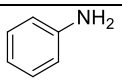	>99 (96)	>99
2	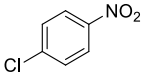	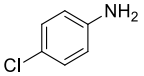	98 (93)	>99
3	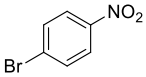	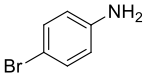	>99 (91)	>99
4	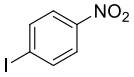	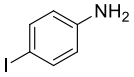	>99 (95)	>99
5	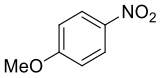	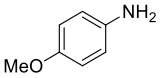	98 (94)	>99
6	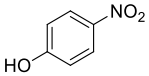	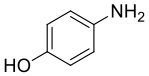	>99 (93)	>99
7	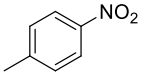	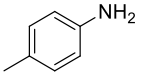	>99 (93)	>99
8	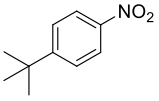	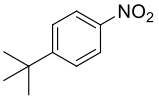	>99 (92)	>99
9	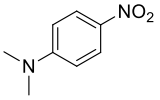	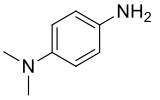	98 (90)	>99
10	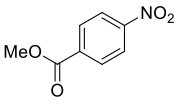	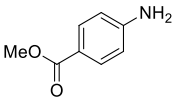	98 (97)	>99

11	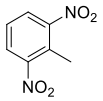	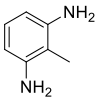	>99 (95)	>99
12	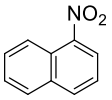	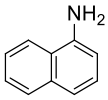	>99 (98)	>99
13	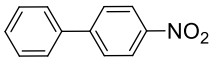	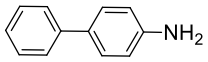	>99 (97)	>99
14[c]	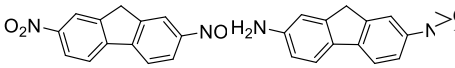		>99 (97)	>99
15	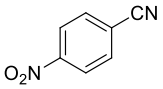	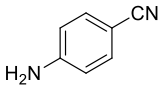	>99 (96)	>99
16	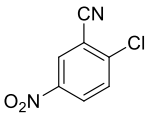	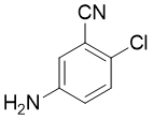	>99 (92)	>99
17	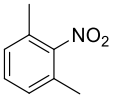	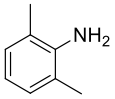	>99 (93)	>99
18[d]	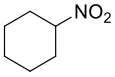	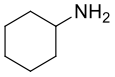	>99 (94)	>99
19	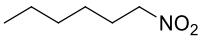	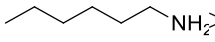	>99 (95)	>99

[a] Reaction conditions: 0.5 mmol substrate, 1.5 mmol NH_3BH_3, 1 mol% Pd–Pt–Fe_3O_4 catalyst, 5 mL methanol, room temperature. [b] Yields were determined via GC analysis using anisole as an internal standard. Parentheses are isolation yield. [c] Reaction time was 30 min instead of 5.

Next, the chemoselectivity of the reduction of 4-nitrostyrene, which has both nitro and olefin moieties (**Table II-7.**), was investigated using the Pd–Pt–Fe_3O_4 catalyst. Reaction of 4-nitrostyrene with 3 equiv of ammonia-borane afforded the completely reduced product B. However, when the amount of ammonia-borane was reduced to 1 equiv, the reaction gave the desired product A with a minimal amount of B (A/B = 94:6). It can thus be concluded that chemoselective reduction of nitro groups in the presence of double bonds was achieved using the Pd–Pt–Fe_3O_4 catalyst through control of the reducing agent stoichiometry.

Table II-7. Chemo-selectivity studies of 4-nitrostyrene reductions[a]

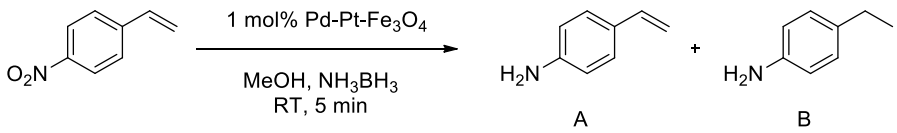

Entry	Equivalent of AB	Conversion (%)[b]	Selectivity (A:B)[b]
1	3 eq	> 99	0:100
2	1 eq	> 99	94:6

[a] Reaction conditions: 0.5 mmol substrate, 1 mol% Pd-Pt-Fe_3O_4 catalyst, 5 mL of methanol and room temperature. [b] Yields were determined by GC analysis using anisole as internal standard.

We also tested the selectivity of aromatic nitro reduction in presence of *O*-allyl, *O*-benzyl, *O*-propargyl groups which frequently used protecting alcohol groups in organic synthesis. When *O*-benzyl protected nitrobenzene was performed 1 eq of AB and 10 min at room temperature, 62% of desired product was obtained. However, upon using 1.5 equiv AB, the product yield went up to 93% (**Table II-8**, entry 2). *O*-allyl and *O*-propagyl protected nitrobenzene were also selectively reduced to *O*-allyl and *O*-propagyl protected anline (**Scheme. II-1**). We also studied the selectivity for *o*-nitroacetophenone and *o*-nitrobenzaldehyde. The reaction on *o*-nitroacetophenone was highly efficient without reduction of the ketone functional group (**Scheme II-2**). When the reduction of *o*-nitrobenzaldehyde was carried out, *o*-nitrobenzyl alcohol was obtained as a major product (95%) under normal reaction conditions employing 3 equiv AB (**Table II-9**). When the same reaction was tested with 1 equiv AB, *o*-nitrobenzyl alcohol and a dimerization product (**Table II-9**, D) were obtained in 1:1 ratio

Table II-8. Chemoselectivity studies of 1-benzyloxy-4-nitrobenzene[a]

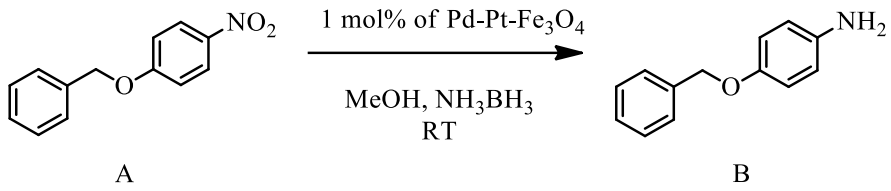

A B

Entry	Eq. of AB	Reaction time	Yield[b]
1	1 eq	10 min	62%
2	1.5 eq	10 min	93%

[a] Reaction conditions: 1 mmol substrate, 1mol% Pd–Pt–Fe_3O_4 catalyst, 10 mL of methanol and room temperature. [b] Yield of isolation product.

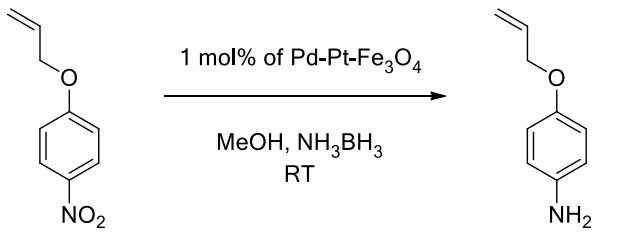

C D: 93%

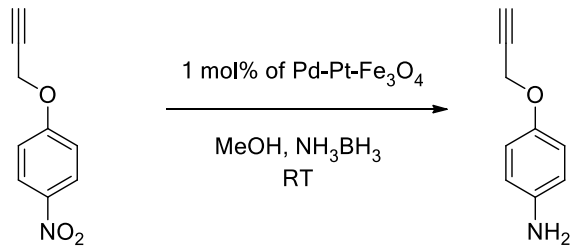

E F: 92%

Scheme II-1. The selectivity test of *O*-ally and *O*-propargyl protected nitrobenzene

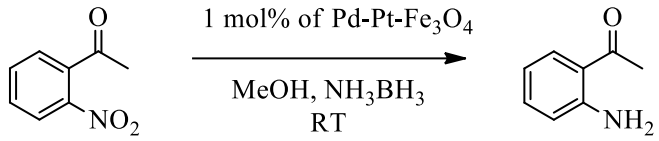

G H: 97%

Scheme II-2. The selectivity test of *o*-nitroacetophenone

Table II-9. Chemoselectivity studies of *o*-nitrobenzaldehyde[a]

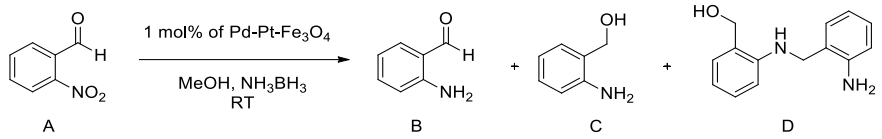

A B C D

Entry	Eq of AB	Reaction time	Yield of B[b]	Yield of C[b]	Yield of D[b]
1	3	5 min	0%	95%	0%
2	1	5 min	0%	49%	48%

[a] Reaction conditions: 1mmol substrate, 1mol% Pd–Pt–Fe_3O_4 catalyst, 10 mL of methanol and room temperature. [b] Yield of isolation product.

The mechanism of the nitro reduction catalyzed by the Pd–Pt–Fe_3O_4 nanoflakes was then studied, based upon which a tandem reaction sequence involving nitrosobenzene and azobenzene as intermediates is proposed as depicted in **Scheme II-3**. First, the Pd–Pt–Fe_3O_4 NPs catalyze the methanolysis of ammonia-borane to generate molecular H_2. Reduction of nitrobenzene to aniline then ensues, consuming the H_2 on the Pd–Pt–Fe_3O_4 NPs catalyst. The reaction intermediates were checked from gas chromatography mass spectrometry (GC-MS) analysis of the reaction mixture at 1, 3 and 5 min from the start of the reaction (**Table II-10**). The presence of the nitrosobenzene was confirmed through comparison with an authentic material on the GC-MS spectrum during the course of reaction. As shown in **Table II-11**, at 3 min the nitrosobenzene and azobenzene peaks were detected in ~1:1 ratio (**Figure II-14**).

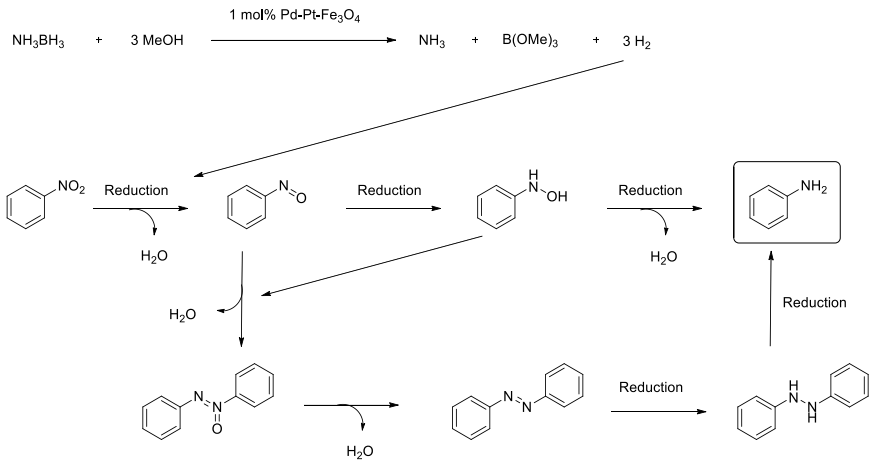

Scheme II-3. The proposed mechanism of nitrobenzene reduction using AB as a hydrogen source**.**

Table II-10. Yields based on GC-MS analyses at 1, 3 and 5 min

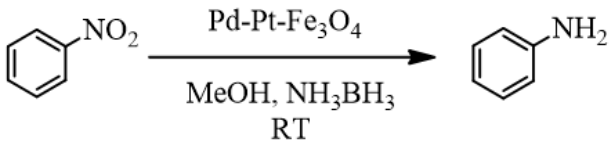

Entry	Time	GC Yield (%)	Conversion (%)
1	1 min	30	88
2	3 min	65	>99
3	5 min	>99	>99

Table II-11. Ratio of nitrosobenzene and azobenzene on GC-MS

Entry	Reaction time	Nitrosobenzne : Azobenzene
1	1 min	1 : 1.5
2	3 mim	1 : 1

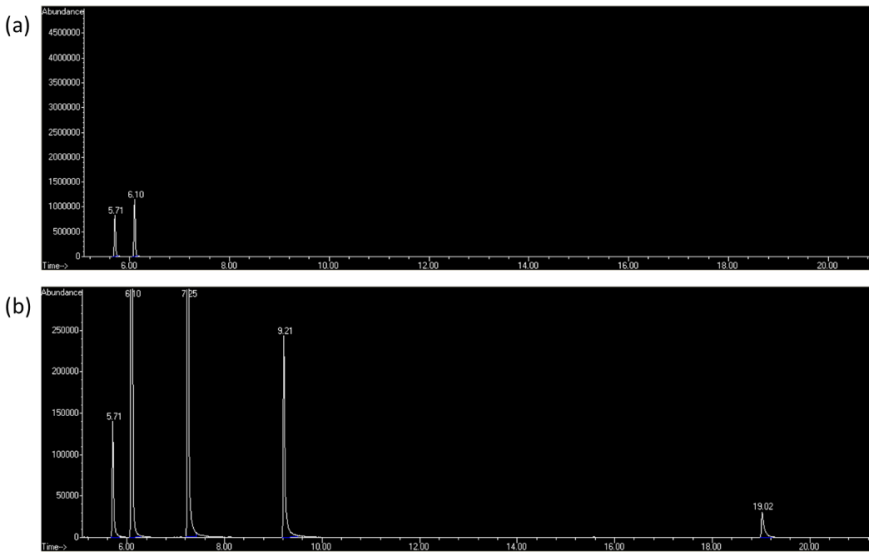

Figure II-14. (a) GC-MS data of the commercially available nitrosobenzene (5.71 min) and anisole (6.10 min) as standards. (b) GC-MS data of the nitrobenzene reduction after 3 min of reaction (nitrosobenzene: 5.71 min, anisole: 6.10 min, aniline: 7.25 min, nitrobenzene: 9.21 min, azobenzene: 19.02 min).

To investigate the recyclability of the Pd–Pt–Fe_3O_4 NPs, they were separated and isolated from the reaction mixture using an external magnet after a catalytic reduction cycle (5 min). The recovered catalyst was immediately reused in the next reduction reaction with fresh substrate and ammonia-borane. The Pd–Pt–Fe_3O_4 NPs were repeatedly used for the reduction of nitrobenzene, and the catalytic performance was monitored. Notably, the catalyst exhibited excellent retention of catalytic activity through 250 cycles (**Figure II-15**), after which, however, a gradual decrease in the conversion and yield was observed. Each of the reactions in the recycling experiment was allowed to run for 5 min.

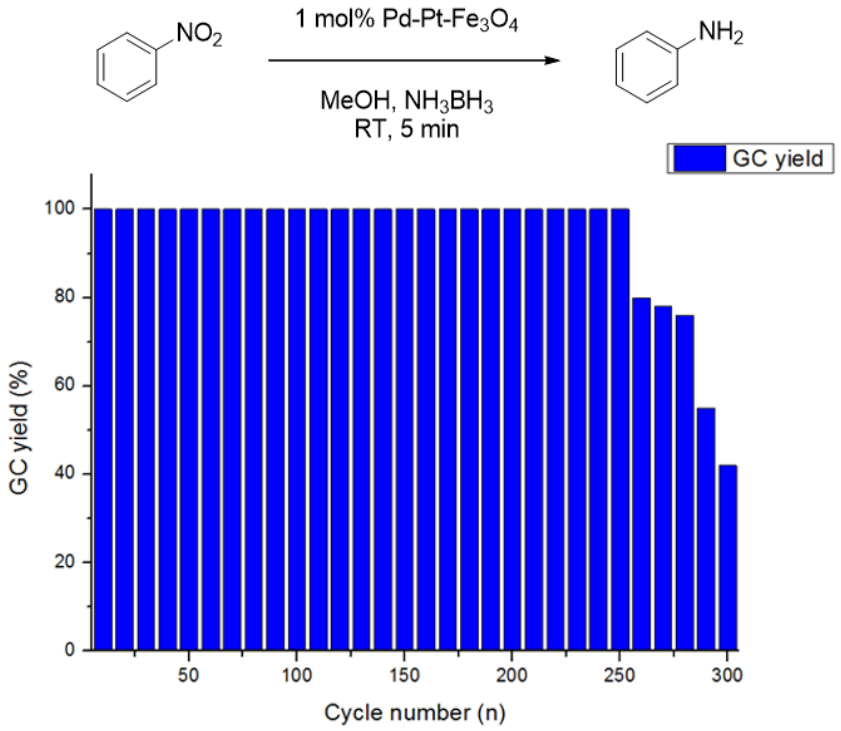

Figure II-15. Recyclability of the Pd–Pt–Fe_3O_4 nanoflake catalyst

SEM, SEM-EDS, XPS, XRD, MPMS, Thermogravimetric analysis (TGA) and Fourier transform infrared spectroscopy (FT-IR) were employed to evaluate the fresh spent (1 cycle) and recycled Pd–Pt–Fe_3O_4 NPs (**Figures II-16–23**, respectively).

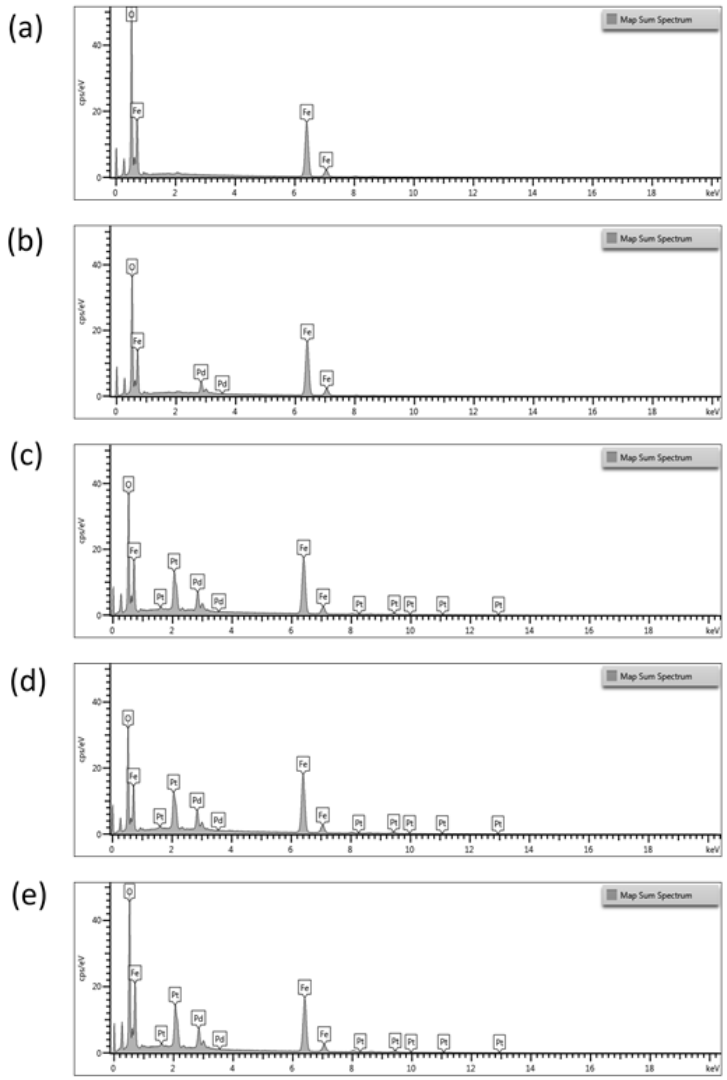

Figure II-16. The energy disperse spectroscopy (EDS) map sum spectrum pattern of NPs: (a) Fe_3O_4 NPs; (b) Pd–Fe_3O_4 NPs; (c) fresh Pd–Pt–Fe_3O_4 NPs; (d) Pd–Pt–Fe_3O_4 NPs after 1 cycle of the catalytic reaction; (e) Pd–Pt–Fe_3O_4 NPs after 10 cycles of the catalytic reaction

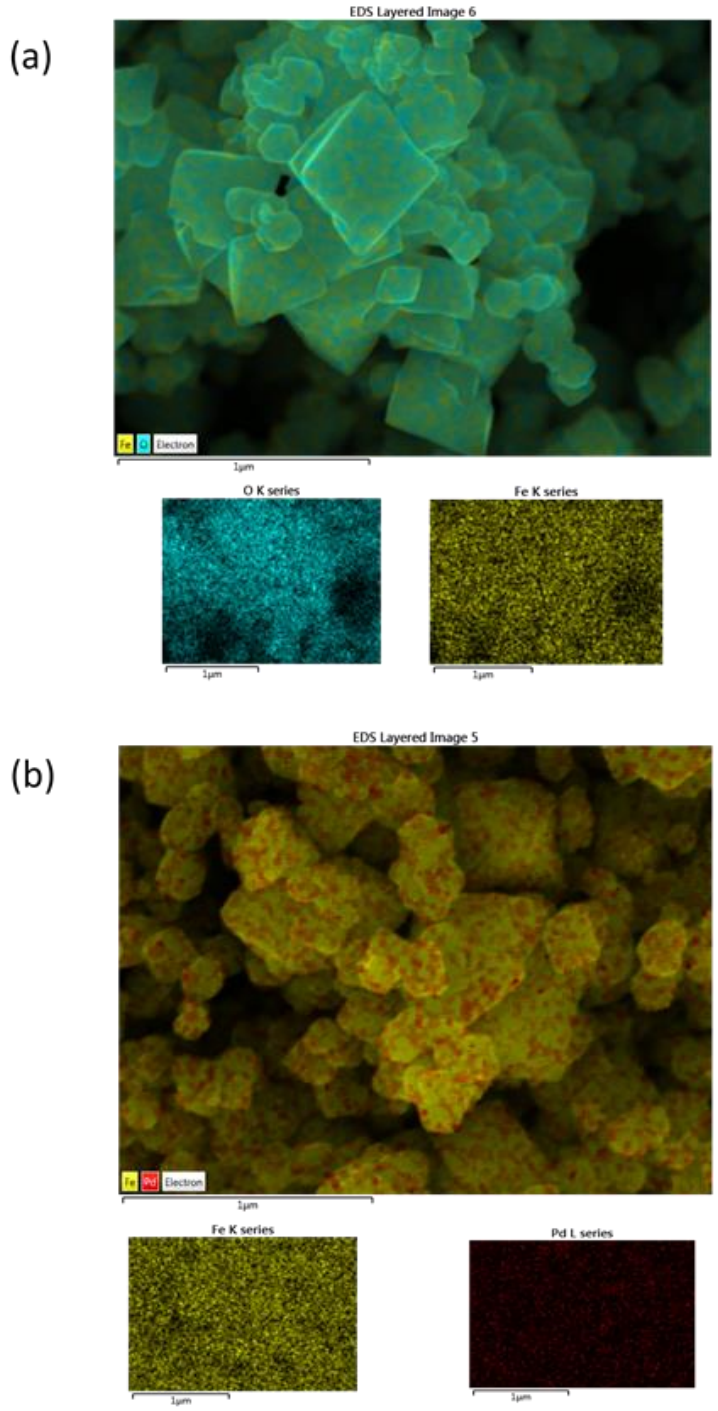

Figure II-17. The elemental analysis of NPs mapping images: (a) Fe_3O_4 NPs; (b) Pd–Fe_3O_4 NP

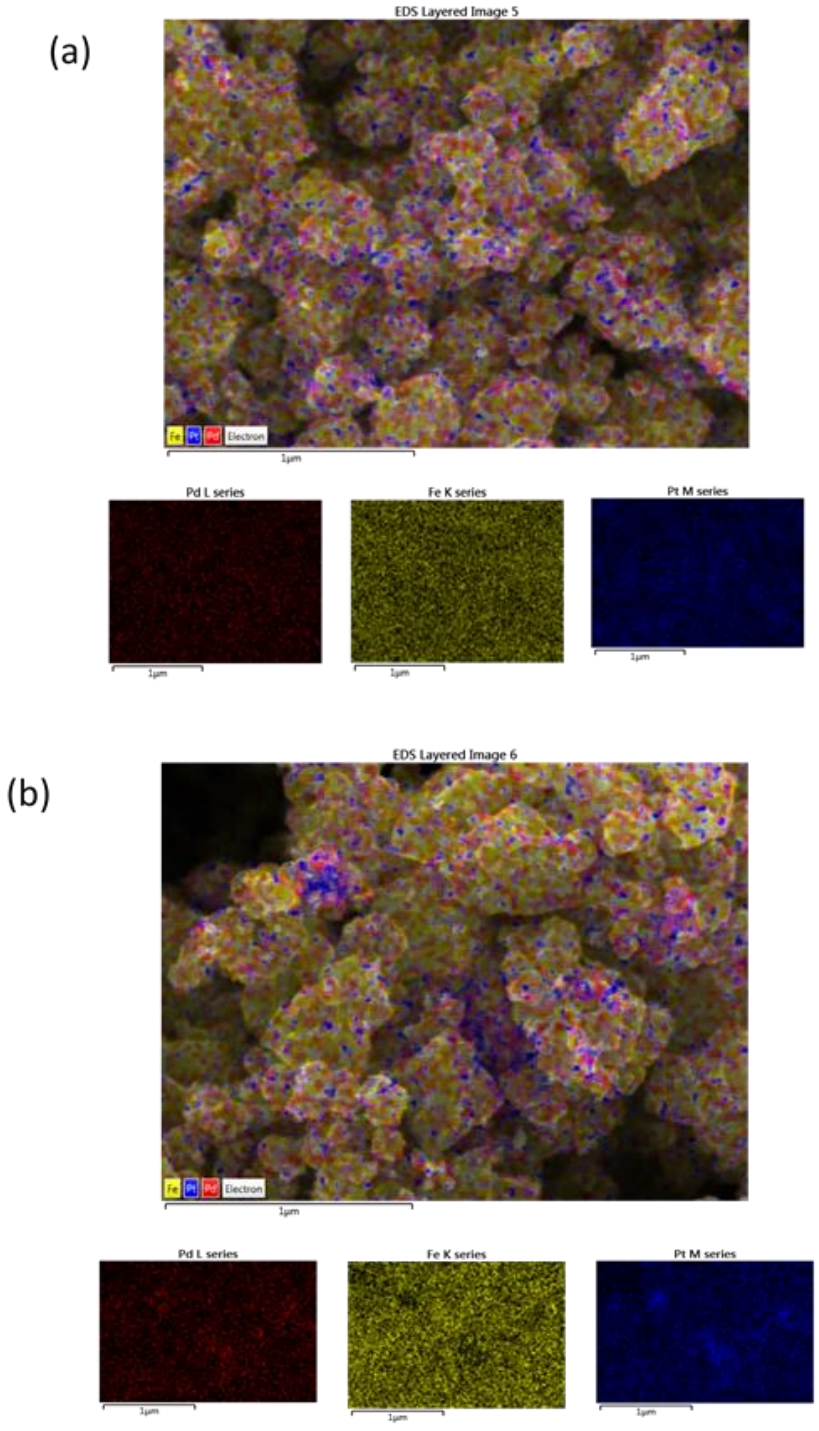

Figure II-18. The elemental analysis of NPs mapping images (a) fresh Pd–Pt–Fe_3O_4 NPs (b) Pd–Pt–Fe_3O_4 NPs after reaction 1 cycle of the catalytic reaction

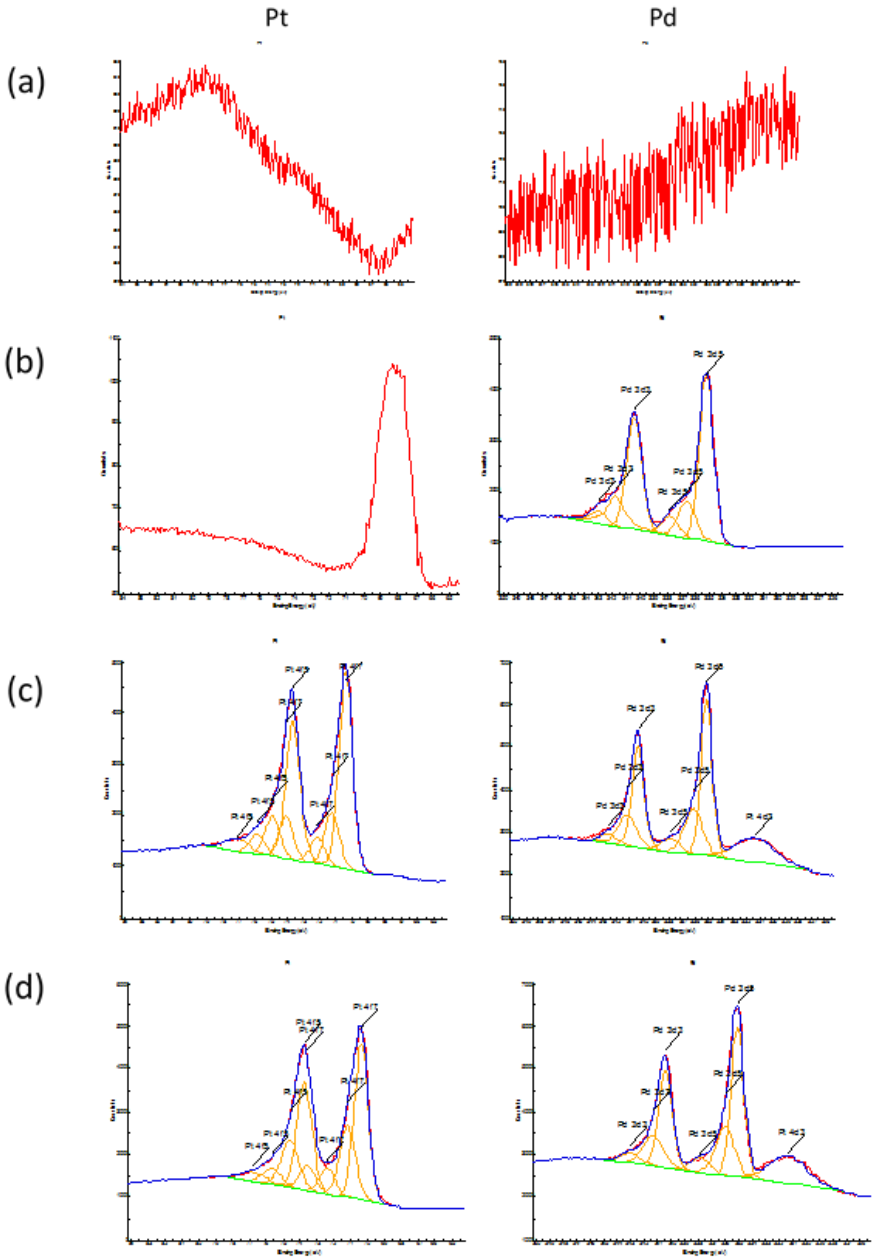

Figure II-19. X-ray photoelectron spectroscopy (XPS) spectrum of NPs: (a) Fe_3O_4 NPs; (b) Pd–Fe_3O_4 NPs; (c) fresh Pd–Pt–Fe_3O_4 NPs; (d) Pd–Pt–Fe_3O_4 NPs after 1 cycle of the catalytic reaction

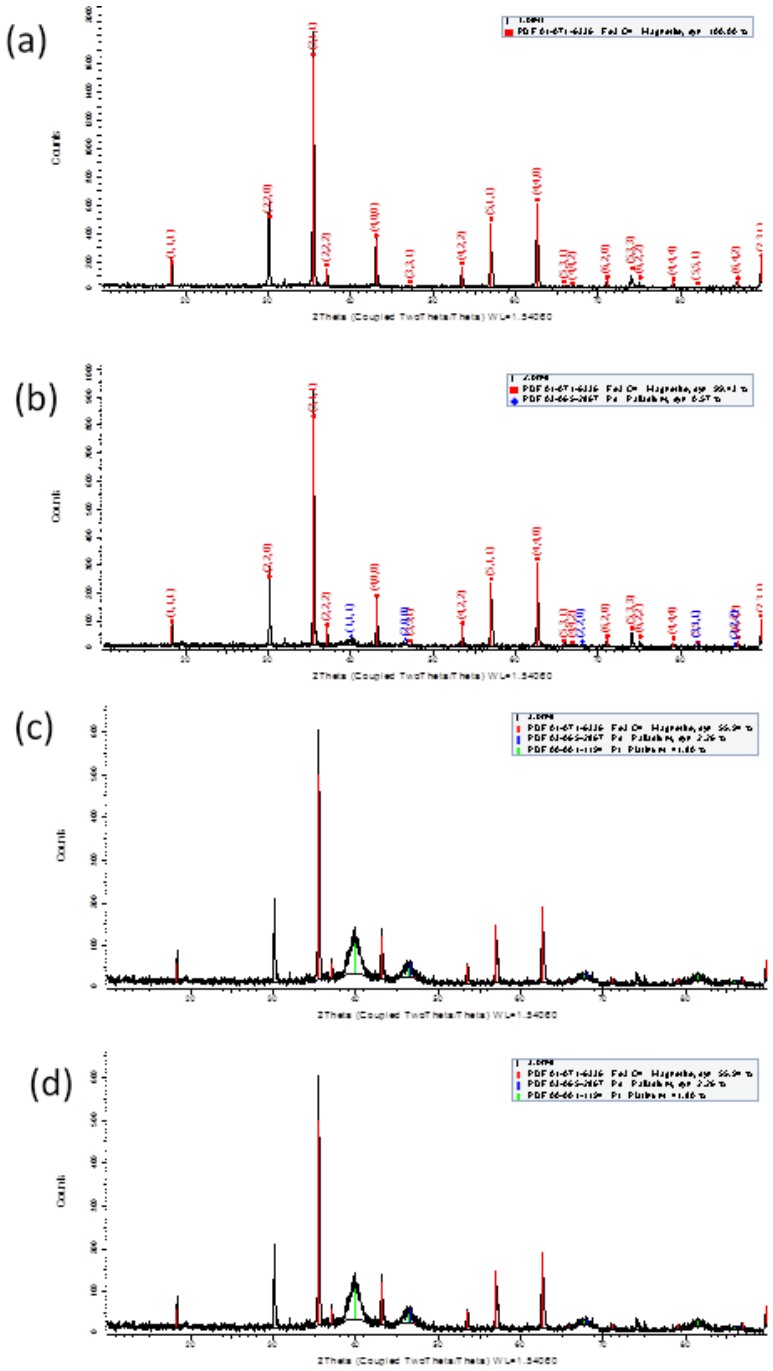

Figure II-20. X-ray diffraction spectroscopy (XRD) spectrum of NPs: (a) Fe_3O_4 NPs; (b) Pd–Fe_3O_4 NPs; (c) fresh Pd–Pt–Fe_3O_4 NPs; (d) Pd–Pt–Fe_3O_4 NPs after 1 cycle of the catalytic reaction

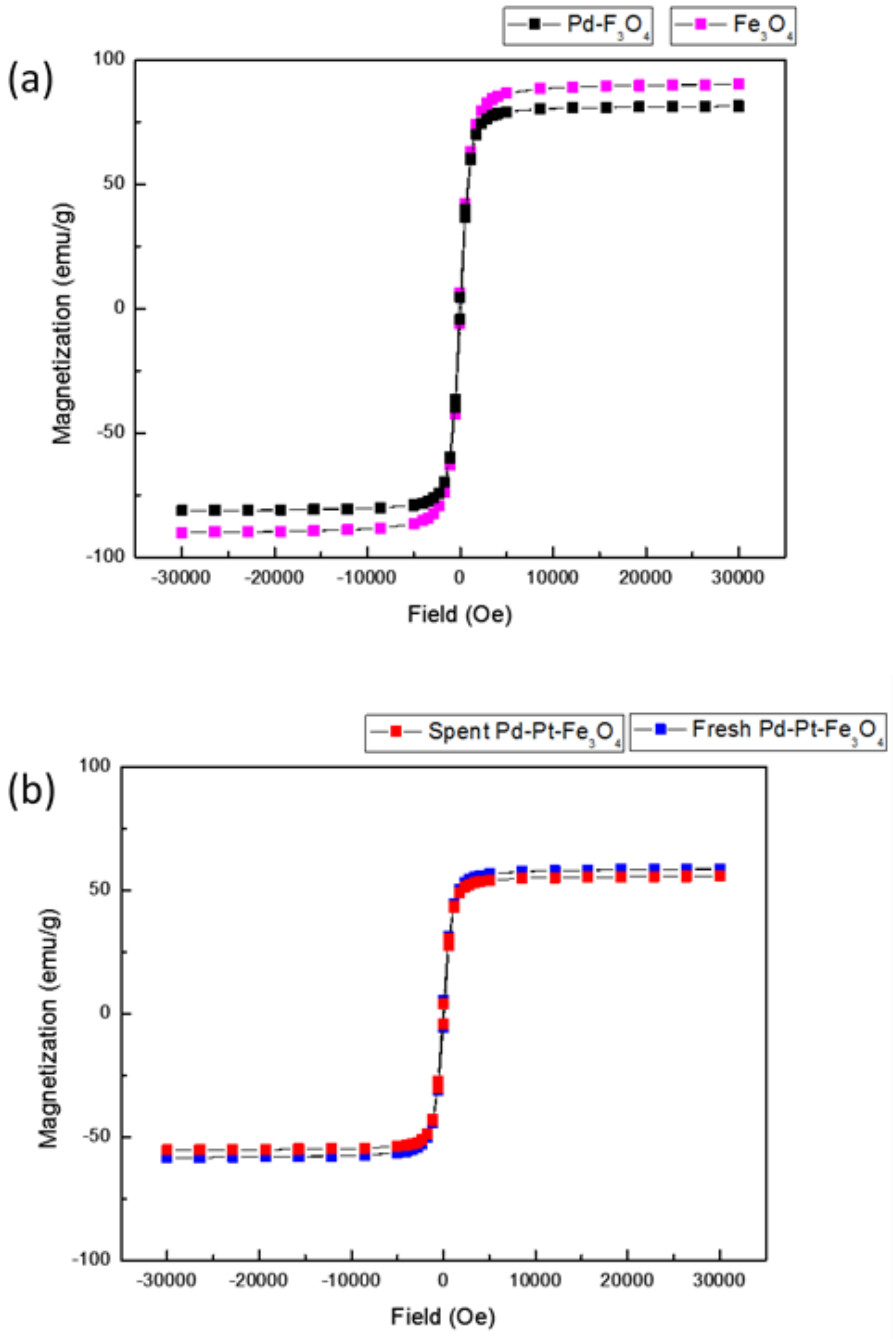

Figure II-21. Magnetic property measurement system (MPMS) spectrum of NPs: (a) Fe_3O_4 NPs (pink) and Pd–Fe_3O_4 NPs (black); (b) fresh Pd–Pt–Fe_3O_4 NPs (blue) and Pd–Pt–Fe_3O_4 NPs after 1 cycle of the catalytic reaction (red)

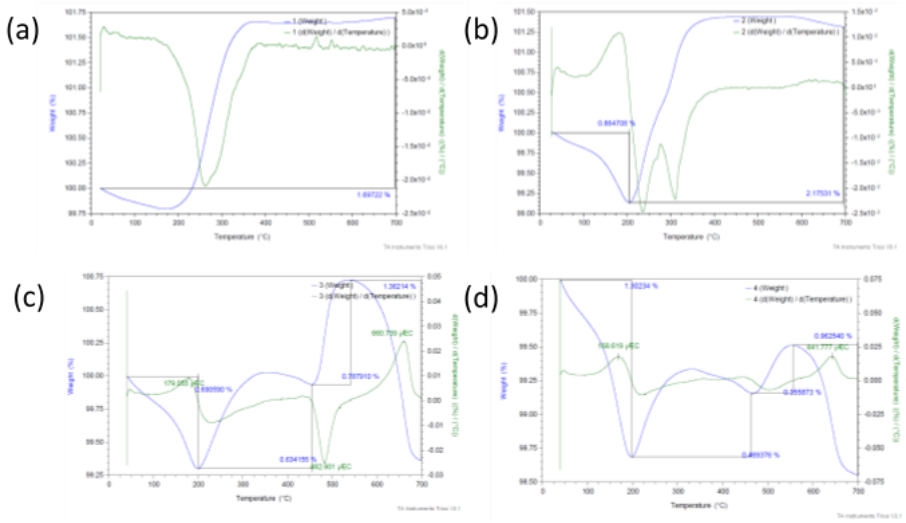

Figure II-22. Thermogravimetric analysis (TGA) curves of NPs: (a) Fe_3O_4 NPs; (b) Pd–Fe_3O_4 NPs; (c) fresh Pd–Pt–Fe_3O_4 NPs; (d) Pd–Pt–Fe_3O_4 NPs after 1 cycle of the catalytic reaction

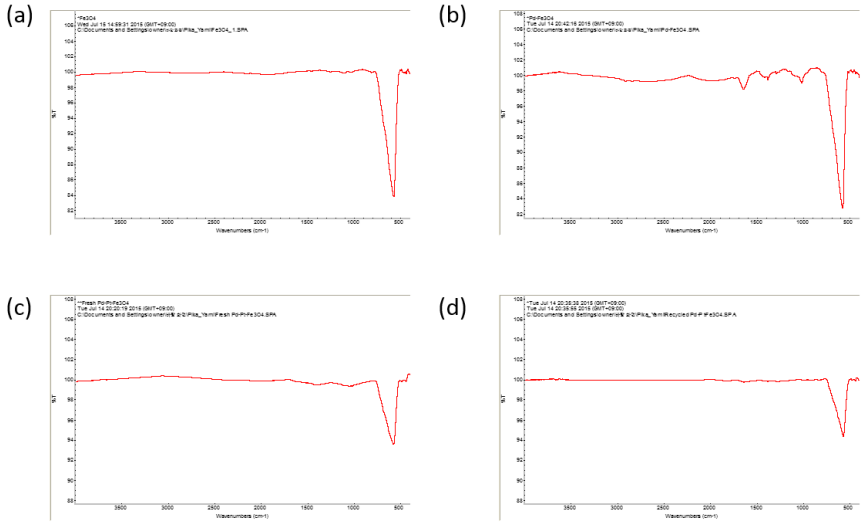

Figure II-23. Fourier transform infrared spectroscopy (FTIR) of NPs: (a) Fe_3O_4 NPs; (b) Pd–Fe_3O_4 NPs; (c) fresh Pd–Pt–Fe_3O_4 NPs; (d) Pd–Pt–Fe_3O_4 NPs after 1 cycle of the catalytic reaction

These analyses revealed that the composition, shape, size, and magnetic properties of the magnetically reusable nanocrystals remained nearly identical upon recycling, which explains the continuous, excellent catalytic activity of the Pd–Pt–Fe_3O_4 NPs. In contrast, the TEM, SEM, EDS, HR-TEM, ICP-AES data for the Pd–Pt–Fe_3O_4 NPs after the 300th cycle revealed significant changes in the physical properties of the catalyst. The TEM, HR-TEM, SEM images and ICP data clearly indicated agglomeration[69] of the loaded Pd and Pt NPs rather than detachment[70] from the support (**Figures II-24–28**, **Table II-12**). Therefore, the reduction in catalytic activity presumably occurred due to agglomeration of the Pd and Pt NPs on the surface of the Fe_3O_4 support.

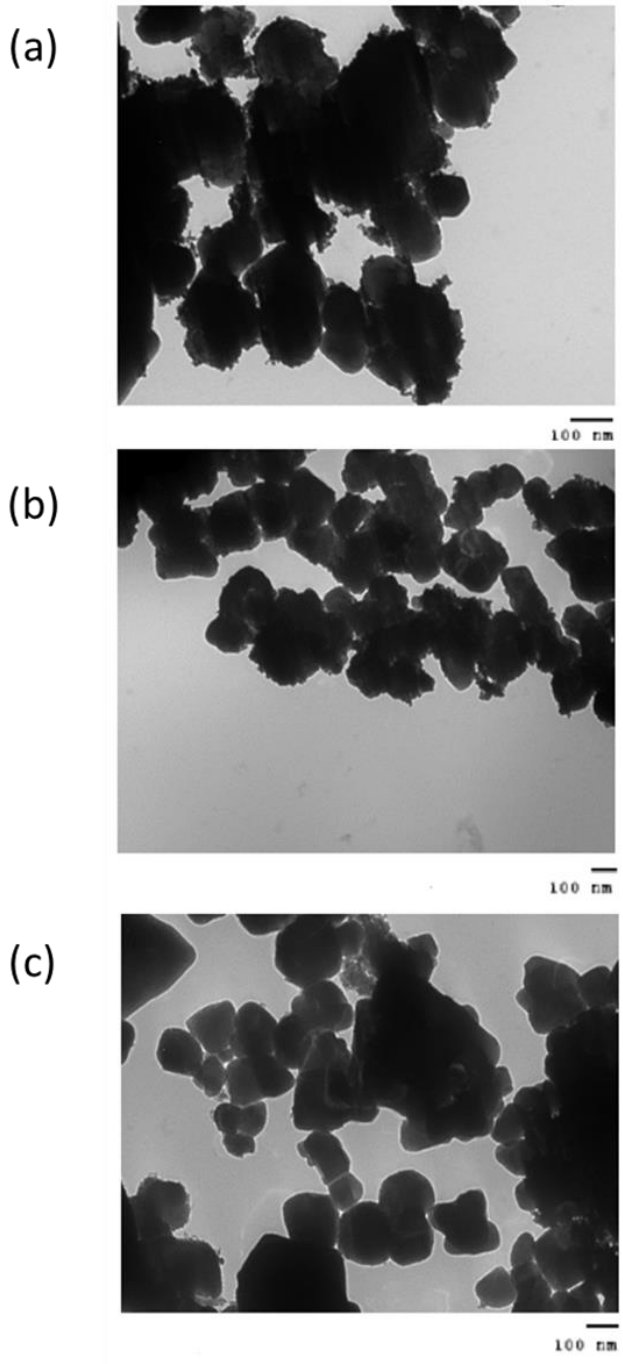

Figure II-24. TEM images of NPs: (a) Pd–Pt–Fe_3O_4 NPs after 10 cycles of the catalytic reaction; (b) Pd–Pt–Fe_3O_4 NPs after 30 cycles of the catalytic reaction; (c) Pd–Pt–Fe_3O_4 NPs after 300 cycles of the catalytic reaction

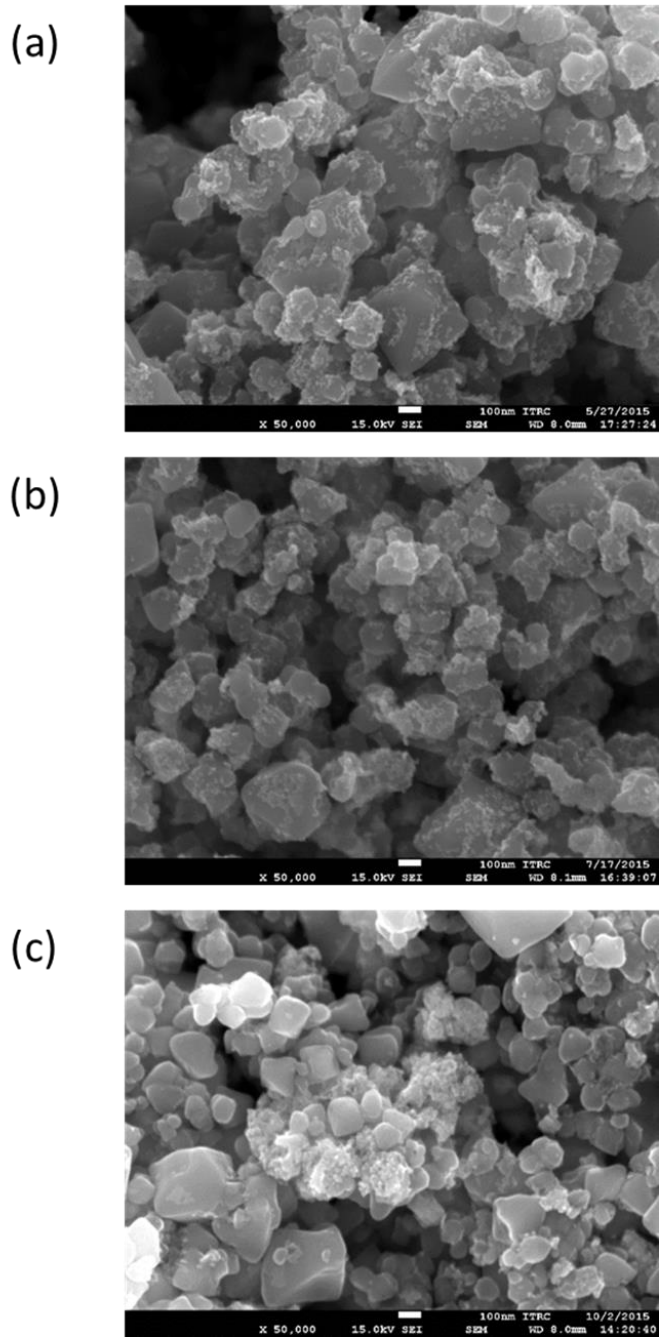

Figure II-25. SEM images of NPs: (a) Pd–Pt–Fe_3O_4 NPs after 10 cycles of the catalytic reaction; (b) Pd–Pt–Fe_3O_4 NPs after 30 cycles of the catalytic reaction; (c) Pd–Pt–Fe_3O_4 NPs after 300 cycles of the catalytic reaction

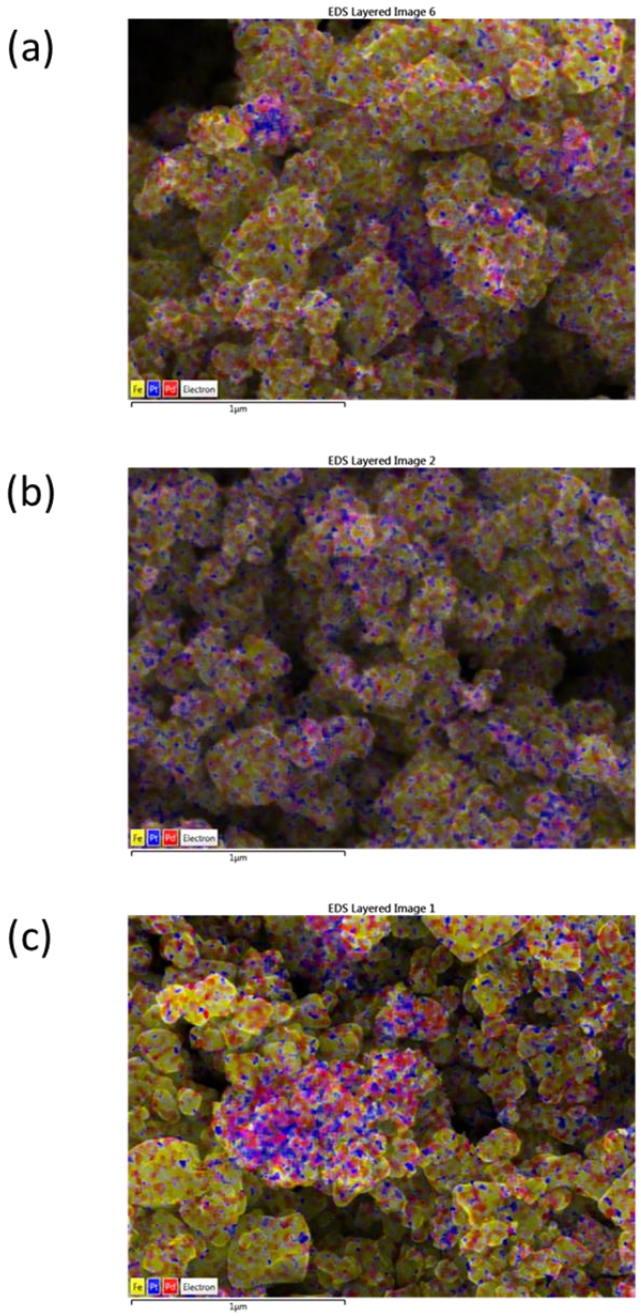

Figure II-26. The elemental analysis of NPs mapping images: (a) Pd–Pt–Fe_3O_4 NPs after 10 cycles of the catalytic reaction; (b) Pd–Pt–Fe_3O_4 NPs after 30 cycles of the catalytic reaction; (c) Pd–Pt–Fe_3O_4 NPs after 300 cycle of the catalytic reaction **(Red=Pd, Blue=Pt, Yellow= Fe)**

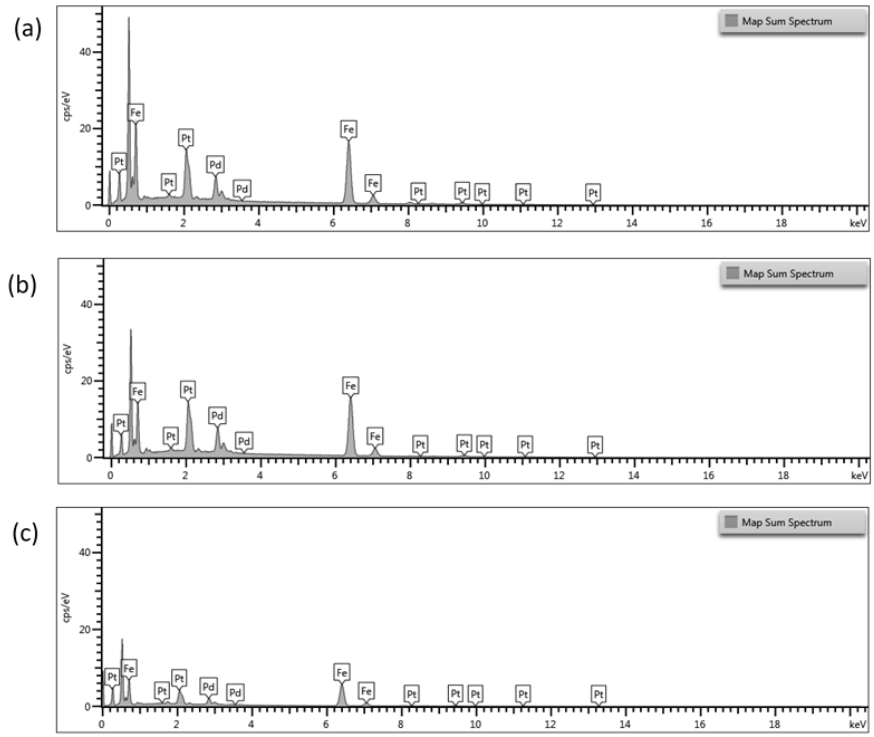

Figure II-27. The energy disperse spectroscopy (EDS) map sum spectrum pattern of NPs: (a) Pd–Pt–Fe_3O_4 NPs after 10 cycles of the catalytic reaction; (b) Pd–Pt–Fe_3O_4 NPs after 30 cycle of the catalytic reaction; (c) Pd–Pt–Fe_3O_4 NPs after 300 cycles of the catalytic reaction

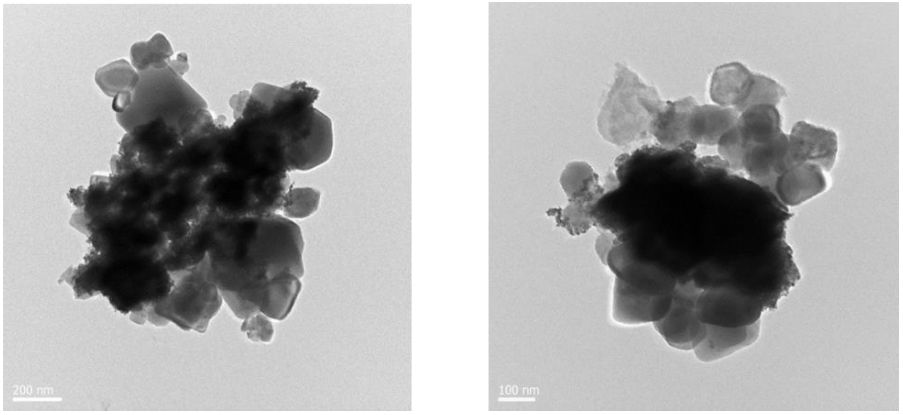

Figure S28. HR-TEM of Pd–Pt–Fe_3O_4 NPs after 300 cycle of the catalytic reaction

Table II-12. The weight % of elements through ICP-MS

Cycle number (n)	Pd (wt%)	Pt(wt%)
0 (Fresh)	5.1	8.3
10	5.0	8.1
30	5.1	8.2
300	5.0	8.0

3. Conclusion

The synthesis of bimetallic Pd–Pt–Fe_3O_4 NPs and their use as a catalyst for the reduction of nitro compounds is described. Using a simple hydrothermal method, nanoscale crystals of palladium and platinum alloy was deposited on the surfaces of Fe_3O_4 NPs. Detailed structural analysis of the catalyst system using HR-TEM, HAADF-STEM, Cs-TEM-EDS and STEM-EDS images was carried out, corroborating the Pd-Pt alloy NPs decorated on the Fe_3O_4 Nps. The nanoflake-shaped Pd-Pt–Fe_3O_4 NPs were superbly effective for catalyzing the dehydrogenation of ammonia-borane and reduction of R-NO_2 to R-NH_2 in methanol at room temperature in one pot. Various nitroarenes and nitroalkanes were smoothly reduced to the corresponding aniline derivatives with excellent conversions and yields in a very short time (5 min). Notably, reactions using the Pd–Pt–Fe_3O_4 catalyst proceeded faster than those using Pd–Fe_3O_4, Pt–Fe_3O_4, or a combination of both Pd–Fe_3O_4 and Pt–Fe_3O_4, revealing a unique synergistic effect of the bimetallic catalyst system. Under optimized conditions, the Pd–Pt–Fe_3O_4 nanocatalyst exhibited great applicability for large-scale reactions. In addition, the performance of the catalyst was excellent at a loading level of 0.001 mol% with high TON and TOF. Extremely good chemoselectivities were observed on nitroarene reduction in presence of *O*-allyl, *O*-benzyl or *O*-propargyl group, which are frequently used protecting groups. Importantly, the catalyst could be recovered using an external magnet in a very straightforward manner and was recycled 250 times without loss of activity. Therefore, this new catalyst system should be a very useful, sustainable, and environmentally friendly solution for industrial applications.

4. Experimental

Materials

All chemicals were commercially available and used as received without further purification. Potassium platinochloride (98 % purity), palladium chloride (99% purity) and polyvinylpyrrolidone (PVP) were purchased from Sigma-Aldrich. Iron oxide was purchased from Skyspring nanomaterials.

Characterization methods

All reaction products were identified through comparison with the authentic compounds and quantified through gas chromatography/mass spectrometry (GC-Mass) analysis using a Hewlett Packard 5890 Gas Chromatograph with anisole as an internal standard. All Transmission Electron Microscopy (TEM) images were obtained on a JEOL EM-2010 microscope at an accelerating voltage of 200 kV. The powder X-ray diffraction (XRD) was performed using a Bruker AXS D8 FOCUS (2 theta: 5-100, scan speed: 2degree/min, Cu Kαradiation: λ=1.54056nm, Generator: 40kV, 40m). Magnetic Property Measurement System (MPMS) was performed using a Quantum Design. The energy disperse spectroscopy (EDS) map sum spectrum pattern performed using an Oxford Instruments X-Maxn. (software: Aztex) Sonication was performed in a 120 W ultrasonic bath (Branson, B-3210) and Sonics & Vibra cell VCX 750. Fourier transform infrared (FT-IR) spectra were recorded on a Nicolet iS10 spectrometer through the use of KBr pellets. Thermogravimetric analysis (TGA) was performed on a TGA Q5000 V3.10 Build 258 instrument at a heating rate of 10 °C min-1 under a nitrogen flow.

Synthesis of the Pd–Pt–Fe_3O_4

The synthesis of Pd-Pt-Fe_3O_4 was performed as follows. First 800mg of potassium platinochloride (K_2PtCl_4), 340 mg of palladium(II) chloride ($PdCl_2$) and 1.00 g of polyvinylpyrrolidone (PVP) (Mw ～10,000) were dissolved in 80 mL of ethylene glycol (EG) in a 250 mL round-bottom flask. This mixture was sonicated for 10 min and heated for 1 h at 100°C in oil bath with magnetic stirring. Meanwhile, 1.00 g of Fe_3O_4 was dissolved in 300 mL of EG in a two-necked 500 mL round-bottom flask and then ultrasonication performed for 40 min. Next, with vigorously stirring of the Fe_3O_4 solution with a mechanical stirrer, the prepared platinum and palladium precursor solution was injected dropwise. The resulting solution was further processed at 100 °C for an additional 24 h. Afterward, the resultant sample could be retrieved via centrifugation and washing with absolute ethanol. Finally, the product was obtained via drying on a rotary evaporator.

General procedure for the catalytic cascade reduction reaction

The nanoflake-shaped Pd-Pt-Fe_3O_4 catalyst (1.00 mol %), R-NO_2 (0.500 mmol), anisole (internal standard, 0.500 mmol) and methanol (5.0 mL) were introduced in a glass vial (10 mL) with a magnetic stirrer bar. The mixture was sonicated for 1 min and stirred at room temperature for 5 min. Then, the ammonia-borane complex (1.50 mmol) was added to the reaction mixture, and the vessel was closed with a Teflon cover. This reaction was vigorously stirred for 5 min at room temperature. After completion of the reaction, an aliquot from the organic layer was analyzed with gas chromatography. The separation of the

catalyst was realized with a small magnet from outside of the vial. The remaining catalyst was washed three times with methanol. The solvent was then removed with the use of a rotary evaporator, therefore allowing the dried catalyst to be reused for a further recycling reaction.

General procedure for the recycling the Pd–Pt–Fe_3O_4

For the recycling test, the reduction of nitrobenzene was scaled up to 1.00 mmol and reductions were run using 1 mol% catalyst. Each reaction cycle was complete within 5 min at room temperature. After each reaction, the catalyst was separated with a magnet and washed with methanol. Nitrobenzene (1.00 mmol), anisole (1.00 mmol) and methanol (10 mL) were then added directly to the washed catalyst. Then the reaction was performed by applying the general procedure for the nitro-reduction reaction. The catalytic reactions were then repeated during 10 cycles. Each cycle was analyzed by gas chromatography mass spectrometry (GC-MS)

Reference of part II

(1) Mori, K.; Hara, T.; Mizugaki, T.; Ebitani, K.; Kaneda, K. Hydroxyapatite-Supported Palladium Nanoclusters: A Highly Active Heterogeneous Catalyst for Selective Oxidation of Alcohols by Use of Molecular Oxygen. *J. Am. Chem. Soc.* **2004**, *126*, 10657-10666.

(2) Wittmann, S.; Schatz, A.; Grass, R. N.; Stark, W. J.; Reiser, O. A Recyclable Nanoparticle-Supported Palladium Catalyst for the Hydroxycarbonylation of Aryl Halides in Water. *Angew. Chem. Int. Ed. Engl.* **2010**, *49*, 1867-1870.

(3) Mori, K.; Hara, T.; Mizugaki, T.; Ebitani, K.; Kaneda, K. Hydroxyapatite-Supported Palladium Nanoclusters: A Highly Active Heterogeneous Catalyst for Selective Oxidation of Alcohols by Use of Molecular Oxygen. *J. Am. Chem. Soc.* **2004**, *126*, 10657-10666.

(4) Karan, N. S.; Keller, A. M.; Sampat, S.; Roslyak, O.; Arefin, A.; Hanson, C. J.; Casson, J. L.; Desireddy, A.; Ghosh, Y.; Piryatinski, A.; Iyer, R.; Htoon, H.; Malko, A. V.; Hollingsworth, J. A. Plasmonic Giant Quantum Dots: Hybrid Nanostructures for Truly Simultaneous Optical Imaging, Photothermal Effect and Thermometry. *Chem Sci* **2015**, *6*, 2224-2236.

(5) Wei, G. F.; Liu, Z. P. Restructuring and Hydrogen Evolution on Pt Nanoparticle. *Chem Sci* **2015**, *6*, 1485-1490.

(6) Priebe, J. B.; Radnik, J.; Lennox, A. J. J.; Pohl, M.-M.; Karnahl, M.; Hollmann, D.; Grabow, K.; Bentrup, U.; Junge, H.; Beller, M.; Brückner, A. Solar Hydrogen Production by Plasmonic Au–Tio2catalysts: Impact of Synthesis Protocol and Tio2phase on Charge Transfer Efficiency and H2evolution Rates. *ACS Catal.* **2015**, *5*, 2137-2148.

(7) Stevens, P. D.; Li, G.; Fan, J.; Yen, M.; Gao, Y. Recycling of Homogeneous Pd Catalysts Using Superparamagnetic Nanoparticles as Novel Soluble Supports for Suzuki, Heck, and Sonogashira Cross-Coupling Reactions. *Chem. Commun.* **2005**, *35*, 4435-4437.

(8) Sun, Y.; Xia, Y. Mechanistic Study on the Replacement Reaction between Silver Nanostructures and Chloroauric Acid in Aqueous Medium. *J. Am. Chem. Soc.* **2004**, *126*, 3892-3901.

(9) Nikoobakht, B.; El-Sayed, M. A. Preparation and Growth Mechanism of Gold Nanorods (Nrs) Using Seed-Mediated Growth Method. *Chem. Mater.* **2003**, *15*, 1957-1962.

(10) Zeng, J.; Zhang, Q.; Chen, J.; Xia, Y. A Comparison Study of the Catalytic Properties of Au-Based Nanocages, Nanoboxes, and Nanoparticles. *Nano Lett.* **2010**, *10*, 30-35.

(11) Xu, Z.; Hou, Y.; Sun, S. Magnetic Core/Shell Fe_3O_4/Au and Fe_3O_4/Au/Ag Nanoparticles with Tunable Plasmonic Properties. *J. Am. Chem. Soc.* **2007**, *129*, 8698-8699.

(12) Bradley, M. J.; Biacchi, A. J.; Schaak, R. E. Chemical Transformation of Pt–Fe_3O4 colloidal Hybrid Nanoparticles into PtPb–Fe_3O_4 and Pt_3Sn–Fe_3O_4 heterodimers and (PtPb–Fe_3O_4) Nanoflowers. *Chem. Mater.* **2013**, *25*, 1886-1892.

(13) Buck, M. R.; Bondi, J. F.; Schaak, R. E. A Total-Synthesis Framework for the Construction of High-Order Colloidal Hybrid Nanoparticles. *Nat. Chem.* **2012,** *4*, 37-44.

(14) Sun, X.; Lin, L.; Li, Z.; Zhang, Z.; Feng, J., Novel Ag–Cu Substrates for Surface-Enhanced Raman Scattering. *Mater. Lett.* **2009,** *63*, 2306-2308.

(15) Maniecki, T. P.; Mierczynski, P.; Maniukiewicz, W.; Bawolak, K.; Gebauer, D.; Jozwiak, W. K. Bimetallic Au–Cu, Ag–Cu/$CrAl_3O_6$ Catalysts for Methanol Synthesis. *Catal. Lett.* **2009**, *130*, 481-488.

(16) Choi, S.-W.; Katoch, A.; Sun, G.-J.; Kim, S. S. Bimetallic Pd/Pt Nanoparticle-Functionalized SnO_2 Nanowires for Fast Response and Recovery to NO_2. *Sens. Actuators, B* **2013**, *181*, 446-453.

(17) Wu, Y.; Cai, S.; Wang, D.; He, W.; Li, Y. Syntheses of Water-Soluble Octahedral, Truncated Octahedral, and Cubic Pt-Ni Nanocrystals and Their Structure-Activity Study in Model Hydrogenation Reactions. *J. Am. Chem. Soc.* **2012**, *134*, 8975-8981.

(18) Wang, Q.; Li, Y.; Liu, B.; Dong, Q.; Xu, G.; Zhang, L.; Zhang, J. Novel Recyclable Dual-Heterostructured Fe_3O_4@CeO_2/M (M = Pt, Pd and Pt–Pd)

Catalysts: Synergetic and Redox Effects for Superior Catalytic Performance. *J. Mater. Chem. A* **2015**, *3*, 139-147.

(19) Li, X.; Wang, X.; Liu, D.; Song, S.; Zhang, H. Multifunctional Nanostructures Based on Porous Silica Covered Fe_3O_4@CeO_2-Pt Composites: A Thermally Stable and Magnetically-Recyclable Catalyst System. *Chem. Commun.* **2014**, *50*, 7198-7201.

(20) Lu, A. H.; Salabas, E. L.; Schuth, F. Magnetic Nanoparticles: Synthesis, Protection, Functionalization, and Application. *Angew. Chem. Int. Ed. Engl.* **2007**, *46*, 1222-1244.

(21) Wang, D.; Astruc, D. Fast-Growing Field of Magnetically Recyclable Nanocatalysts. *Chem. Rev.* **2014**, *114*, 6949-6985.

(22) Polshettiwar, V.; Luque, R.; Fihri, A.; Zhu, H.; Bouhrara, M.; Basset, J. M. Magnetically Recoverable Nanocatalysts. *Chem. Rev.* **2011**, *111*, 3036-3075.

(23) Gawande, M. B.; Branco, P. S.; Varma, R. S. Nano-Magnetite (Fe_3O_4) as a Support for Recyclable Catalysts in the Development of Sustainable Methodologies. *Chem. Soc. Rev.* **2013**, *42*, 3371-3393.

(24) Lim, C. W.; Lee, I. S. Magnetically Recyclable Nanocatalyst Systems for the Organic Reactions. *Nano Today* **2010**, *5*, 412-434.

(25) Vernekar, A. A.; Patil, S.; Bhat, C.; Tilve, S. G. Magnetically Recoverable Catalytic Co–Co_2B Nanocomposites for the Chemoselective Reduction of Aromatic Nitro Compounds. *RSC Adv.* **2013,** *3*, 13243-13250.

(26) Kim, D.; Guengerich, F. P. Cytochrome P450 Activation of Arylamines and Heterocyclic Amines. *Annu. Rev. Pharmacol. Toxicol.* **2005**, *45*, 27-49.

(27) Tafesh, A. M.; Weiguny, J. A Review of the Selective Catalytic Reduction of Aromatic Nitro Compounds into Aromatic Amines, Isocyanates, Carbamates, and Ureas Using CO. *Chem. Rev.* **1996**, *96*, 2035-2052.

(28) Merlic, C. A.; Motamed, S.; Quinn, B. Structure Determination and Synthesis of Fluoro Nissl Green: An Rna-Binding Fluorochrome. *J. Org. Chem.* **1995**, *60*, 3365-3369.

(29) Wegener, G.; Brandt, M.; Duda, L.; Hofmann, J.; Klesczewski, B.; Koch, D.; Kumpf, R. J.; Orzesek, H.; Pirkl, H. G.; Six, C.; Steinlein, C.; Weisbeck, M. Trends in Industrial Catalysis in the Polyurethane Industry. *Appl. Catal., A* **2001**, *221*, 303-335.

(30) Kantam, M. L.; Chakravarti, R.; Pal, U.; Sreedhar, B.; Bhargava, S. Nanocrystalline Magnesium Oxide-Stabilized Palladium(0): An Efficient and Reusable Catalyst for Selective Reduction of Nitro Compounds. *Adv. Synth. Catal.* **2008**, *350*, 822-827.

(31) Mandal, P. K.; McMurray, J. S. Pd-C-Induced Catalytic Transfer Hydrogenation with Triethylsilane. *J. Org. Chem.* **2007**, *72*, 6599-6601.

(32) Corma, A.; Serna, P.; Concepcion, P.; Calvino, J. J. Transforming Nonselective into Chemoselective Metal Catalysts for the Hydrogenation of Substituted Nitroaromatics. *J. Am. Chem. Soc.* **2008**, *130*, 8748-8753.

(33) Maity, P.; Basu, S.; Bhaduri, S.; Lahiri, G. K. Superior Performance of a Nanostructured Platinum Catalyst in Water: Hydrogenations of Alkenes, Aldehydes and Nitroaromatics. *Adv. Synth. Catal.* **2007**, *349*, 1955-1962.

(34) Takasaki, M.; Motoyama, Y.; Higashi, K.; Yoon, S. H.; Mochida, I.; Nagashima, H. Chemoselective Hydrogenation of Nitroarenes with Carbon Nanofiber-Supported Platinum and Palladium Nanoparticles. *Org. Lett.* **2008**, *10*, 1601-1604.

(35) Corma, A.; Serna, P. Chemoselective Hydrogenation of Nitro Compounds with Supported Gold Catalysts. *Science* **2006**, *313*, 332-334.

(36) He, L.; Wang, L. C.; Sun, H.; Ni, J.; Cao, Y.; He, H. Y.; Fan, K. N. Efficient and Selective Room-Temperature Gold-Catalyzed Reduction of Nitro Compounds with CO and H_2O as the Hydrogen Source. *Angew. Chem. Int. Ed. Engl.* **2009**, *48*, 9538-9541.

(37) Yamane, Y.; Liu, X.; Hamasaki, A.; Ishida, T.; Haruta, M.; Yokoyama, T.; Tokunaga, M.,One-Pot Synthesis of Indoles and Aniline Derivatives from Nitroarenes under Hydrogenation Condition with Supported Gold Nanoparticles. *Org. Lett.* **2009**, *11*, 5162-5165.

(38) Jagadeesh, R. V.; Surkus, A. E.; Junge, H.; Pohl, M. M.; Radnik, J.; Rabeah, J.; Huan, H.; Schunemann, V.; Bruckner, A.; Beller, M. Nanoscale Fe_2O_3-Based Catalysts for Selective Hydrogenation of Nitroarenes to Anilines. *Science* **2013**, *342*, 1073-1076.

(39) Wienhofer, G.; Baseda-Kruger, M.; Ziebart, C.; Westerhaus, F. A.; Baumann, W.; Jackstell, R.; Junge, K.; Beller, M. Hydrogenation of Nitroarenes Using Defined Iron-Phosphine Catalysts. *Chem. Commun.* **2013**, *49*, 9089-9091.

(40) Westerhaus, F. A.; Jagadeesh, R. V.; Wienhofer, G.; Pohl, M. M.; Radnik, J.; Surkus, A. E.; Rabeah, J.; Junge, K.; Junge, H.; Nielsen, M.; Bruckner, A.; Beller, M. Heterogenized Cobalt Oxide Catalysts for Nitroarene Reduction by Pyrolysis of Molecularly Defined Complexes. *Nat. Chem.* **2013**, *5*, 537-543.

(41) Shi, Q.; Lu, R.; Lu, L.; Fu, X.; Zhao, D. Efficient Reduction of Nitroarenes over Nickel-Iron Mixed Oxide Catalyst Prepared from a Nickel-Iron Hydrotalcite Precursor. *Adv. Synth. Catal.* **2007**, *349*, 1877-1881.

(42) Saha, A.; Ranu, B. Highly Chemoselective Reduction of Aromatic Nitro Compounds by Copper Nanoparticles/Ammonium Formate. *J. Org. Chem.* **2008**, *73*, 6867-6870.

(43) Blaser, H.-U.; Steiner, H.; Studer, M. Selective Catalytic Hydrogenation of Functionalized Nitroarenes: An Update. *ChemCatChem* **2009**, *1*, 210-221.

(44) Kadam, H. K.; Tilve, S. G. Advancement in Methodologies for Reduction of Nitroarenes. *RSC Adv.* **2015,** *5*, 83391-83407.

(45) Mohapatra, S. K.; Sonavane, S. U.; Jayaram, R. V.; Selvam, P. Heterogeneous Catalytic Transfer Hydrogenation of Aromatic Nitro and Carbonyl Compounds over Cobalt(II) Substituted Hexagonal Mesoporous Aluminophosphate Molecular Sieves. *Tetrahedron Lett*. **2002**, 43, 8527-8529.

(46) Gawande, M. B.; Rathi, A. K.; Branco, P. S.; Nogueira, I. D.; Velhinho, A.; Shrikhande, J. J.; Indulkar, U. U.; Jayaram, R. V.; Ghumman, C. A.; Bundaleski, N.; Teodoro, O. M. Regio- and Chemoselective Reduction of Nitroarenes and Carbonyl Compounds over Recyclable Magnetic Ferrite-Nickel Nanoparticles (Fe_3O_4-Ni) by Using Glycerol as a Hydrogen Source. *Chem. Eur. J.* **2012**, 18, 12628-12632.

(47) Kim, J. H.; Park, J. H.; Chung, Y. K.; Park, K. H. Ruthenium Nanoparticle-Catalyzed, Controlled and Chemoselective Hydrogenation of Nitroarenes Using Ethanol as a Hydrogen Source. *Adv. Synth. Catal.* **2012**, *354*, 2412-2418.

(48) Vasilikogiannaki, E.; Gryparis, C.; Kotzabasaki, V.; Lykakis, I. N.; Stratakis, M. Facile Reduction of Nitroarenes into Anilines and Nitroalkanes into Hydroxylaminesviathe Rapid Activation of Ammonia· Borane Complex by Supported Gold Nanoparticles. *Adv. Synth. Catal.* **2013**, *355*, 907-911.

(49) Couturier, M.; Tucker, J. L.; Andresen, B. M.; Dube, P.; Negri, J. T. Palladium and Raney Nickel Catalyzed Methanolic Cleavage of Stable Borane-Amine Complexes. *Org. Lett.* **2001**, *3*, 465-467.

(50) Göksu, H.; Ho, S. F.; Metin, Ö.; Korkmaz, K.; Mendoza Garcia, A.; Gültekin, M. S.; Sun, S. Tandem Dehydrogenation of Ammonia Borane and Hydrogenation of Nitro/Nitrile Compounds Catalyzed by Graphene-Supported Nipd Alloy Nanoparticles. *ACS Catal.* **2014**, *4*, 1777-1782.

(51) Jang, Y.; Kim, S.; Jun, S. W.; Kim, B. H.; Hwang, S.; Song, I. K.; Kim, B. M.; Hyeon, T. Simple One-Pot Synthesis of Rh–Fe_3O_4 Heterodimer Nanocrystals and Their Applications to a Magnetically Recyclable Catalyst for Efficient and Selective Reduction of Nitroarenes and Alkenes. *Chem. Commun.* **2011**, *47*, 3601-3603.

(52) Jang, Y.; Chung, J.; Kim, S.; Jun, S. W.; Kim, B. H.; Lee, D. W.; Kim, B. M.; Hyeon, T. Simple Synthesis of Pd–Fe_3O_4 Heterodimer Nanocrystals and Their Application as a Magnetically Recyclable Catalyst for Suzuki Cross-Coupling Reactions. *Phys. Chem. Chem. Phys.* **2011**, *13*, 2512-2516.

(53) Chung, J.; Kim, J.; Jang, Y.; Byun, S.; Hyeon, T.; Kim, B. M. Heck and Sonogashira Cross-Coupling Reactions Using Recyclable Pd–Fe_3O_4 Heterodimeric Nanocrystal Catalysts. *Tetrahedron Lett.* **2013**, *54* (38), 5192-5196.

(54) Lee, J.; Chung, J.; Byun, S. M.; Kim, B. M.; Lee, C. Direct Catalytic C–H Arylation of Imidazo[1,2-*a*]Pyridine with Aryl Bromides Using Magnetically Recyclable Pd–Fe_3O_4 Nanoparticles. *Tetrahedron* **2013**, *69*, 5660-5664.

(55) Bae, I. H.; Lee, I.-H.; Byun, S.; Chung, J.; Kim, B. M.; Choi, T.-L. Magnetically Recyclable Pd–Fe_3O_4 heterodimer Nanocrystals for the Synthesis of Conjugated Polymers Via Suzuki Polycondensation: Toward Green Chemistry. *J. Polym. Sci., Part A: Polym. Chem.* **2014**, *52*, 1525-1528.

(56) Byun, S.; Chung, J.; Jang, Y.; Kwon, J.; Hyeon, T.; Kim, B. M. Highly Selective Wacker Oxidation of Terminal Olefins Using Magnetically Recyclable Pd–Fe_3O_4 Heterodimer Nanocrystals. *RSC Adv.* **2013**, *3*, 16296-16299.

(57) Byun, S.; Chung, J.; Lim, T.; Kwon, J.; Kim, B. M. Synthesis of Benzil Derivatives Via Oxidation of Alkynes Catalyzed by Pd–Fe_3O_4 Heterodimer Nanocrystals. *RSC Adv.* **2014**, *4*, 34084-34088.

(58) Byun, S.; Chung, J.; Kwon, J.; Moon Kim, B. Mechanistic Studies of Magnetically Recyclable Pd – Fe_3O_4 Heterodimeric Nanocrystal-Catalyzed Organic Reactions. *Chem. Asian. J.* **2015**, *10*, 982-988.

(59) Wang, H.; Qiao, X.; Chen, J.; Wang, X.; Ding, S. Mechanisms of PVP in the Preparation of Silver Nanoparticles. *Mater. Chem. Phys.* **2005**, *94*, 449-453.

(60) Fernandez-Lopez, C.; Mateo-Mateo, C.; Alvarez-Puebla, R. A.; Perez-Juste, J.; Pastoriza-Santos, I.; Liz-Marzan, L. M. Highly Controlled Silica Coating of Peg-Capped Metal Nanoparticles and Preparation of Sers-Encoded Particles. *Langmuir* **2009**, *25*, 13894-13899.

(61) Yang, W.; Yang, C.; Sun, M.; Yang, F.; Ma, Y.; Zhang, Z.; Yang, X. Green Synthesis of Nanowire-Like Pt Nanostructures and Their Catalytic Properties. *Talanta* **2009**, *78*, 557-564.

(62) Peuckert, M.; Bonzel, H. P. Characterization of Oxidized Platinum Surfaces by X-Ray Photoelectron Spectroscopy. *Surf. Sci.* **1984**, *145*, 239-259.

(63) Kim, K. S.; Gossmann, A. F.; Winograd, N. X-Ray Photoelectron Spectroscopic Studies of Palladium Oxides and the Palladium-Oxygen Electrode. *Anal. Chem.* **1974**, *46*, 197-200.

(64) Wang, W.; Huang, Q.; Liu, J.; Zou, Z.; Li, Z.; Yang, H. One-Step Synthesis of Carbon-Supported Pd–Pt Alloy Electrocatalysts for Methanol Tolerant Oxygen Reduction. *Electrochem. Commun.* **2008**, *10*, 1396-1399.

(65) Kim, E.; Jeong, H. S.; Kim, B. M. Efficient Chemoselective Reduction of Nitro Compounds and Olefins Using Pd–Pt Bimetallic Nanoparticles on Functionalized Multi-Wall-Carbon Nanotubes. *Catal. Commun.* **2014**, *45*, 25-29.

(66) Ramachandran, P. V.; Gagare, P. D. Preparation of Ammonia Borane in High Yield and Purity, Methanolysis, and Regeneration. *Inorg. Chem.* **2007**, *46*, 7810-7817.

(67) Kim, S.; Kim, E.; Kim, B. M. Fe_3O_4 Nanoparticles: A Conveniently Reusable Catalyst for the Reduction of Nitroarenes Using Hydrazine Hydrate. *Chem. Asian J.* **2011**, *6*, 1921-1925.

(68) Bhattacharjya, A.; Klumphu, P.; Lipshutz, B. H. Ligand-Free, Palladium-Catalyzed Dihydrogen Generation from Tmds: Dehalogenation of Aryl Halides on Water. *Org. Lett.* **2015**, *17*, 1122-1125.

(69) Liang, S.; Jasinski, J.; Hammond, G. B.; Xu, B. Supported Gold Nanoparticle-Catalyzed Hydration of Alkynes under Basic Conditions. *Org. Lett.* **2015**, *17*, 162-165.

(70) Bartholomew, C. H. Mechanisms of Catalyst Deactivation. *Appl. Catal., A* **2001**, *212*, 17-60.

Appendix A (NMR data)

Part I. Chapter 2

Table I-2.3

1. Benzil

^{1}H NMR (CD_3Cl_3) δ 7.49 (4H, dd, *J* = 6.8, 7.3 Hz), 7.64 (2H, t, *J* = 6.8 Hz), 7.89 (4H, t, *J* = 7.3 Hz); ^{13}C NMR (CD_3Cl_3) δ 128.9, 129.8, 132.9, 134.8, 194.5; MS (EI) m/z 210 (M^+, 10%),105 (100), 77 (50), 51 (20); HRMS (EI) calcd for $C_{14}H_{10}O_2$ (M^+) 210.06808. Found 210.06771. These ^{1}H NMR and ^{13}C NMR were identical with those reported in the literature.[1]

2. 1-Phenyl-2-*p*-tolylethane-1,2-dione

^{1}H NMR ($CDCl_3$) δ 2.41 (3H, s), 7.29 (2H, d, *J* = 8.3 Hz),7.48 (2H, dd, *J* = 7.2, 7.3 Hz), 7.63 (1H, t, *J* = 7.3 Hz), 7.86 (2H, d, *J* = 8.3 Hz), 7.96 (2H, d, *J* = 7.2Hz); ^{13}C NMR ($CDCl_3$) δ 21.8, 128.9, 129.6, 129.7, 129.9, 130.4, 133.0, 134.7, 194.2, 194.7; MS (EI) m/z 224 (M^+, 10%), 119 (100), 105 (20), 77 (15); HRMS (EI) calcd for $C_{15}H_{12}O_2$ (M^+) 224.06808. Found 224.08295. The ^{1}H and ^{13}C NMR spectra were identical with those reported in the literature.[2]

3. 1-(4-Methoxyphenyl)-2-phenylethane-1,2-dione

^{1}H NMR ($CDCl_3$) δ 3.88 (3H, s), 6.97 (2H, d, *J* = 8.8 Hz),7.50 (2H, dd, *J* = 7.9, 8.0 Hz), 7.64 (1H, t, *J* = 8.0 Hz), 7.94–7.98 (4H, m); ^{13}C NMR ($CDCl_3$) δ 55.6,114.3, 126.1, 128.9, 129.9, 132.3, 133.2, 134.7, 165.0, 193.1, 194.7; MS (EI) m/z 240 (M^+, 5%), 135(100), 92 (10), 77 (20); HRMS (EI) calcd for $C_{15}H_{12}O_3$ (M^+) 240.07865. Found 240.07806. The ^{1}H and ^{13}C NMR spectra were identical with those reported in the literature.[2]

4. 1-(3-Methoxyphenyl)-2-phenylethane-1,2-dione

^{1}H NMR ($CDCl_3$) δ 3.86 (3H, s), 7.21 (1H, dd, *J* = 1.6, 8.2 Hz), 7.40 (1H, t, *J* = 8.2 Hz), 7.47–7.55 (4H, m), 7.66 (1H, t, *J* = 7.2 Hz), 7.97 (2H, d, 7.7 Hz); ^{13}C NMR ($CDCl_3$) δ 55.4, 112.8, 121.8, 123.1, 129.0, 129.8, 130.0, 132.9, 134.2, 134.8, 160.0, 194.4, 194.4; MS (EI) m/z 240 (M^+, 20%), 135 (100), 105 (40), 77 (40); HRMS (EI) calcd for $C_{15}H_{12}O_3$ (M^+) 240.07865. Found 240.07833. The ^{1}H and ^{13}C NMR spectra were identical with those reported in the literature.[2]

5. 1-(2-Methoxyphenyl)-2-phenylethane-1,2-dione

^{1}H NMR ($CDCl_3$) δ 3.56 (3H, s), 6.93 (1H, d, *J* = 8.0 Hz), 7.13 (1H, t, *J* = 8.0 Hz), 7.49 (2H, dd, *J* = 1.2, 8.1 Hz), 7.58–7.63 (2H, m), 7.92 (2H, dd, *J* = 8.0, 8.1 Hz), 8.03 (1H, dd, *J* = 1.2, 8.1 Hz); ^{13}C NMR ($CDCl_3$) δ 55.7, 112.4, 121.6, 123.9, 128.7, 129.3, 130.6, 133.0,133.7, 136.4, 160.4, 193.4, 194.6; MS (EI) m/z 240 (M^+, 20%), 135 (100), 105 (45), 77 (40); HRMS (EI) calcd for $C_{15}H_{12}O_3$ (M^+) 240.07865. Found 240.07912. The ^{1}H and ^{13}C NMR spectra were identical with those reported in the literature.[2]

6. 1,2-Bis(4-methoxyphenyl)ethane-1,2-dione

^{1}H NMR ($CDCl_3$) δ 3.88 (6H, s), 6.97 (4H, d, *J* = 9.0 Hz), 7.96 (4H, d, *J* = 9.0 Hz); ^{13}C NMR ($CDCl_3$) δ 55.6, 114.2, 126.2, 132.1, 132.3, 164.8, 193.4; MS (EI) m/z 270 (M^+, 10%), 135 (100), 120 (10), 105 (20), 77 (20); HRMS (EI) calcd for $C_{16}H_{14}O$ (M^+) 270.08921. Found 270.08973. The ^{1}H and ^{13}C NMR spectra were identical with those reported in theliterature.[2]

7. 1-(4-Ethylphenyl)-2-(4-methoxyphenyl)ethane-1,2-dione

^{1}H NMR ($CDCl_3$): δ 7.94-7.89 (m, 2H),7.86 (d, 2H, *J*=8.2 Hz), 7.29 (d, 2H, *J*=8.2 Hz), 6.96-6.92 (m, 2H), 3.85 (s, 3H), 2.69 (q, 2H, *J*=7.6 Hz), 1.22 (t, 3H, *J*=7.6 Hz); ^{13}C NMR ($CDCl_3$): δ 194.59, 193.37, 164.86, 152.06, 132.29, 130.93, 130.08, 128.46, 126.14, 114.27, 55.57, 29.11, 15.00; IR (KBr, $cm^{-}1$): ν 2968, 2934, 2841, 1665; HRMS-ESI (m/z): $[M^{+}Na]^{+}$ calcd for $C_{17}H_{16}O_3Na$ 291.0997; found 291.0994.[3]

8. 1-(4-Trimethylsilylphenyl)-2-phenylethane-1,2-dione

Yellow solid, mp 60-63ºC; ^{1}H NMR ($CDCl_3$, 400 MHz): δ 7.97-7.90 (m, 4H), 7.67-7.63 (m, 3H), 7.48 (t, 2H, *J* = 7.8 Hz), 0.29(s, 9H); ^{13}C NMR ($CDCl_3$): δ 194.85, 194.61, 149.89, 134.79,133.79, 133.00, 132.96, 129.83, 128.96, 128.61, -1.49; IR (KBr, $cm^{-}1$): ν 3066, 2957, 2897, 2802, 1675; HRMS-ESI (m/z): $[M^{+}Na]^{+}$ calcd for $C_{17}H_{18}O_2SiNa$ 305.0974; found 305.0971.[3]

9. 1-(4-Chlorophenyl)-2-phenylethane-1,2-dione

^{1}H NMR ($CDCl_3$) δ 7.45–7.51 (4H, m), 7.64 (1H, t, 7.4 Hz), 7.89–7.96 (4H, m); ^{13}C NMR ($CDCl_3$) δ 129.0, 129.4, 129.9, 131.1, 131.2, 131.3, 132.7, 135.0, 141.5, 193.0, 193.8; MS (EI) m/z 244 (M^+, 5%), 139 (40), 105 (100), 77 (40); HRMS (EI) calcd for $C_{14}H_9Cl$ (M^+) 244.02911. Found 240.03001. The ^{1}H and ^{13}C NMR spectra were identical with those reported in the literature.[2]

10. 1-(4-bromophenyl)-2-phenylethane-1,2-dione

^{1}H NMR (400 MHz, $CDCl_3$) δ 7.89 (d, *J* = 7.6Hz, 2H), 7.77 (d, *J* = 8.4 Hz, 2H), 7.60 (t, *J* = 8.4 Hz, 3H), 7.45 (t, *J* = 7.6 Hz, 2H). ^{13}C NMR (101MHz, CDCl3) δ 193.8, 193.3, 135.1, 132.7, 132.4, 131.7, 131.2, 130.5, 129.9, 129.1.[4]

11. 1,2-Bis(4-bromophenyl)ethane-1,2-dione

H NMR ($CDCl_3$) δ 7.83 (4H, d, *J* = 8.5 Hz), 7.67 (4H, d, *J* = 8.5 Hz)ppm.[5]

12. 1-(4-acetylphenyl)-2-phenylethane-1,2-dione

^{1}H NMR (400 MHz, $CDCl_3$) δ 8.08 (s, 4H), 7.98 (d, *J* = 7.6 Hz, 2H), 7.69 (t, *J* = 7.6 Hz, 1H), 7.54 (t, *J* = 7.8 Hz, 2H), 2.66 (s, 3H).[6]

13. 1-(4-Nitrophenyl)-2-phenylethane-1,2-dione

^{1}H NMR ($CDCl_3$) δ 7.55 (2H, dd, *J* = 7.2, 7.7 Hz), 7.71 (1H, t, *J* = 7.2 Hz), 7.99 (2H, d, *J* = 7.7 Hz), 8.17 (2H, d, 8.8 Hz), 8.34 (2H, d, 8.8 Hz); ^{13}C NMR ($CDCl_3$) δ 124.1, 129.2, 130.0, 130.9, 132.4, 135.4, 137.3, 151.1, 192.0, 192.8; MS (M^+H^+ m/z 256 (M^+, 10%), 154 (100), 136 (70), 105 (60); HRMS (FAB^+, m-nitrobenzylalchol) calcd for $C_{14}H_9NO_4$ (M^+H^+) 256.06098. Found 256.06021. The ^{1}H and ^{13}C NMR spectra were identical with those reported in the literature.[2]

14. 4-(2-Oxo)-2-phenylacetyl benzonitrile

^{1}H NMR ($CDCl_3$) δ 7.55 (2H, t, *J* = 8.0 Hz), 7.69 (1H, t, *J* = 8.0Hz), 7.80 (2H, d, *J* = 8.6 Hz), 7.96 (2H, d, 8.6 Hz), 8.08 (2H, d, 8.0 Hz); ^{13}C NMR ($CDCl_3$) δ 117.4,117.8, 129.1, 129.9, 130.1, 132.3, 132.6, 135.2, 135.7, 192.2, 192.8; MS (EI) m/z 235 (M^+, 5%), 135(10), 105 (100), 77 (40); HRMS (EI) calcd for $C_{15}H_9NO_2$ (M^+) 235.06333. Found 235.06300. The ^{1}H and ^{13}C NMR spectra were identical with those reported in the literature.[1]

References

1. S. Urgaonkar and J. G. Verkade, *J. Org. Chem.*, 2004, **69**, 5752-5755.

2. A. Giraud, O. Provot, J.-F. Peyrat, M. Alami and J.-D. Brion, *Tetrahedron*, 2006, **62**, 7667-7673.

3. A. Gao, F. Yang, J. Li and Y. Wu, *Tetrahedron*, 2012, **68**, 4950-4954.

4. W. Ren, Y. Xia, S. J. Ji, Y. Zhang, X. Wan and J. Zhao, *Org. Lett.*, 2009, **11**, 1841-1844.

5. F. Romanov-Michailidis, C. Besnard and A. Alexakis, *Org. Lett.*, 2012, **14**, 4906-4909.

6. M.-J. Wu, J.-H. Chu and Y.-J. Chen, *Synthesis*, **2009**, 2155-2162.

Part II

Table II-6.

NMR S1. Aniline[1]

^{1}H-NMR (400 MHz, $CDCl_3$) δ: 7.16 (m, 2H), 6.77 (m, 1H), 6.69 (m, 2H), 3.35 (s, 2H). ^{13}C-NMR (100 MHz, $CDCl_3$) δ: 146.41, 129.41, 118.73, 115.26

NMR S2. Amino-4-chlorobenzene[2]

^{1}H-NMR (400 MHz, $CDCl_3$) δ: 7.08 (d, J = 8.4 Hz, 2 H), 6.58 (d, J = 8.8 Hz, 2 H), 3.63 (s, br, 2 H). ^{13}C-NMR (100 MHz, $CDCl_3$) δ: 144.90, 129.05, 123.05, 116.17

NMR S3. Amino-4-bromobenzene[3]

^{1}H-NMR (400 MHz, $CDCl_3$) **δ:** 7.24 (d, **J**=8.72 Hz, 2 H), 6.55 (d, **J**=8.72 Hz, 2 H), 3.67 (br s, 2 H). ^{13}C-NMR (100 MHz, $CDCl_3$) **δ**: 146.0, 131.8, 117.1, 109.0

NMR S4. 4- Iodoaniline[4]

^{1}H-NMR (400 MHz, $CDCl_3$) δ: 7.44 (d, *J*=8.6 Hz, 2H), 6.48 (d, *J*=8.6 Hz, 2H), 3.69 (bs, 2H, NH). ^{13}C-NMR (100 MHz, $CDCl_3$) δ: 79.6, 117.5, 138.1, 146.3.

NMR S5. 4- Methoxyaniline[5]

^{1}H-NMR (400 MHz, $CDCl_3$) δ: 6.75 (d, J = 8.9 Hz, 2H), 6.65 (d, J = 8.9 Hz, 2H), 3.75 (s, 3H), 3.41 (s, 2H, NH). ^{13}C-NMR (100 MHz, $CDCl_3$) δ: 152.9, 140.0, 116.6, 114.9, 55.9

NMR S6. 4-Aminophenol[1]

^{1}H-NMR (400 MHz, DMSO-d6) δ: 6.45 (d, J = 8.56 Hz, 2H), 6.38 (d, J = 8.56 Hz, 2H), 4.35 (br. s, 2H). ^{13}C-NMR (100 MHz, DMSO-d6) δ: 149.10, 141.12, 115.98, 115.66

NMR S7. *p*- Toluidine[5]

^{1}H-NMR (400 MHz, $CDCl_3$) δ: 6.99 (d, J = 8.3 Hz, 2H), 6.63 (d, J = 8.3 Hz, 2H), 3.53 (s, 2H, NH), 2.26 (s, 3H). ^{13}C-NMR (100 MHz, $CDCl_3$) δ: 143.9, 129.9, 127.9, 115.4, 20.6

NMR S8. 4-*tert*-Butylaniline[2]

^{1}H-NMR (400 MHz, $CDCl_3$) δ: 7.05 (d, J = 8.4 Hz, 2 H), 6.55 (d, J = 8.8 Hz, 2 H), 3.44 (s, br, 2 H), 1.20 (s, 9 H). ^{13}C-NMR (100 MHz, $CDCl_3$) δ: 143.74, 141.32, 125.98, 114.86, 33.85, 31.49

NMR S9. N, N-Dimethyl-p-phenylenediamine[6]

^{1}H-NMR (400 MHz, $CDCl_3$) δ: 6.71 – 6.64 (4H, m), 3.19 (2H, s, br), 2.82

(6H, s). ^{13}C-NMR (100 MHz, $CDCl_3$) δ: 144.7, 138.0, 116.5, 115.5, 42.0

NMR S10. Methyl-4-aminobenzoate[5]

^{1}H-NMR (400 MHz, $CDCl_3$) δ: 7.84 (d, J = 8.1 Hz, 2H), 6.63 (d, J = 8.1 Hz, 2H), 4.05 (s, 2H, NH), 3.85 (s, 3H). ^{13}C-NMR (100 MHz, $CDCl_3$) δ: 167.3, 151.0, 131.7, 119.7, 113.9, 51.8

NMR S11. 2, 6-Diaminotoluene[7]

^{1}H-NMR (400 MHz, $CDCl_3$) δ: 6.84 (t, J = 8.0 Hz, 1H), 6.20 (d, J = 8.0 Hz, 2H), 3.56 (bs, 4H), 1.98 (s, 3H). ^{13}C-NMR (100 MHz, $CDCl_3$) δ: 145.3, 126.9, 107.4, 106.8, 10.3

NMR S12. Aminonaphthalene[8]

^{1}H-NMR (400 MHz, DMSO-d6) δ: 7.95 (m, 1H), 7.73 (m, 1H), 7.39 (m, 2H), 7.22 (m, 2H), 6.80 (m, 1H). ^{13}C-NMR (100 MHz, DMSO-d6) δ: 143.3, 134.8, 128.0, 126.2, 125.4, 124.2, 121.4, 118.1, 109.5

NMR S13. 4-Aminobiphenyl[1]

^{1}H-NMR (400 MHz, $CDCl_3$) δ: 7.34 (m, 5H), 7.53 (m, 4H). ^{13}C-NMR (100 MHz, $CDCl_3$) δ: 144.79, 129.58, 129.06, 123.17, 120.52, 116.25, 115.47, 115.26

NMR S14. 2, 7- Diaminofluorene[9]

^{1}H-NMR (400 MHz, $CDCl_3$) δ: 7.75 (d, 3 JH,H = 7.0 Hz, 4 H), 7.46 (t, 3 JH,H = 7.3 Hz, 2 H), 7.42–7.38 (m, 6 H), 7.28–7.23 (m, 6 H), 7.17–7.13 (m, 4 H), 6.89–6.86 (m, 2 H), 6.66 (dd, 3 JH,H = 8.0, 4 JH,H = 1.9 Hz, 2 H), 3.62 (s, 2 H). ^{13}C-NMR (100 MHz, $CDCl_3$): δ = 167.8, 149.7, 143.7, 139.9, 137.1, 136.4, 130.6, 129.6, 129.3, 128.5, 128.2, 128.0, 119.9, 119.2, 118.0, 36.8

NMR S15. 4-cyanoaniline[1]

^{1}H-NMR (400 MHz, $CDCl_3$) δ: 7.41 (d, J = 8.36 Hz, 2H), 6.62 (d, J = 11.48 Hz, 2H), 4.13 (br. s, 2H). ^{13}C-NMR (100 MHz, $CDCl_3$) δ: 150.45, 133.96, 120.20, 114.58, 100.50

NMR S16. 5- Amino-2-chlorobenzonitrile[10]

^{1}H-NMR (400 MHz, $CDCl_3$) δ: 7.24 (d, 1H), 6.91 (d, 1H), 6.8 (dd, 1H), 3.91 (s, 2H)

NMR S17. 2, 6-Dimethylaniline[11]

^{1}H-NMR (400 MHz, $CDCl_3$) δ: 6.83 (2H, d, J = 7.5 Hz), 6.46 (1H, t, J = 7.5 Hz), 4.49 (2H, br s), 2.12 (6H, s). ^{13}C-NMR (100 MHz, $CDCl_3$) δ: 144.16, 127.81, 120.60, 115.89, 17.8

NMR S18. Cyclohexylamine[12]

^{1}H-NMR (400 MHz, $CDCl_3$) δ: 2.67-2.58 (m, 1H), 2.01-1.56(m, 6H), 1.32-0.98 (m, 4H); ^{13}C-NMR (100 MHz, $CDCl_3$) δ: 49.78, 36.01, 25.00, 24.46

NMR S19. Aminohexane[4]

^{1}H-NMR (400 MHz, $CDCl_3$) δ: 2.69 (t, *J*=6.5 Hz, 2H), 1.50-1.05 (m, 10H), 0.89 (t, *J*=5.6 Hz, 3H). ^{13}C-NMR (100 MHz, $CDCl_3$) δ: 42.3, 34.1, 31.7, 26.3, 22.8, 14.0

Scheme II-1 and 2

NMR S20. Nitro-4-(vinyloxy)benzene[13]

^{1}H-NMR (400 MHz, $CDCl_3$) δ 4.72 (dd, J = 6.0,2.0 Hz, 1H), 5.02 (dd, J = 13.6, 2.0 Hz, 1H), 6.70 (dd, J = 13.6, 6.0 Hz, 1H), 7.10 (m, 2H), 8.26 (m, 2H); ^{13}C-NMR(100 MHz, $CDCl_3$): δ 99.1, 116.3, 125.8, 142.9, 145.8, 161.5

NMR S21. 1-Nitro-4-(prop-2-ynyloxy)benzene[14]

^{1}H-NMR (400 MHz, $CDCl_3$): 8.22 (d, J = 9.5 Hz, 2H), 7.05 (d, J = 9.5 Hz, 2H), 4.79 (d, J = 2.5 Hz, 2H), 2.58 (t, J = 2.5 Hz, 1H). ^{13}C NMR (100 MHz, $CDCl_3$): 162.3, 142.2, 125.8, 115.0, 77.1, 76.7, 56.3

NMR S22. 4-Allyloxyaniline[4]

^{1}H-NMR (400 MHz, $CDCl_3$) δ: 6.62 (d, J=6.2 Hz, 2H), 6.51 (d, J=6.2 Hz, 2H), 5.89 (ddt, J=16.3 Hz, 11.9 Hz, 2.8 Hz, 1H), 5.16 (d, J=16.3 Hz, 1H), 4.97

(d, J=11.9 Hz, 1H), 4.21 (d, J=2.8 Hz, 2H). 13C-NMR (100 MHz, $CDCl_3$) δ: 152.0, 140.3, 134.1, 117.5, 116.7, 116.2, 69.9.

NMR S23. 4-(Ethynyloxy)) aniline[15]

^{1}H-NMR (400 MHz, $CDCl_3$): δ 7.29 (d, 2H, J = 8.64 Hz), 6.59 (d, 2H, J = 8.67 Hz), 3.81 (s, 2H), 2.96 (s, 1H). ^{13}C-NMR (100 MHz, $CDCl_3$): δ 146.98, 133.41, 114.53, 111.21, 84.36, 74.89.

NMR S24. 4-benzyloxyaniline[4]

^{1}H-NMR (400 MHz, $CDCl_3$) δ: 7.40 (m, 5H), 6.85 (d, *J*=8.7 Hz, 2H), 6.66 (s, *J*=8.7 Hz, 2H), 5.02 (s, 2H), 3.37 (bs, 2H). ^{13}C-NMR (100 MHz, $CDCl_3$) δ: 152.0, 140.3, 137.6, 128.4, 127.7, 127.4, 116.3, 116.2, 70.9

NMR S25. Aminoacetophenone[15]

^{1}H-NMR (400 MHz, $CDCl_3$) δ: 7.71 (1H, d, *J* = 8.0 Hz), 7.30–7.10 (3H, m), 6.76 (1H, d, *J* = 8.0 Hz), 6.53 (1H, t, *J* = 8.0 Hz), 2.50 (3H, s). ^{13}C-NMR (100 MHz, $CDCl_3$) δ: 200.15, 151.04, 134.17, 132.22, 116.85, 114.38, 27.84

REFERENCES

(1) Kumar, A.; Purkait, K.; Dey, S. K.; Sarkar, A.; Mukherjee, A. A Hydroquinone Based Palladium Catalyst for Room Temperature Nitro Reduction in Water. *RSC Advances* **2014**, *4*, 35233-35237.

(2) Shen, Q.; Hartwig, J. F. Palladium-Catalyzed Coupling of Ammonia and Lithium Amide with Aryl Halides. *J. Am. Chem. Soc.* **2006**, *128*, 10028-10029.

(3) Kamal, A.; Markandeya, N.; Shankaraiah, N.; Reddy, C. R.; Prabhakar, S.; Reddy, C. S.; Eberlin, M. N.; Silva Santos, L. Chemoselective Aromatic Azido Reduction with Concomitant Aliphatic Azide Employing Al/Gd Triflates/NaI and ESI-Ms Mechanistic Studies. *Chem. Eur. J.* **2009**, *15*, 7215-7224.

(4) Orlandi, M.; Tosi, F.; Bonsignore, M.; Benaglia, M. Metal-Free Reduction of Aromatic and Aliphatic Nitro Compounds to Amines: A $HSiCl_3$-Mediated Reaction of Wide General Applicability. *Org. Lett.* **2015**, *17*, 3941-3943.

(5) Lee, D. Y.; Hartwig, J. F. Zinc Trimethylsilylamide as a Mild Ammonia Equivalent and Base for the Amination of Aryl Halides and Triflates. *Org. Lett.* **2005**, *7*, 1169-1172.

(6) Tao, C.-Z.; Li, J.; Fu, Y.; Liu, L.; Guo, Q.-X. Copper-Catalyzed Synthesis of Primary Arylamines from Aryl Halides and 2,2,2-Trifluoroacetamide. *Tetrahedron Lett.* **2008**, *49*, 70-75

(7) Wu, G. G.; Chen, F. X.; LaFrance, D.; Liu, Z.; Greene, S. G.; Wong, Y. S.; Xie, J. A Novel Iodide-Catalyzed Reduction of Nitroarenes and Aryl Ketones with H_3PO_2 or H_3PO_3: Its Application to the Synthesis of a Potential Anticancer Agent. *Org. Lett.* **2011**, *13*, 5220-5223.

(8) Göksu, H. Recyclable Aluminium Oxy-Hydroxide Supported Pd Nanoparticles for Selective Hydrogenation of Nitro Compounds Via Sodium Borohydride Hydrolysis. *New J. Chem.* **2015**, *39*, 8498-8504.

(9) Rotzler, J.; Vonlanthen, D.; Barsella, A.; Boeglin, A.; Fort, A.; Mayor, M. Variation of the Backbone Conjugation in Nlo Model Compounds: Torsion-

Angle-Restricted, Biphenyl-Based Push-Pull-Systems. *Eur. J. Org. Chem.* **2010**, *2010*, 1096-1110.

(10) Uthuppu, B.; Aamand, J.; Jorgensen, C.; Kiersgaard, S. M.; Kostesha, N.; Jakobsen, M. H. Optimization of an Immunoassay of 2,6-Dichlorobenzamide (BAM) and Development of Regenerative Surfaces by Immunosorbent Modification with Newly Synthesised Bam Hapten Library. *Anal. Chim. Acta* **2012**, *748*, 95-103.

(11) Ntaganda, R.; Dhudshia, B.; Macdonald, C. L.; Thadani, A. N. Cross-Coupling of Aryl/Heteroaryl Bromides with Ammonia Using a Copper-Carbene Catalyst. *Chem. Commun.* **2008**, 6200-6202.

(12) Damodara, D.; Arundhathi, R.; Ramesh Babu, T. V.; Legan, M. K.; Kumpaty, H. J.; Likhar, P. R. Polymethylhydrosiloxane Derived Palladium Nanoparticles for Chemo- and Regioselective Hydrogenation of Aliphatic and Aromatic Nitro Compounds in Water. *RSC Adv.* **2014**, *4*, 22567-22574.

(13) Blouin, M.; Frenette, R., A New Method for the Preparation of Aryl Vinyl Ethers. *J. Org. Chem* **2001**, *66*, 9043-9045.

(14) Lykakis, I. N.; Efe, C.; Gryparis, C.; Stratakis, M., $Ph_3PAuNTf_2$ as a Superior Catalyst for the Selective Synthesis of *2H*-Chromenes: Application to the Concise Synthesis of Benzopyran Natural Products. *Eur. J. Org. Chem.* **2011**, *2011*, 2334-2338.

(15) Udumula, V.; Tyler, J. H.; Davis, D. A.; Wang, H.; Linford, M. R.; Minson, P. S.; Michaelis, D. J., Dual Optimization Approach to Bimetallic Nanoparticle Catalysis: Impact of M_1/M_2 ratio and Supporting Polymer Structure on Reactivity. *ACS Catal.* **2015**, *5*, 3457-3462.

국문초록

I. 재사용 가능한 이종 팔라듐–산화철 나노결정을 이용한 효과적인 유기 반응 개발 및 메커니즘 규명

제 1장에서는, 이종 팔라듐-산화철 나노촉매를 이용한 웨커 산화 반응을 진행하였다. 일반적으로 웨커 산화 반응은 말단기의 이중결합을 케톤으로 바꾸는 유기화학적 프로세스에서 매우 중요한 반응이다. 우리는 초상자성 이종 나노 크리스탈을 기반으로 하는 팔라듐-산화철 입자를 이용하여 높은 선택성과, 좋은 반응성, 친환적 조건을 충족시키는 웨커 반응 프로세스에 대한 연구를 진행하였다. 다양한 반응조건을 탐색하던 도중, 원하는 종류의 유기물질을 높은 선택성으로 확인하였다. 친환경적 조건으로 용매를 물과 에탄올을 사용하였으며, 1 기압의 산소 조건을 이용하였다. 또한 산화반응의 프로세스 후에, 손쉽게 팔라듐-산화철 나노촉매를 외부 자석을 이용하여 여러 번의 재사용 가능하게 하였다.

제 2장에서는, 팔라듐-산화철 나노 촉매를 이용한 웨커 타입의 산화 반응을 효과적이며성공적으로 반복적 수행이 가능하였다. 1,2-다이케톤기를 가진 벤질 구조의 물질들은 구조의 특이성 때문에 유기합성적으로 매우 다양한 방법을 통하여 합성 되어 왔다. 본연구는 이러한 벤질 구조는 철의 부식을 막는 물질, 카르복실레이즈 인히비터, 광민감성 물질들에서 많은 구조를 보임에 이러한 구조를 팔라듐-산화철 나노 촉매를 적용하여 재사용 가능하고 효과인 시스템을 만들고자 하였다. 1 몰퍼센트의 낮은 촉매를 이용하여 산소 조건하에서 좋은 수득과 5번의 재사용 가능성을 확인하였다.

제 3장에서는, 현재까지 재사용 가능한 팔라듐-산화철 나노입자를 이용한 다양한 유기반응 적용에 대하여 본실험실은 계속적인 연구를 하였다. 유기반응 적용에는 탄소-탄소 결합 반응의 대표주자인 스즈키, 헥, 소노가시라 반응과 탄소-수소 사이의 아릴레이션 반응 스즈키를 기반으로 하는 폴리머리제이션 반응 웨커와 웨커 타입의 산화반응을 성공적으로 수행하였다. 여러가지 유기반응들의 성공적인 적용에도 불고하고, 비균질성의 팔라듐-산화철의 실제 반응에 참가하는 메커니즘에 자세하게 알려지지 않았다. 팔라듐-산화철 나노입자의 표면에서 반응이 진행되는 것인지 혹은 소량의 균일화된 팔라듐이 소량 녹아나와 반응이 진행되는 것을 확인하기 위하여 키네틱 실험, 핫-필터레이션 실험, 3상 반응 실험 등 3 가지의 실험을 스즈키 반응과 웨커 산화반응에 동시에 수행하였다.

II. 재사용 가능한 코어-쉘 구조의 팔라듐-백금-산화철 나노입자의 합성 및 유기반응의 촉매 활성 연구

본 연구는 산화철 나노 입자 위에 균일한 분포로 전이금속 혹은 합금 형태의 전이금속을 코어-쉘 구조로 만들며 만든 입자를 기존에 알려진 유기반응에 적용하여 독특한 촉매활성을 보는 연구이다. 하이드로서멀 기법을 이용한 방법을 토대로 나노 크기의 산화 철 입자에 전이금속의 종류인 팔라듐과 플레티늄을 팔라듐-플레티늄 합금을 고정화 시키는 새로운 전이금속-산화철 성공적으로 합성하였다. 세가지 형태의 코어-쉘 구조의 산화철 나노입자를 기본적인 니트로 환원반응에 적용하여 팔라듐-플레티늄 합금 산화철 나노입자의 우수성을 확인하였다. 독성이 없으며 높은 수소 보존력을 가지고 물이나 알코올 용매에 잘 녹으며 전이금속을 통한 가수분해를 통하여 수소를 잘 내놓는 아민보레인을 환원제로 이용하여 니트로 환원 반응을 수행하였다. 한가지 전이 금속이 고정화 된 팔라듐-산화철, 플레티늄-산화철 나노 입자들 보다 같은 조건에서 더 좋은 촉매활성을 보이는 합금형태의 팔라듐-프레티늄-산화철 나노 입자는 1 몰퍼센트라는 적은 양과 5 분이라는 짧은 시간에 높고 수득율을 보였다. 두 가지 전이 금속의 합금이라는 독특한 물성을 통한 촉매반응의 상승효과를 가져다 주었다. 또한 산화철의 초상자기성에 의한 자성으로 반응 후 촉매 회수를 쉽고 효과적으로 할 수 있는 장점을 동시에 가지었다. 300 번의 재사용 실험을 반복 실험 하였으며, 250번 정도는 동일 조건 하에 99%의 높은 수득률을 보이며 다양한 치환기에 대한 선택적인 반응성을 보였다. 반응 전/후의 촉매의 구조를 전자현미경 및 다양한 기기를 이용하여 반응성이 줄어드는 이유를 논리적으로 규명 하였다.